8-19-2015 12:00 AM

Self-Assembly and Stimuli-Responsive Properties of Amphiphilic Self-Immolative Block Co-Polymers

Thomas Mackenzie Gungor
The University of Western Ontario

Supervisor
Dr Elizabeth Gillies
The University of Western Ontario

SELF-ASSEMBLY AND STIMULI-RESPONSIVE PROPERTIES OF AMPHIPHILIC
SELF-IMMOLATIVE BLOCK CO-POLYMERS

by

Thomas Mackenzie Güngör

Graduate Program in Chemistry

A thesis submitted in partial fulfillment
of the requirements for the degree of
Master of Science (MSc)

The School of Graduate and Postdoctoral Studies
The University of Western Ontario
London, Ontario, Canada

© Thomas Mackenzie Güngör 2015

Abstract

In recent years, degradable polymers have become increasingly researched for their applications in drug delivery systems, adhesives, and tissue engineering. Self-immolative polymers (SIPs) are of particular utility due to predictable end-to-end backbone depolymerization after a stimuli-responsive end-cap cleavage. There are examples of incorporating a hydrophobic SIP into an amphiphilic block-copolymer, followed by self-assembly in aqueous media forming various nanoparticle morphologies. However, their self-assembly behaviour has not been described in detail, and there are no general synthetic methods that allow for their synthesis with good control over the relative hydrophilic block ratio, the major factor controlling their morphology. This thesis presents the synthesis of a self-immolative poly(carbamate) with a photo-active end-cap linked to a poly(ethylene)glycol (PEG) hydrophilic block and an attempt at poly(2-(*N*,*N*-dimethylamine)-ethyl-methacrylate) (PDMAEMA). These copolymers were self-assembled in aqueous media to form vesicles, micelles and inverted micelles. These nanoparticles were loaded with nile red, and their degradation was monitored by the release of the cargo.

Keywords and Abbreviations

Boc	*tert*-butoxycarbonyl
br	broad
d	Doublet
$Đ$	Polymer Dispersity
DLS	Dynamic Light Scattering
DMAP	4-(dimethylamino)pyridine
DMF	N,N-dimethylformamide
EDC	1-Ethyl-3-(3-dimethylaminopropyl)carbodiimide
$f_{hydrophilic}$	Hydrophilic Volume Fraction
HPLC	High-Pressure Liquid Chromatography
IR	Infrared
M	Molar
m	multiplet
M_n	Number-Average Molecular Weight
M_w	Weight-Average Molecular Weight
MWCO	Molecular Weight Cut-off
NIR	Near-Infrared
NMR	Nuclear Magnetic Resonance
PDMAEMA	poly(2-dimethylaminoethyl methacrylate)
PEG	Poly(ethylene glycol)
s	Singlet
SEC	Size-Exclusion Chromatography
SIP	Self-Immolative Polymer
t	Triplet
TBS	*tert*-Butyldimethylsilyl ether
TEM	Transmission Electron Microscopy
TFA	Trifluoroacetic Acid
THF	Tetrahydrofuran
UV	Ultraviolet

Acknowledgments

I would like to first thank Dr. Elizabeth Gillies for taking me on as one of her students, and giving me the opportunity to succeed in the group. She has genuinely cared for my progress both as a student and a researcher by going above and beyond what a supervisor needs to do.

I would like to thank all of the members of the Gillies group who have made my experience in the group not only hugely enlightening, but also quite a bit of fun. I would especially like to thank Trevor McIntosh for being my comrade through every step of this degree, Andrew Wong for directing me to produce the best chemistry I could, and Bo Fan for his patient and helpful collaboration. I would also like to thank Aneta Borecki for teaching me how to properly run a SEC instrument, and all her good advice.

I would like to thank my examiners Dr. Robert Hudson, Dr. Ken Yeung, and Dr. Martin Houde for taking the time to read my thesis. I would also like to thank Dr. Mathew Willans for his patience through helping me with many NMR spectra.

Lastly I would like to thank my family for letting me comfortably live at home for my entire university education rent-free, and my girlfriend Anne Isobel McDonald for her support through anything and everything.

To whoever else helped me along the way, I thank you.

Table of Contents

List of Schemes

List of Figures

List of Tables

List of Appendices

1   Introduction

1.1   General Introduction

In the past 50 years, the development of biodegradable polymers has led to their widespread usage in many different fields of science. A direct result of intensive research for this period of time has led to the introduction of biodegradable polymers into areas where environmentally-friendly plastics could replace commodity plastics. Applications like tissue engineering, drug-delivery systems and chemical sensors are a few examples where these biodegradable polymers find considerable use[1-3]. In general, a degradable polymer is a polymeric system that undergoes a deleterious change in its chemical structure and physical properties under specific, practical environmental conditions. Ideally, these polymers should be biologically non-toxic and environmentally friendly, and not produce any toxic by-products following the degradation process.

Biodegradable polymers are typically composed of systems with hydrolysable bonds in the polymer backbone. Examples of these kind of polymers with a biological origin are polysaccharides, peptides, and natural polyesters, and examples of artificially synthesized polymers include polyurethanes, polyamides, polyethers, and many more[1,2]. The mechanism of the polymer's degradation depends on its chemical and physical characteristics such as polymer length, dispersity, solubility and crystallinity[1]. Therefore, the design of biodegradable polymers is essential in deciding what application they may be useful in, and the extent to which they can be applied in that area.

1.2   Biodegradable Polymers

Aliphatic polyesters have received the most attention out of all possible biodegradable polymer backbones due to their ease of synthesis, desirable mechanical properties and high biocompatibility[4]. Additionally, the degradation of these polymers is tolerable *in vivo* because the hydroxy and carboxylate groups resulting from backbone hydrolysis are metabolized in a biological setting[1]. Examples of common synthetic biodegradable polyesters include poly(ε-capro lactone) (PCL), poly(glycolic acid) (PGA), and poly-3-hydroxybutyrate (PHB), used in fields like biomedicine as biodegradable stents and sutures[5,6], tissue engineering scaffolds[7,8], and drug delivery vehicles[9-13].
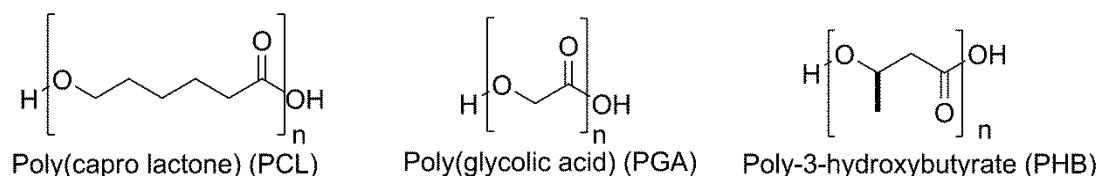
Scheme 1: Common examples of biodegradable polyesters

Due to the extensive exposure of polyesters in the field of chemistry, highly effective methods of their preparation have been reported. Ring-opening of lactones is the typical method to produce high-molecular weight polyesters and is conducted with catalysts, or with anionic or cationic initiators[2,14]. This method allows for significant control over the polymerization reaction, including factors such as polymer composition length, dispersity, and stereochemistry. Additionally, this high degree of control over the polymerization process can be used to tune biodegradable polyesters to degrade completely in the time span of weeks to years in a biological setting[4].
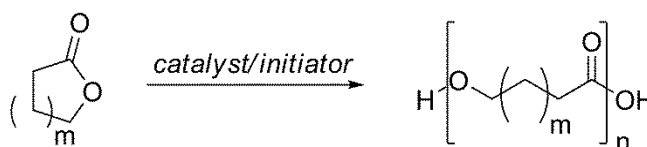
Scheme 2: The synthesis of polyesters can be done under many conditions and with variously sized lactone rings.

Unfortunately, polyesters suffer a drawback: limited fine control over the degradation process. In a biological setting, the mechanism of degradation of polyesters is achieved by random backbone hydrolysis events. This is a concern because the degradation isn't stimulated by a specific stimulus, only the presence of an environment which can lead to the scission of an ester functionality. Additionally, an entire polymer chain can be halved in size by only one cleavage event[15]. Although the polymer length and pH of the environment are factors that can partially change the degradation rate, they do not confer the polymeric system with a predictable framework for depolymerization rate or the mechanism of said degradation.
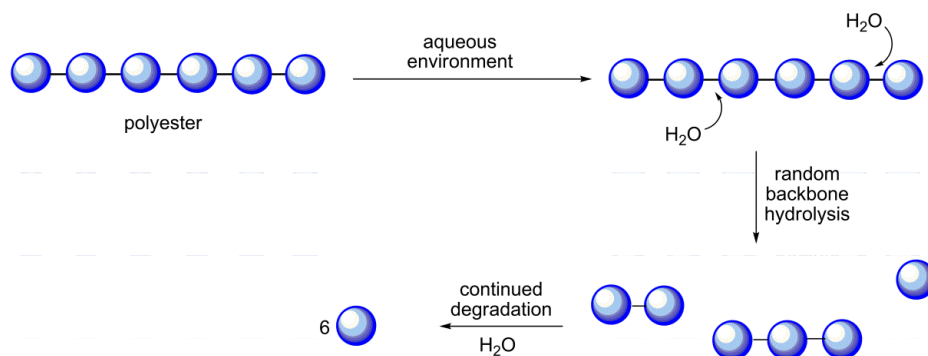
Scheme 3: The mechanism by which polyesters degrade is a series of random backbone ester hydrolyses.

1.3   Stimuli-Responsive Polymers

The issue of a non-specific degradation of a polymer has been resolved in the field of stimuli-responsive degradable polymers. These polymers undergo complete depolymerization only under a specific stimulus that triggers a functionality located in the polymer backbone[15-17]. There are examples of polymers that depolymerize when stimulated with acids, reducing agents, and light. Examples of each of these will be outline below.

1.3.1   Reduction-Sensitive Degradable Polymers

Disulfide bonds have been incorporated into degradable polymer backbones because they cleave under reducing conditions to produce two thiols. Additionally, organisms implement the cleavage and formation of the disulfide bond using the difference between the extracellular/intracellular redox potential. This gives disulfide systems the ability to degrade under certain stimuli, but also reform into a polymer again under oxidizing conditions[18]. These degradable di-sulfide polymers are stable in the context of the extracellular matrix where the concentration of glutathione is under $1\mu M$, but susbsequently degrade when introduced to the intracellular environment which has a glutathione concentrations above $1mM$[19-23].
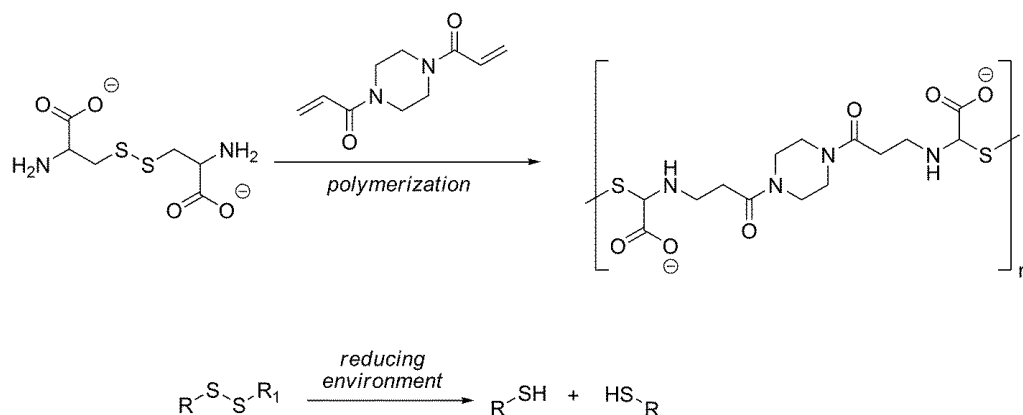
Scheme 4: The preparation of a reduction-sensitive degradable polymer, and the reaction equation of a general di-sulfide bond cleavage with a reducing agent.

1.3.2 Acid-Sensitive Degradable Polymers

There are many functionalities that undergo a chemical rearrangement when the pH of the environment has been lowered (**Scheme 5**). Under basic or neutral conditions these polymers are stable and do not degrade, but when introduced into an acidic setting they degrade completely[24]. This property has led to the application of these acid-degradable polymers in biological settings like the acidic lysosome or endosomes as drug-delivery vehicles[25-30]. Ultimately, these polymers could be used to deliver drugs into cancerous tumours, which are more acidic than typical biological conditions.
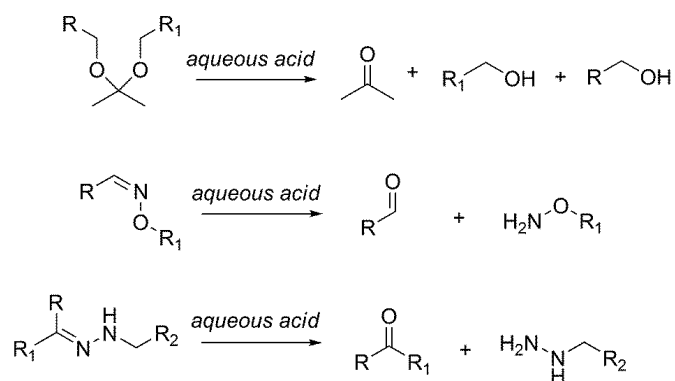
Scheme 5: Various functionalities which undergo a cleavage reaction under mildly acidic conditions. From top to bottom: acetal being cleaved into a ketone and two alcohols, an oxime being cleaved into an aldehyde and a hydroxylamine, and a hydrazone being cleaved into a ketone and a hydrazine molecule.

1.3.3   Photo-Sensitive Degradable Polymers

The degradation of a polymer that is stimulated by light is particularly attractive due to the ease of application of the stimulus. The type of light that has led to depolymerization of polymers is typically UV or near-infra-red (NIR). These systems commonly employ *o*-nitrobenzyl alcohol functionalities within the polymer backbone that undergo a chemical rearrangement following the absorption of one photon[31]. UV light has the drawback that it is harmful in biological conditions, and that UV light cannot penetrate deeper than 1mm under human skin. To contrast this NIR light is biologically harmless and can penetrate much deeper into tissue. To mediate the UV problem, 4-bromo 7-hydroxycoumarin functionalities have been incorporated into these polymer backbones because they cleave following the application of NIR light[32].

o-nitrobenzyl alcohol
derivative

4-bromo 7-hydroxycoumarin
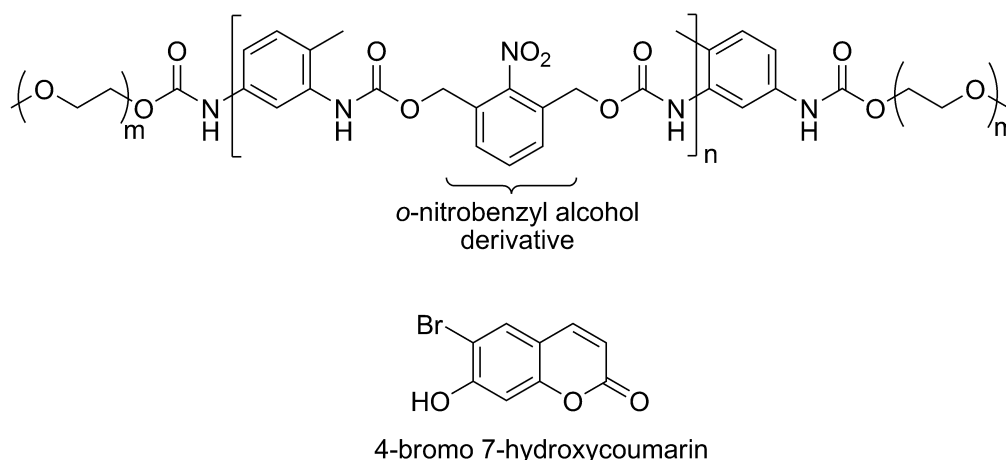
Scheme 6: The UV-sensitive *o*-nitrobenzyl derivative incorporated into a stimuli-responsive tri-block co-polymer, and the NIR-sensitive hydroxycumarin molecule.

1.4   Limitations of Stimuli-Responsive Degradable Polymers

The polyesters and stimuli-responsive polymers still suffer from the random and undesirable mechanism of depolymerization. This limits the overall control of the degradation process, and ultimately how these polymers will behave in a biological setting. Additionally, for complete degradation to occur there must be an abundance of the stimuli to ensure every single bond has been cleaved in the polymer backbone. The limits the systems to environments where there is a high concentration of the stimulus to

ensure degradation is complete, and thus restricts the extent to which these polymer systems are sensitive.

1.5   Self-Immolative Polymers

The requirement for degradable polymers needing a more specific stimulus to achieve a more predictable degradation has been resolved with the work on stimuli-responsive polymers (SIPs). SIPs are a class of stimuli-responsive degradable polymers that have emerged in the past 15 years to address the issues that previous degradable polymers suffer from. SIPs undergo end-to-end depolymerization in a cascade of intramolecular reactions following the removal of the end-cap which stabilizes the polymer[33-35]. SIPs are typically composed of monomeric spacers that are covalently arranged in an iterative manner and terminated with an end-cap which affords the polymer with stability. Ideally these SIPs do not degrade by backbone scissions, but only when the end-cap is cleaved ("triggered"). When this occurs, the adjacent terminal monomer undergoes a spontaneous intramolecular reaction and is released, leaving the polymer chain one unit shorter. This process repeats continuously down the chain of the polymer like a zipper, until the polymer has been completely transformed into small molecules.
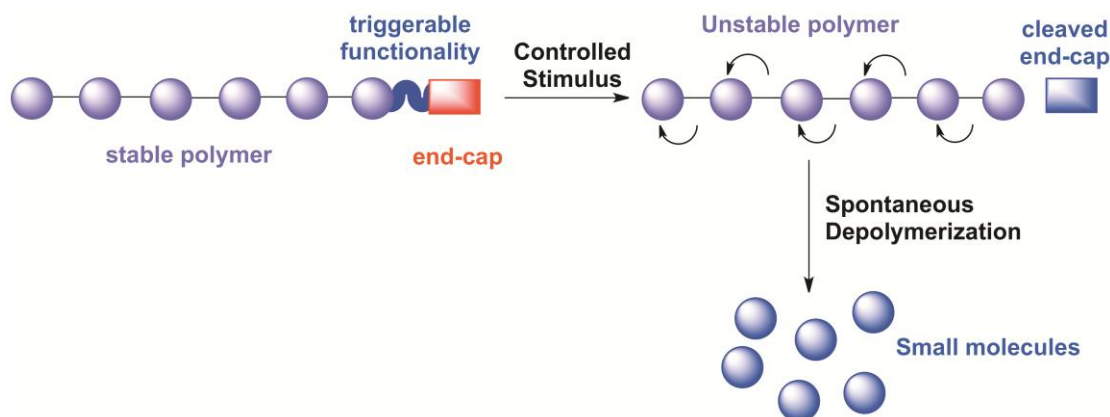
Scheme 7: A representation of the head-to-tail zip mechanism by which SIPs depolymerize into monomeric units following end-cap cleavage.

SIPs have been shown to depolymerize following end-cap cleavage triggered by conditions like changes in pH, temperature, redox environment, mechanical stress, and light[36]. Additionally, to address the issues with previous degradable polymer systems,

SIPs have been shown to depolymerize predictably under zero-order kinetics, and their full degradation time is correlated to the length of the polymer, ie the number of units[37].

1.5.1   Self-Immolative Dendrimers: the Inspiration for SIPs

The inspiration for the development of SIPs began in the area of stimuli-responsive dendrimers. These are molecules which contain a focal point on one end and branch outwards in the other direction in a series of generations. Self-immolative dendrimers were independently developed in 2003 by three groups to degrade under unique environmental triggers [38-40]. The trigger can be incorporated as the focal point which, upon the specific stimulus, leads to the downstream generations becoming unstable and being released in an exponential manner. This is important because the single stimulus leads to an amplification of released reporter molecules. Additionally, the dispersity of these large dendrimers are low (<1.1), which makes the behaviour of these molecules very consistent and predictable[41-45]. Unfortunately self-immolative dendrimers are limited in their use due to their complicated multi-step synthesis, and the increasing steric bulk that each successive generation gains, rendering high-generation functionalization difficult. The synthesis of SIPs contrasts that of dendrimers in that they can be produced in one polymerization reaction with no further transformations, and suffer less from steric hindrance in comparison with dendrimers.
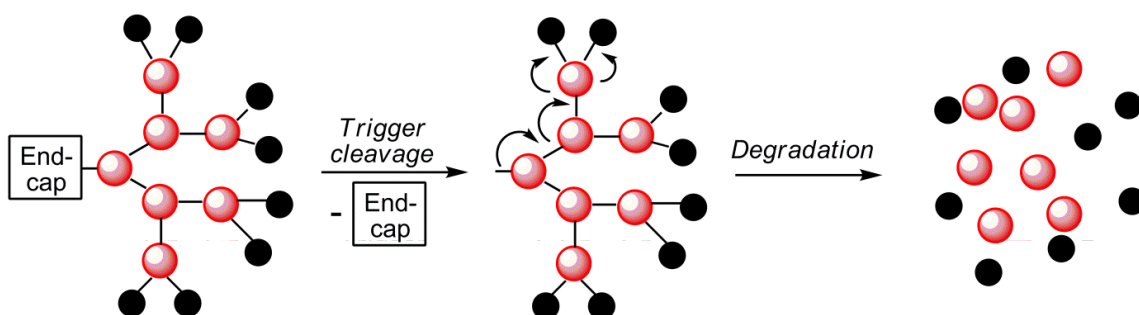
Scheme 8: A representation of the degradation of a dendrimer following one end-cap cleavage event, releasing a reporter molecule in an amplified manner (black circles).

1.5.2   The Elimination Poly(benzyl) Carbamate

The first backbone incorporated into a self-immolative linear polymer was a poly(benzyl carbamate), using a 4-aminobenzyl spacer, previously used in self-immolative dendrimers and oligomers[46]. The mechanism by which these polymers degrade the 1,6-elimination reaction of the benzylcarbamate backbone to form azaquinone methide, releasing the substituent on the benzylic position. The resulting carbamic acid functionality releases CO_2, and the self-immolation mechanism starts over. This methide is unstable, and is readily quenched with a nucleophile, usually being water, regenerating aromaticity.
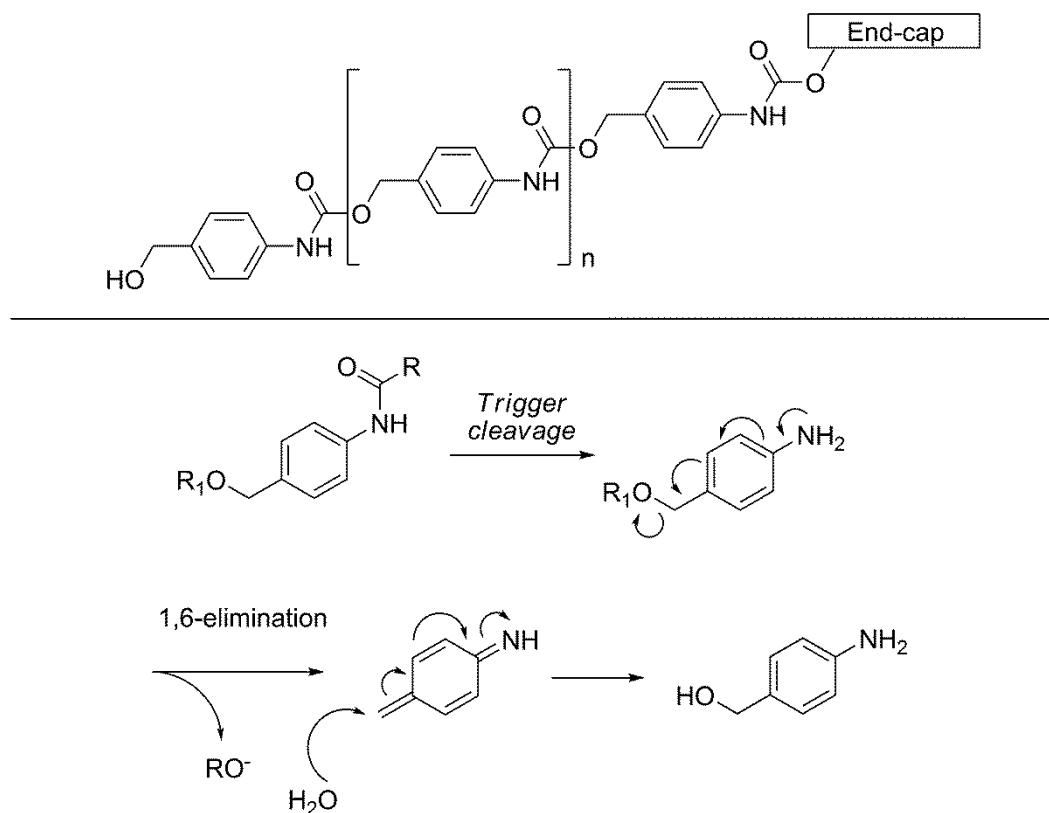
Scheme 9: A general poly(benzyl carbamate) SIP, and the 1,6-elimination reaction by which these systems depolymerize.

The degradation rate of these poly-(benzyl carbamate) is significantly limited by the loss of aromaticity when the azaquinone methide is released. Therefore, it was proposed to construct a monomer that would more favourably form the azaquinone methide by lowering the energy of breaking aromaticity. One method was adding one

methyl ether group to the benzyl ring which gives the benzyl ring more electrondensity, thus raising the energy of the Highest Occupied Molecular Orbital (HOMO). The other method was to use a naphthyl ring instead of a benzyl ring, decreasing the aromaticity (thus stability) of the parent structure. The latter approach afforded a 113-fold increase in the rate of the 1,6-elimination reaction, while the former approach afforded a 143-fold increase in the rate of formation of the azaquinone methide[47]. These results demonstrate that a SIP's degradation rate can be tuned not only by the length of polymer, but also by small structural changes in the repeat unit.

Relative Rate: 1   113   143

Scheme 10: The repeat unit of this SIP can be modified to tune the relative rate of degradation. Left to right: benzyl carbmate, naphthyl carbamate, and methoxy-substituted benzyl carbamate.

One end-cap chosen for this polymer was 4-hydroxy-2-butanone because it can be triggered enzymatically. Bovine serum albumin (BSA) cleaves the hydroxy-butanone end-cap via β-elimination, resulting in depolymerization of the polycarbamate[46]. To impart fluorescence to the monomer, the aniline monomer was functionalized with an acrylate group *ortho* to the amine. The equivalent carbamate formed from the amino group exhibited weak fluorescence in the resulting polymer, but following end-cap cleavage with BSA, the free amine of the monomer acted as a reporter molecule and greatly increased the fluoroescence of the sample. As was mentioned previously, the azaquinone methide, resulting from the depolymerization of these polycarbamates is electrophilic, and can be quenched with surrounding nucleophiles, usually being water. Therefore it was thought that the unstable quinone methide could label a larger molecule, perhaps a protein. Thus, depolymerization was monitored by the labelling of the anti-body Ab38C2 in the presence of penicillin-G amidase (PGA)[48]. It was shown that, upon depolymerization, labelling of these proteins occured and PGA did not suffer a decrease

in activity. Interestingly, as the concentration of the SIP increased,the activity of Ab38C2 declined, implying the azaquinone methide was labelling the lysine ε-amine located in active site on this protein.

Scheme 11: Bovine serum albumin (BSA) selectively cleaves the 4-hydroxybutanone end-cap. An enzyme is labelled with the azaquinone methide.

1.5.3   Poly(phthalaldehyde)s, a Class of Polyacetal SIP

Another class of SIPs is the polyacetal, of which there are two main types in the area of SIPs: poly(phthalaldehyde)s (PPHAs), and poly(glyoxylate)s (PGs). Due to their low ceiling temperature (T_c) these polymers tend to degrade spontaneously under ambient conditions[49], and this characteristic makes them promising candidates in the area of SIPs because, under low-energy conditions, they will degrade in a head-to-tail fashion. Unfortunately, this unstable nature of poly(acetal)s makes them difficult to synthesize, difficult to store over long periods, and incompatible in environments where stability is desired.
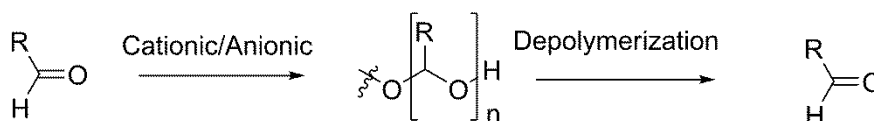
Scheme 12: The general synthesis and depolymerization of a polyacetal.

To address the problem of low ceiling temperatures, it was shown that PPHAs can be stabilized with a triggerable end-cap, after which the T_c was significantly raised. Upon cleavage under photochemically generated acid conditions, the PPHA completely depolymerized[50,51]. Following this work, a PPHA SIP system was developed where the ends of the polymer were terminated with multiple responsive end-caps. Upon anionic polymerization, three end-caps were attached to the PPHA termini to form three unique polymers: a Pd(0)-sensitive allyl carbonate end-cap, a fluoride-sensitive *tert*-butyl silyl end-cap, and a vinyl control end-cap[52]. It was shown that the resulting PPHAs were stable in THF under ambient conditions for over 15 hours, but once triggered with the appropriate stimulus, the metal-sensitive and fluoride-sensitive end-capped polymers completely depolymerized within minutes. To contrast this, the control underwent no degradation under these conditions.
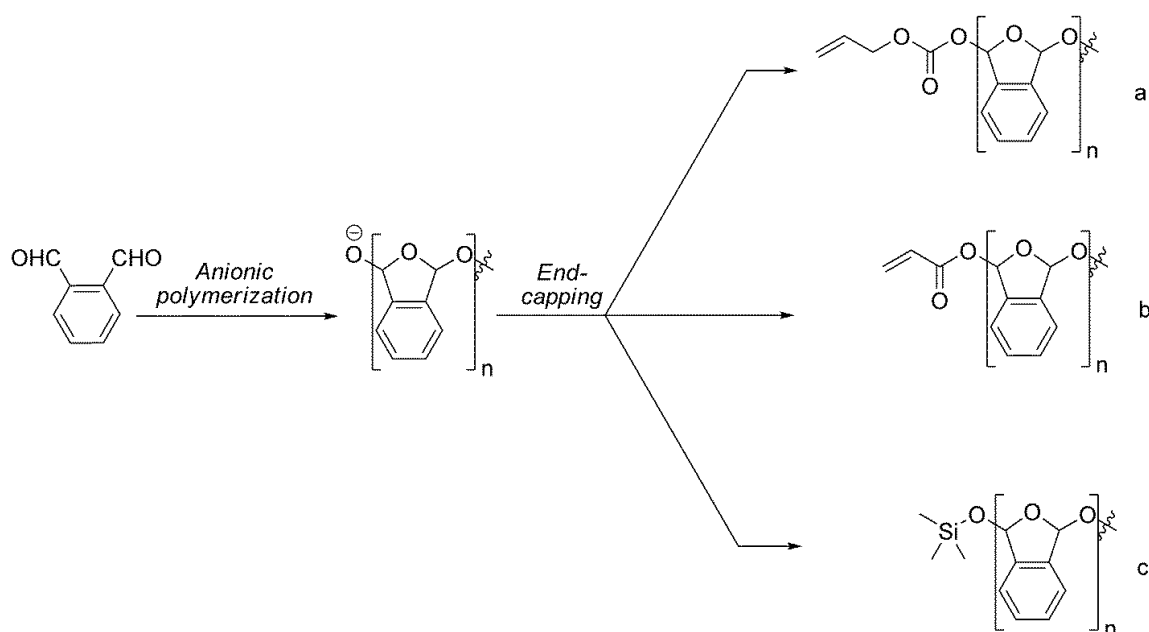
Scheme 13: Preparation of three PPHA SIPs. a) responds to Pd(0) metal catalysts, b) is a control polymer, and c) responds to F⁻ anions.

Post-polymerization functionalization of PPHA homo-polymers isn't feasible because of the sensitive nature of the acetal backbone. To address this issue, it was shown that PPHAs could be randomly co-polymerized with functionalized benzaldehyde monomers to form chemically modifiable polymers[53]. Although benzaldehydes are usually impossible to polymerize into poly(benzaldehydes) due to their low ceiling temperature, they are stabilized in the form of a random poly(phthaldehyde)-r-poly(benzaldehyde) co-polymer. The benzaldehyde monomer was functionalized with bromide, a partner in cross-coupling reactions like Sonogashira or Stille, to attach vinyl and alkynyl groups to the benzladehyde ring post-polymerization. Additionally, pendant aldehyde groups were attached to the benzaldehyde units in the random co-polymer and were subsequently reduced to form alcohols. Primary alcohols are highly versatile functional handles, and were combined with isocyanates to form cross-linked carbamate groups throughout the SIP.
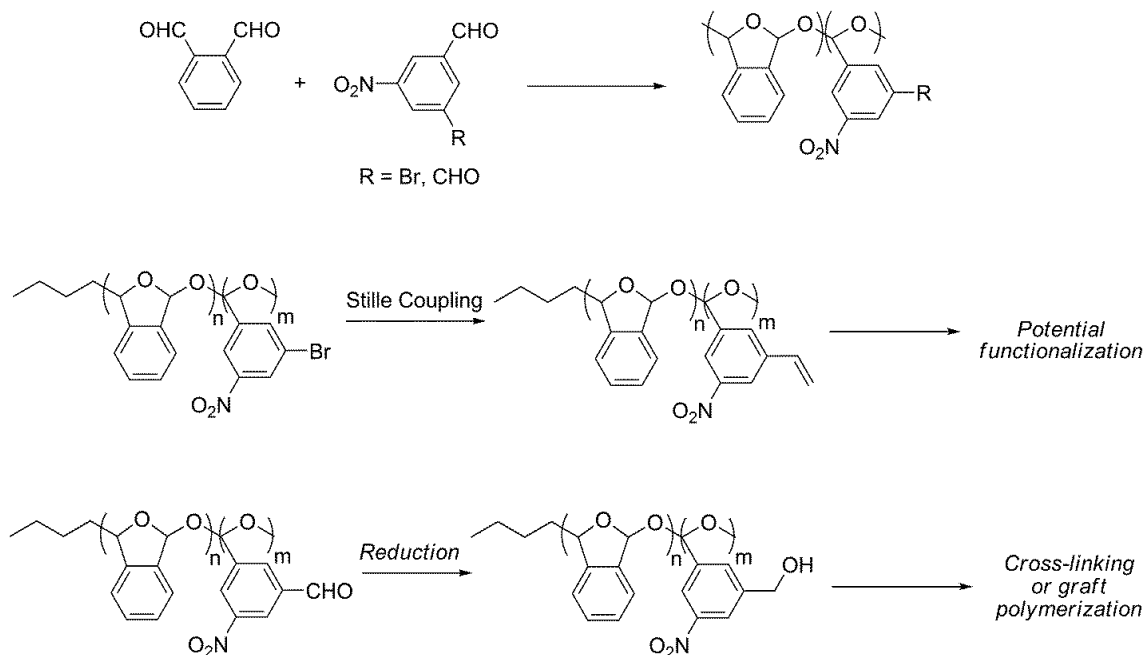
Scheme 14: Random copolymerization with functionalized benzaldehydes gives these PPHAs post-polymerization characteristics aside from depolymerization.

Using the PPHA homo-polymer, it has been shown that, under cationic polymerization conditions with $BF_3 \cdot Et_2O$, stable polymers can be synthesized without end-capping[54]. Anionic polymerization usually affords a PPHA with visible end-cap peaks, thus making the absence of end-cap peaks for this cationic polymerization novel. The authors speculated that the polymer products may be cyclic species, and this was confirmed with matrix assisted laser desorption/ionization-time of flight mass spectrometry (MALDI-TOF MS) and size-exclusion chromatography (SEC). Additionally, it was observed that these cyclic species are not stimuli-responsive, confirming the lack of end-cap. However, the formation of these cyclic polymers was a reversible process, which gives these systems the potential to incorporate new monomers as the polymerization progresses in a living-manner. Although not what was originally intended, these cyclic polymers are intriguing due to their reversible formation, and that large macrocycles are typically difficult to synthesize.

1.5.4   Poly(glyoxylate)s, Another Class of Poly(acetal) SIP

Poly(glyoxylate)s (PGs) are the other major backbone of the more general class of self-immolative poly(acetal)s, whose properties and applications have seen large advances in recent years due to their potential applications in areas like drug-delivery, and detergent buiders[55-59]. The monomer unit of these poly(acetal)s is a glyoxylate molecule, essentially being an aldehyde bonded directly to an ester functionality. PGs can be polymerized in either acidic or basic conditions, and the ester functionality is essential to making the aldehyde electrophilic enough to facilitate attack from another monomer's nucleophilic oxygen. PGs have relatively low ceiling temperatures (below 100 ºC) and like PPHAs, require end-capping to prevent rapid depolymerization. PGs are of particular interest due to their non-toxic degradation products, being glyoxylic acid hydrate in aqueous conditions, which can be incorporated into the glyoxylic acid cycle present in all plants, bacteria, fungi and protists[60]. This gives these polymers the advantage of being environmentally friendly and potentially biocompatible. Additionally, the PG monomer requires few synthetic steps prior to polymerization, contrasting many other SIP monomers.
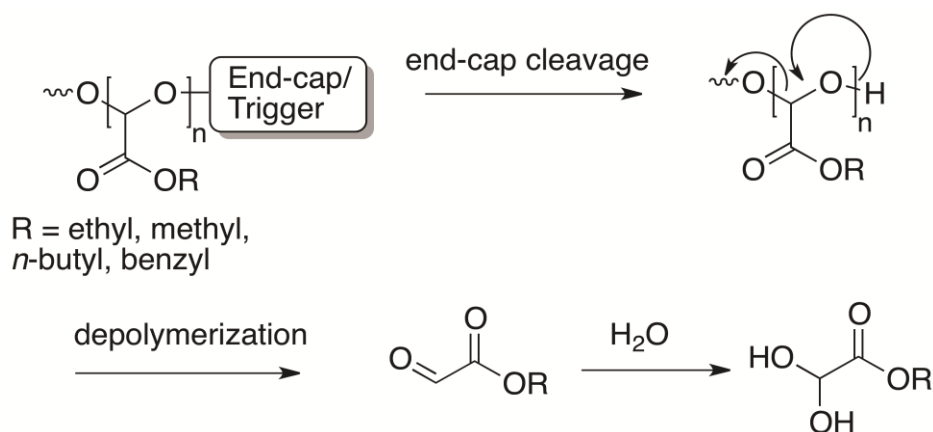
Scheme 15: Depolymerization following end-cap cleavage in polyglyoxylates, resulting in the production of glyoxyl hydrate.

The first reported self-immolative PG was poly(ethyl glyoxylate) (PEtG), and was chosen due to the commercial availability of the ethyl version of the monomer[61]. A photo-triggerable 6-nitroveratryl (6-NVOC) moiety was chosen as the end-cap. High monomer purity was essential to producing high molecular-weight polymers with low

dispersities (Đ), facilitated by multiple distillations of the monomer. These conditions produced polymers end-capped with the UV light-sensitive 6-NVOC group with molecular weights ranging from 31 - 53 kg mol^{-1}. Under the application of UV-B light, the 6-NVOC end-cap will undergo an intramolecular rearrangement and presumably be cleaved from the PEtG, leading to downstream depolymerization. This PEtG was dissolved in 9:1 acetonitrile: water and irradiated with UV light, and depolymerized completely over several days into the ethyl glyoxylate hydrate. The progression of the degradation was monitored by ^{1}H-NMR spectroscopy, confirmed by the appearance of the sharp hydrate peaks, and disappearance of the broad polymer peaks. To broaden the scope of using poly(glyoxylate) SIPs, a poly(methyl glyoxylate) was prepared from commercially available starting materials like maleic or fumaric acid. Varying the R group on the monomer ester would potentially have an effect on the steric bulk and hydrophobicity of the polymer, giving this type of poly(acetal) additional tunability.
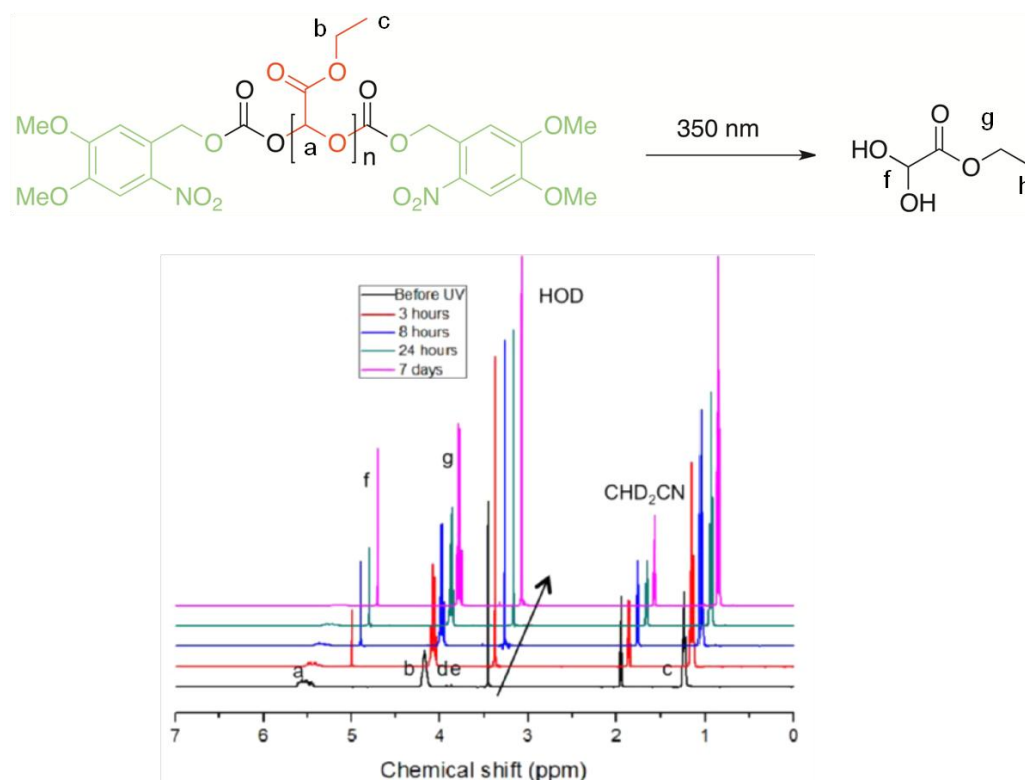
Scheme 16: The NMR-monitored depolymerization of NVOC-end-capped PEtG.

1.5.5   Incorporation of a Cyclization Spacer into Poly(carbamate) SIPs

The rapid kinetics of the 1,6-elimination limits the scope of the previously reported poly(benzyl carbamate)s because they degrade almost completely within minutes in aqueous solution. This problem has been mediated by the development of a new monomer which is comprised of a cyclization spacer[62]. This backbone compromises alternating 1,6-elimination spacers and cyclization spacers, and is based on 4-hydroxybenzyl alcohol and *N*,*N'*-dimethylethylenediamine. This polymer is prepared in a step-growth polycondensation reaction, and the conditions of this reaction can be used to control the length of the polymer produced. Selective removal of the Boc end-cap with TFA led to complete depolymerization of the polymer in a 3:2 pH 7.4 buffer:acetone mixture at 37°C (**Scheme 17**).
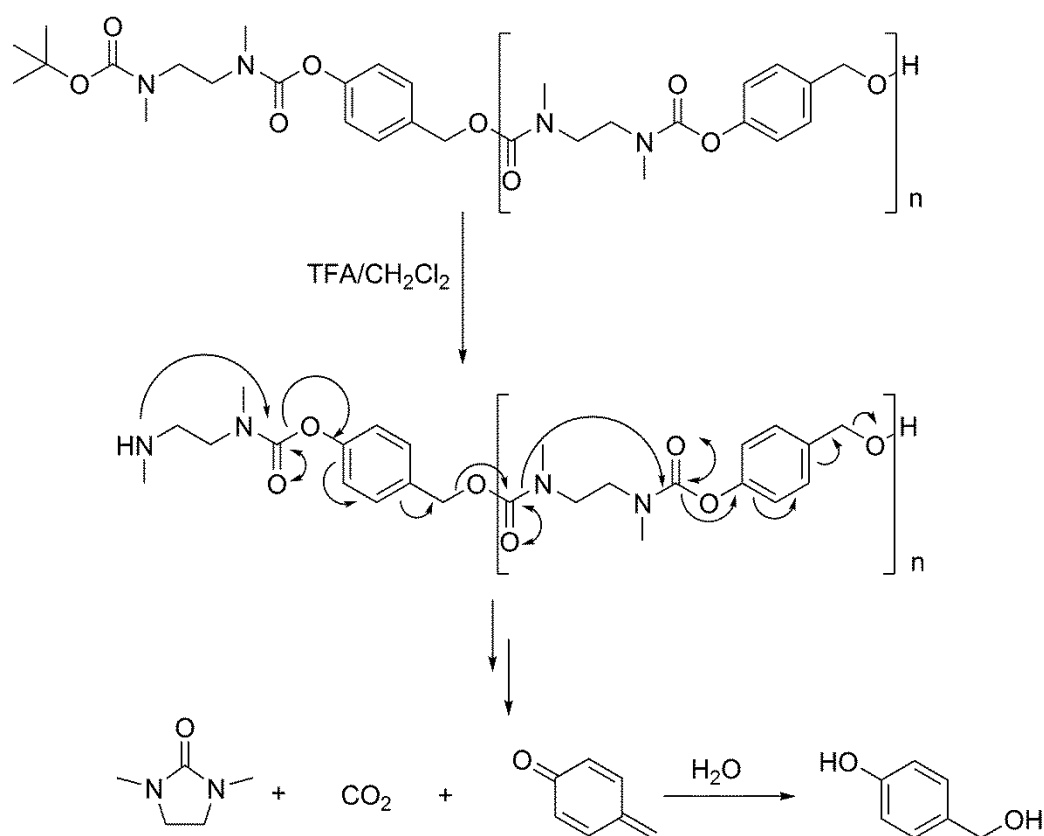
Scheme 17: Upon removal of the end-cap, this alternating 1,6-elimination cyclization SIP depolymerizes completely into small molecules.

The depolymerization process leads to the production of water-soluble small molecules: a cyclic urea, CO_2, and *p*- quinone methide which is subsequently quenched by water to regenerate 4-hydroxybenzyl alcohol. The degradation rate can be further modified by modifying the nucleophilic and electrophilic sites in the spacer by changing the type of cyclization spacer. Instead of using the diamine spacer mentioned previously, *N*-methylaminoethanol and 2-mercaptoethanol were integrated into this polymer with the aim to change the degradation profile of this SIP[63]. The incorporation of *N*-methylaminoethanol decreased the time required for 80% depolymerization to 4 hours from 2 days, and the 2-mercaptoethanol further reduced this time to only 2 hours (**Scheme 18**). The introduction of these new spacers decrease the degradation time by increasing the rate of cyclization reaction of the spacer itself. *N*-methylaminoethanol increases the electrophilicity of the carbonyl group by incorporating a carbonate group next to the spacer, and the 2-mercaptoethanol further increases the cyclization reaction rate by incorporating a sulfur, a better nucleophile than nitrogen in this context.
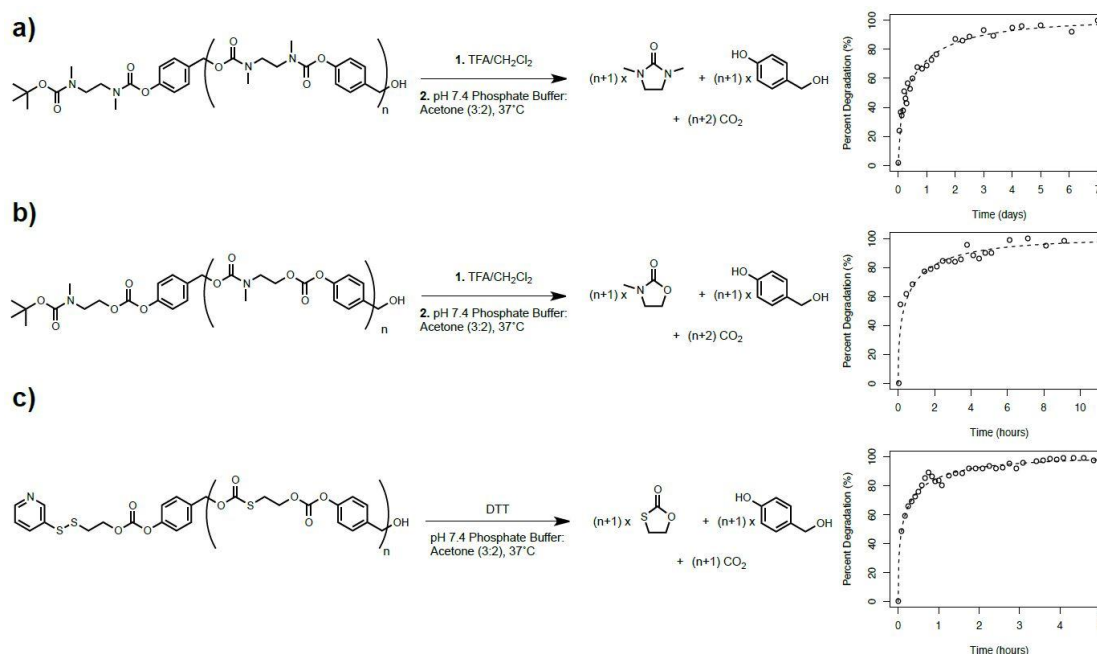
Scheme 18: Linear SIP depolymerizations following end-cap removal and their relative degradation kinetics. a) diamine cyclization spacer, b) *N*-methylaminoethanol cyclization spacer, and c) 2-mercaptoethanol cyclization spacer.

1.6   Amphiphilic Block Co-Polymers

An amphiphile is a molecule that possesses both hydrophobic and hydrophilic properties. When an amphiphile is introduced into a solvent, the molecules arrange themselves into thermodynamically favourable particles by displaying the solvophilic portion towards the exterior, and hiding the solvophobic portion inside these particles. A common example of an amphiphilic molecule is soap, which contains a hydrophobic tail and a polar (hydrophilic) head that forms small micelles in an aqueous environment.

Block co-polymers also display amphiphilic characteristics when one block is designed to be hydrophobic and the other is hydrophilic. Once introduced to a solvent (typically water) they self-assemble into nanoparticles with properties such as unique morphologes and distributions of sizes . The formation of these morphologies in aqueous media is attributed to two competing thermodynamic parameters: a) the enthalpic contribution from the interfacial energy between the two blocks, and b) the entropic contribution due to chain stretching. The co-polymers attempt to minimize the interfacial energy while maximizing the entropic stretching[64]. These amphiphilic co-polymers can assume various nanoparticle morphologies including spherical micelles, cylindrical micelles, lamellar structures, and vesicles. The factors that dictate the type and size of the nanoparticle morphology that results from self-assembly are: i) the hydrophilic block volume fraction ($f_{hydrophilic}$), ii) the random coil nature of the two chains comprising the co-polymer, and iii) the extent to which each block is hydrophilic and hydrophobic respectively.

The last two points ii) and iii) both depend on the composition and chemical structure of the two polymers involved in the block co-polymer, but the first point i) does not. A rough guideline which estimates any given block co-polymer's morphology following self-assembly has been reported[65, 66]. The $f_{hydrophilic}$ of an amphiphilic block co-polymers has a direct effect on the size and morphology of the nanoparticles formed in aqueous solution. A co-polymer with a $f_{hydrophilic}$ of 25% or below forms inverted microstructures, $f_{hydrophilic}$ of $35 \pm 10\%$ forms vesicles (polymersomes), and $f_{hydrophilic}$ of 45% and above forms spherical micelles.
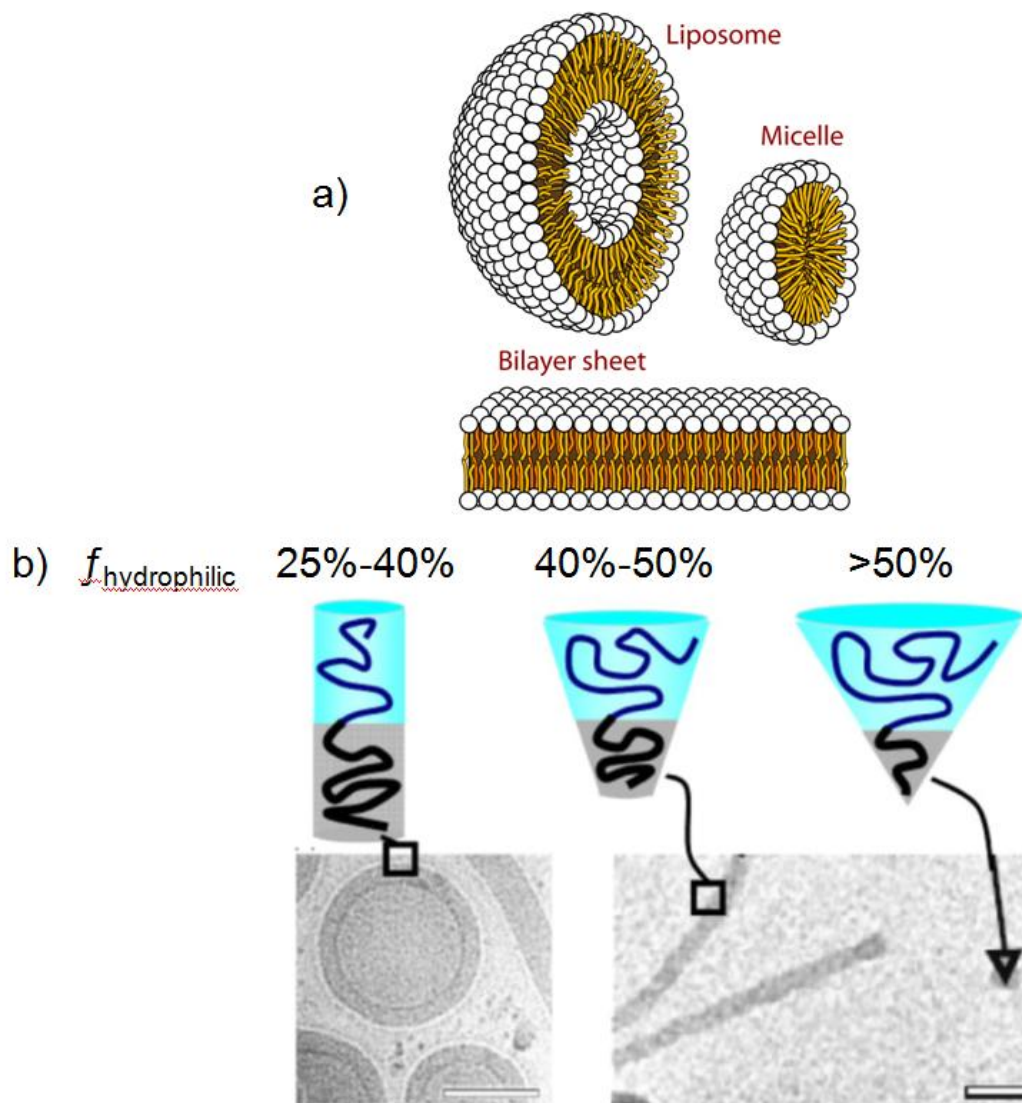
Scheme 19: a) representation of liposomes (vesicles) and micelles where the yellow lines represent the hydrophobic tail and the white spheres are the hydrophilic head, b) from left to right: TEM images of vesicles, cylindrical micelles, and spherical micelles. (adapted with permission from reference 74 Copyright **2006** Wiley Online Library.)

The nanoparticles formed from these amphiphilic co-polymers are important because they can be used as drug-delivery vehicles *in vivo*. Hydrophobic drugs can be loaded into the interior of the hydrophobic core of a micelle, or sandwiched into the interior of the bi-layer of a vesicle. Vesicles are unique in that they contain a hollow

hydrophilic interior that can be loaded with hydrophilic drugs, an ability that micelles do not possess. Nanoparticles acting as drug-delivery vehicles can transport their drug throughout an organism, but will eventually release their cargo. Biodegradable polymers become a useful tool in this area because they can be incorporated into the block co-polymer as one of the blocks. The biodegradable polymer is typically the hydrophobic block, and poly(ethylene glycol) (PEG) is the most commonly implemented hydrophilic block[67-69].

The various desirable properties of SIPs make them attractive candidates for the degradable hydrophobic block of a co-polymer. In the context of drug-delivery, it would be desirable to achieve the production of nanoparticles that could carry both hydrophilic and hydrophobic drugs through the body, and then depolymerize under a specific stimulus to release their cargo at a certain time in a specific location.

1.6.1 Poly(benzyl carbamate)s as the Hydrophobic Block of Polymersomes

A responsive SIP block co-polymer system was developed in response to the potential applications for drug-delivery. An array of poly(benzyl carbamate) (PBC) SIPs were prepared using a polycondensation reaction followed by end-capping with three stimuli-responsive end-caps cleaved with: UV-light (~360nm), visible light (420nm), and reducing conditions, respectively[70]. The opposite end of each SIP was covalently linked to a reversible addition−fragmentation chain-transfer (RAFT) initiator which was used to grow a hydrophilic poly(*N*,*N*-dimethylacrylamide) (PDMA) block to produce PBC-*b*-PDMA co-polymers. These co-polymers self-assembled in aqueous media to form polymersomes, which were confirmed by TEM and SEM images, and DLS data. To confirm the self-immolative properties of this system, the polymersomes formed containing the visible- light-sensitive end-cap were irradiated with 420nm light for 30 minutes. Their depolymerization was monitored by the appearance of the main degradation product, 4-hydroxybenzyl aniline via HPLC, and the decreasing M_n was monitored by SEC over time to confirm the disappearance of the poly(benzyl carbamate) chain. The remaining M_n in the SEC was the same as the molecular weight of the PDMA hydrophilic block (~6,500 g/mol) that was originally grown off the SIP. TEM images were taken following depolymerization and it was observed that the polymersomes

became ruptured with pores, and after 12 hours of incubation time, led to complete degradation into aggregates.
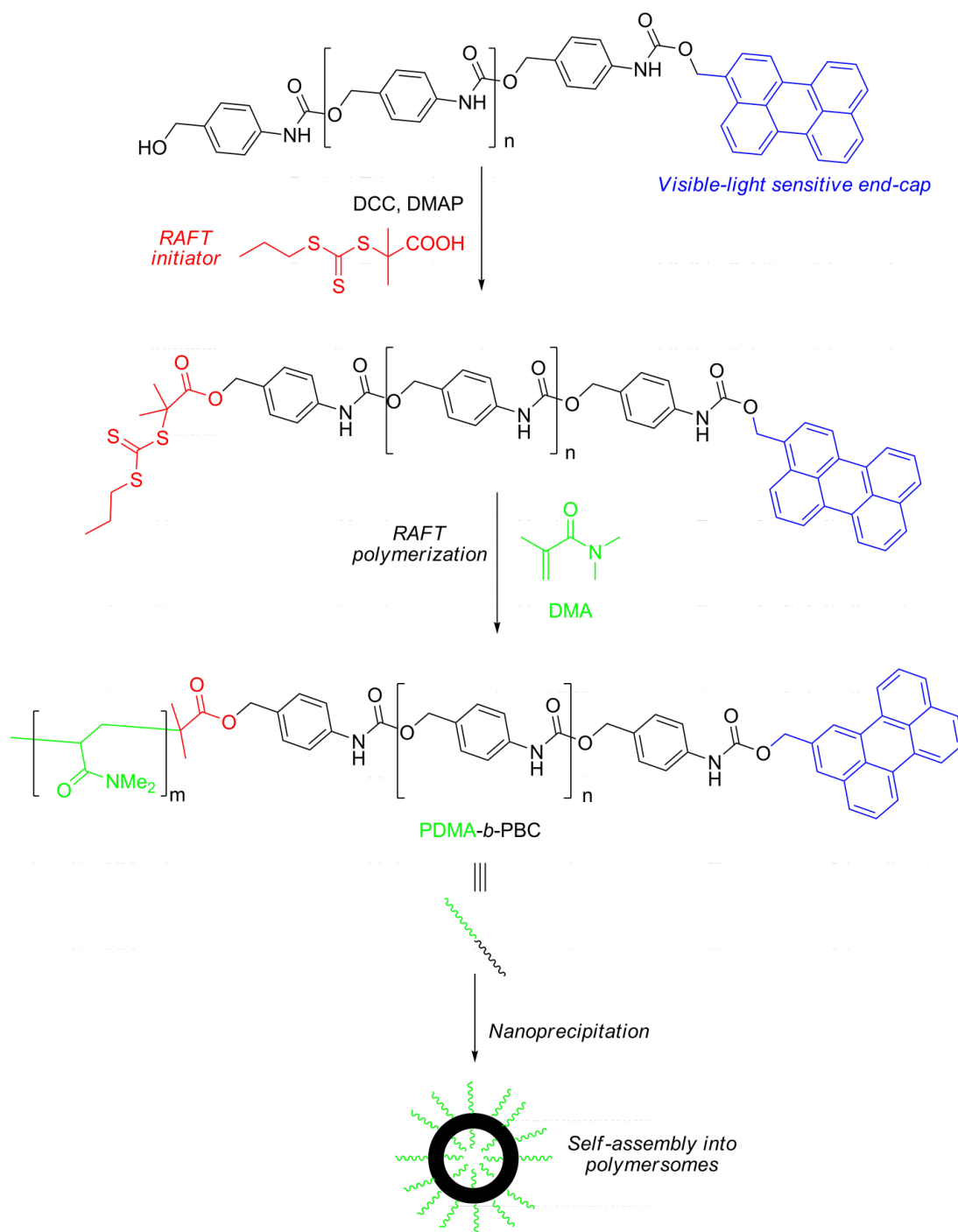
Scheme 20: The synthesis and self-assembly of PDMA-*b*-PBC block co-polymers.

The logical next step was the loading of these polymersomes with a drug to further demonstrate that these systems are applicable in the drug-delivery area. The PBC-*b*-PDMAEMA co-polymer chosen for this study implemented the reduction-sensitive end-cap due to its biological relevance. Two drugs were chosen: a hydrophobic amptothecin (CPT) and hydrophilic doxorubicin (DOX). In the absence of glutathione (the reducing stimulus), these polymersomes only released 4% of DOX and 19% of CPT over the period of 20hrs. When these polymersomes were introduced to 10mM glutathione, 82% of DOX and 86% of CPT were released under the same 20hr period. This shows that the triggering of the end-cap and subsequent depolymerization of the PBC hydrophobic block is essential to the release of the drugs.

1.6.2 CO_2-Responsive Block Co-polymer Nanoparticles

There are also examples of block-co-polymers whose nanoparticles undergo reversible morphological changes under the influence of a certain stimulus. PEG is the usual choice for the hydrophilic block due its commercial availability and low dispersity, but PDMAEMA was chosen for this system due to its unique thermal and pH responsive properties. The pendant tertiary amine groups on each repeat unit can be protonated and positively charged or unprotonated and neutral, giving the polymer the ability to have varying degrees of protonation and therefore charge. Additionally, PDMAEMA has been shown to have unique thermo-responsiveness; as the temperature is increased from 30 to 50 °C, the polymer chains undergoes a "chain collapse" phenomenon whereby its hydrodynamic volume significantly decreases[71]. A tri-block co-polymer was prepared which contained this multi-responsive polymer: poly(ethylene glycol)-*b*-polystyrene-*b*-poly(2-dimethylaminoethyl methacrylate) (**PEG-*b*-PS-*b*-PDMAEMA**)[72]. Although the hydrophobic polymer in this case is a non-degradable polystyrene (PS) chain, this system nonetheless demonstrates the morphological versatility of co-polymers that incorporate PDMAEMA. In this work, the pH responsiveness of PDMAEMA was utilized by varying the acidity of the aqueous medium that the nanoparticles were assembled in. Three tri-block co-polymers were prepared, each possessing a unique hydrophilic weight ratio by way of varying the lengths of the PS and PDMAEMA blocks. This was done in aim to form three distinct morphologies which would undergo unique morphological changes

following the purging of CO_2. Following the purging of the aqueous medium with CO_2, the pH steadily decreased while the pendant amine groups on the PDMAEMA block became protonated. The parent morphology underwent an increase in volume (swelling) due to the strong cationic repulsion in the PDMAEMA chain.
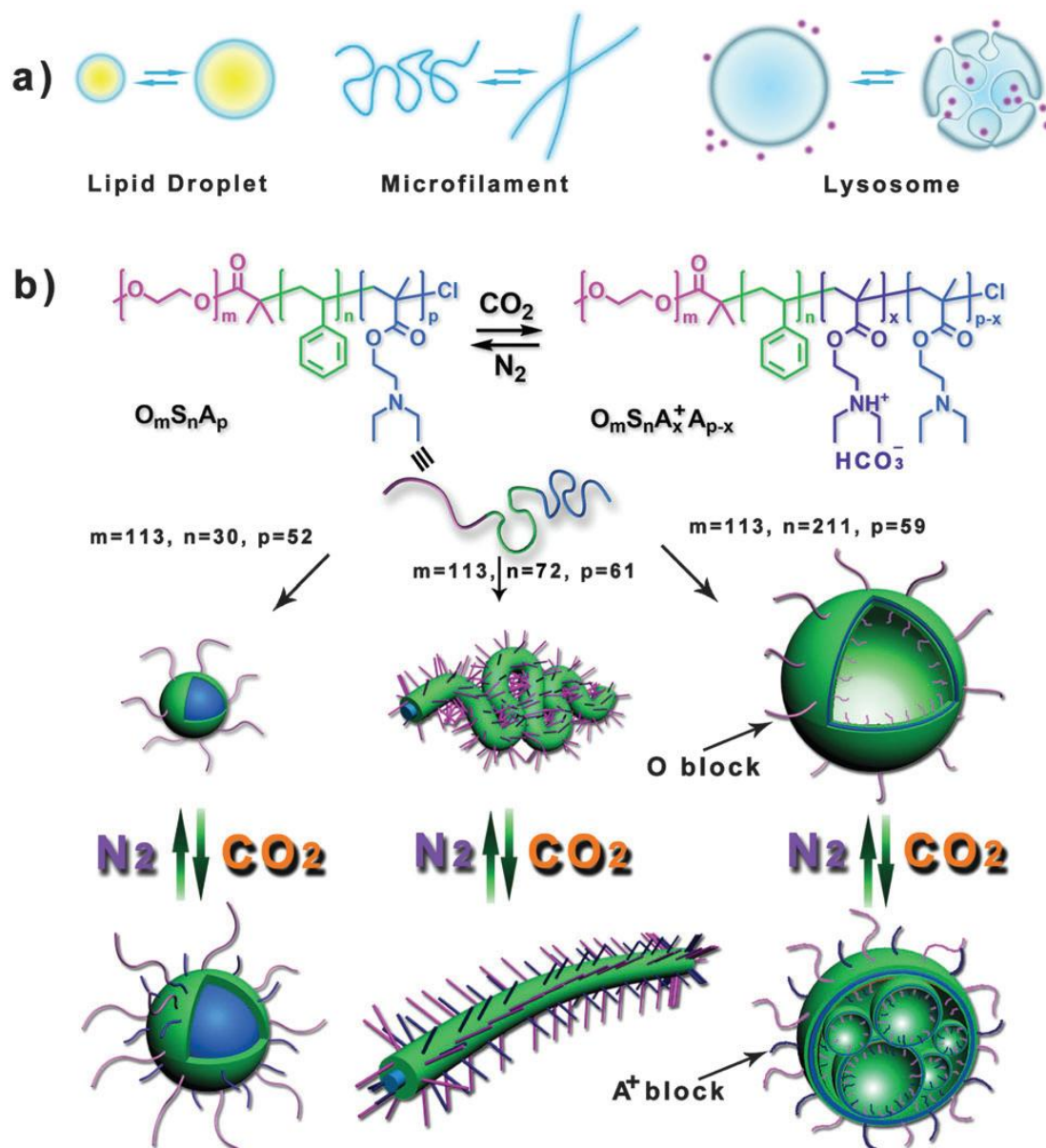
Scheme 21: The shape regulation of different morphologies after both CO_2 purging (adapted with permission from reference 72. Copyright 2009 American Chemical Society.)

PEG$_{113}$-*b*-PS$_{30}$-*b*-PDMAEMA$_{52}$ formed micelles, PEG$_{113}$-*b*-PS$_{72}$-*b*-PDMAEMA$_{61}$ formed cylindrical micelles, and PEG$_{113}$-*b*-PS$_{211}$-*b*-PDMAEMA$_{59}$ formed polymersomes. As the number of pendant amine groups on the PDMAEMA chain became increasingly protonated, these chains repelled each other and consequently swelled this portion of the nanoparticle. The micelle interior became more voluminous, causing an increase in the micelle diameter. The cylindrical micelles became rigid rods, and the polymersomes began to form pockets of smaller vesicles within its interior. Additionally, after purging these systems with N_2 to remove CO_2 and regenerate the neutral pH, the morphologies returned to their parent nanoparticle structures, giving these systems the property of convenient reversibility.

1.7   Thesis Goals

The goal of this thesis is to create a unique co-polymer system composed of the hydrophobic poly (benzyl carbamate) with a diamine linker and a hydrophilic PEG which has the following properties: depolymerizes following a specific stimulus, self-assembles in aqueous media, can be tuned to form various morphologies, can be loaded with a cargo, and is reversibly multi-responsive under various stimuli. An array of co-polymers will be produced, each with a unique hydrophilic volume ratio so that the self-assembly nature of the co-polymers can be studied. To begin depolymerisation of the nanoparticles UV light will be used to trigger the cleavage of the *o*-nitrobenzyl end-cap of the SIP, and the degradation profile will be monitored using spectroscopic and imaging techniques. PDMAEMA has been shown to be an increasingly attractive hydrophilic block due to its various multi-responsiveness. An attempt to covalently link this hydrophilic block to the UV-sensitive SIP will be undertaken so form an amphiphilic co-polymeric system that is responsive to light, and changes in both pH and temperature.

2   Results and Discussion

2.1   Small Molecule Synthesis

The synthesis of the monomer required for the preparation of the target poly(carbamate) SIP has been previously reported. To form the 1,6-elimination spacer, benzyl alcohol was protected using *tert*-butyldimethyl silyl chloride (TBSCl) under basic conditions to afford **2**. To form the cyclization spacer *N,N*-dimethylethylenediamine was protected with di-*tert*-butyl-dicarbonate (Boc$_2$O) to yield mono-Boc protected **5**. The phenol group on **2** was transformed into the "activated" carbonate **3** using 4-nitrophenyl chloroformate (PNP-COCl). The mono-Boc protected **5** was then coupled to activated carbonate (due to the carbonate's electrophilicty) **3**, releasing the PNP phenol, and affording carbamate **6** (**Scheme 22**).The synthetic steps leading to the final monomer preceding polymerization were straightforward, but the previously reported synthesis could be improved upon.
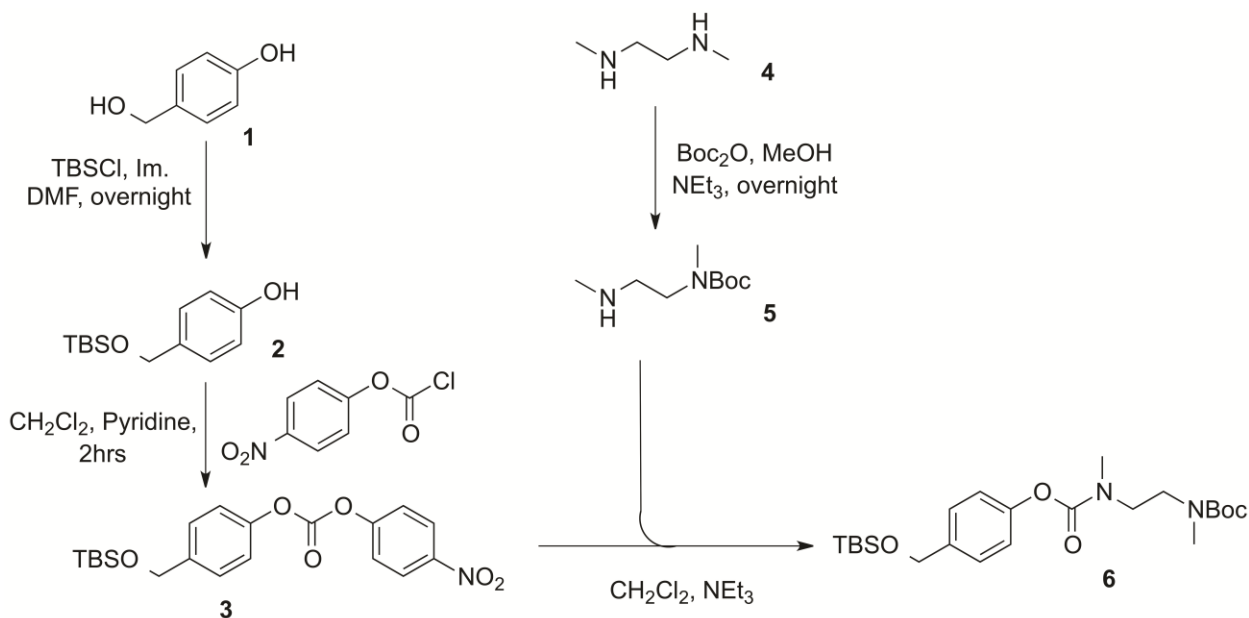
Scheme 22: The first steps of the previously reported monomer synthesis.

Instead of forming an activated carbamate, it was thought that the benzyl and diamine spacers could be combined in one step following the protection reactions. A revised synthesis (**Scheme 23**) was proposed to shorten the synthetic route by one step, thus avoiding chromatography purification. The synthesis was simplified by replacing the

PNP- activation and purification with a one-step chloroformate formation of **2** with triphosgene and immediate in-situ condensation with **5**. The monomer requires an electrophilic site on one end, and a nucleophilic site on the other for polymerization to occur. To form the nucleophile, the alcohol was activated using PNP-OCClto form a carbonate. This allowed for the synthesis of the Boc-protected monomer in 5 steps.
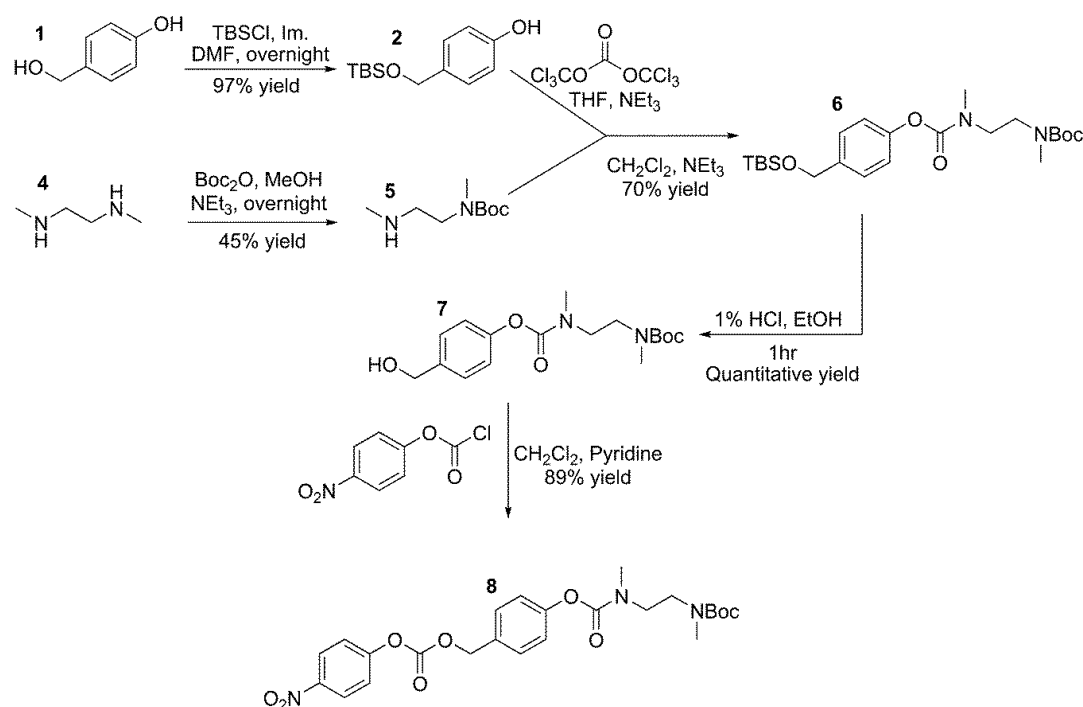
Scheme 23: Convergent synthesis of the activated monomer.

An *o*-nitro benzyl end-cap was chosen as the stimulus-responsive terminus of the SIP, whose chromophore absorbs ~300nm light to undergo an intramolecular rearrangement (**Scheme 24**). This photochemical reaction releases the polymer, and leads to depolymerization. In practise this means that under the brief application of UV-B light, the polymer should theoretically begin its degradation.
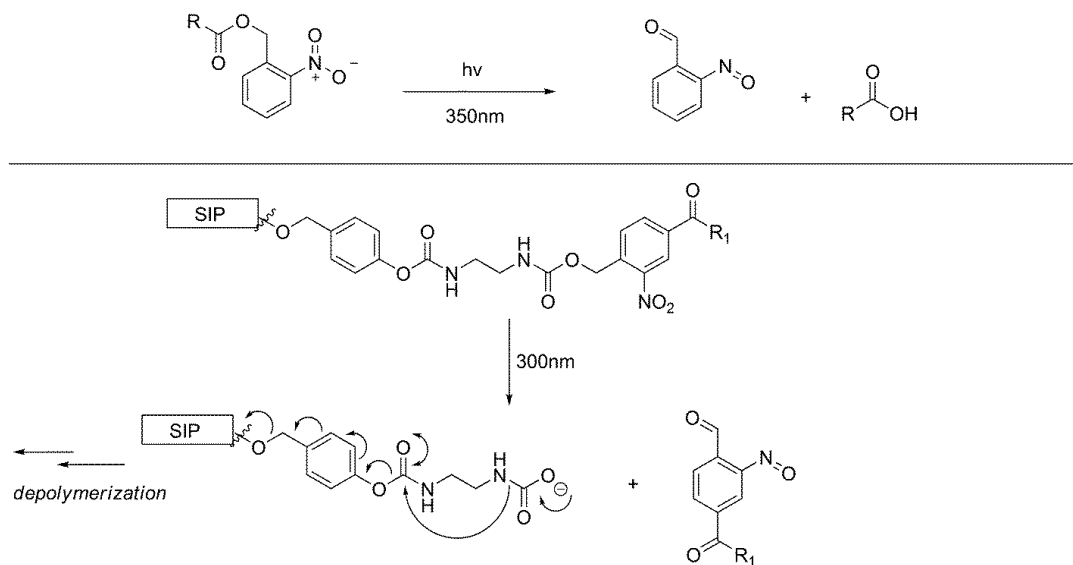
Scheme 24: The intramolecular rearrangement that *o*-nitro benzyl groups undergo following application of UV light.

The synthesis of the end-cap began with the commercially available acid **9**. Nucleophilic substitution of the bromide with a hydroxyl group yielded the benzyl alcohol **10**. Propargyl amine was attached to **10** using 1-ethyl-3-(3-dimethylaminopropyl)carbodiimide (EDC) to form amide **11**. The alkyne was chosen so that an azide functionality on a hydrophilic polymer could be coupled under click conditions in future steps. Amide **11** was then activated using PNP-OCCl to form the end-cap **12**, ready for end-capping during polymerization (**Scheme 25**).
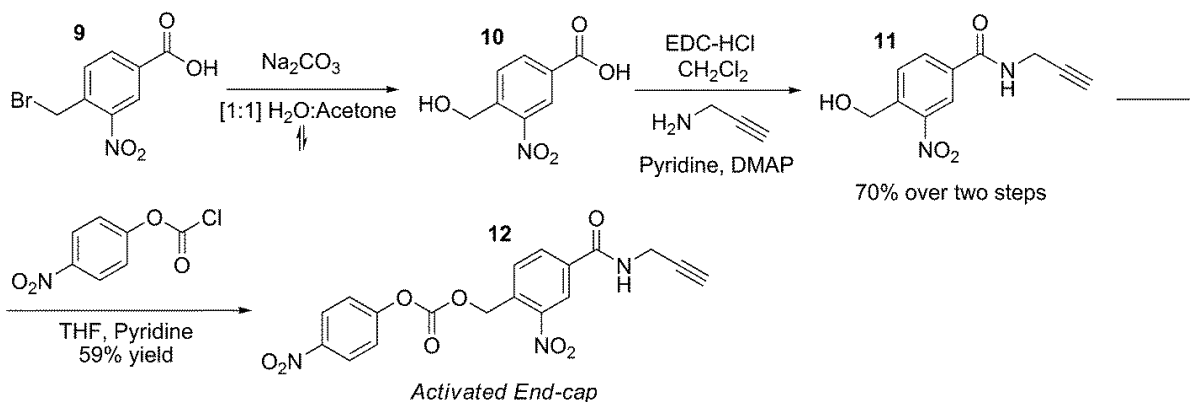
Scheme 25: The synthesis of the photo-responsive end-cap, activated with a carbonate group.

2.2   Polymer Syntheses and Characterization

With both the monomer and end-cap synthesized, polymerizations were subsequently performed. With the aim of preparing a set of co-polymers whose hydrophobic block ratios are varied, it was decided to synthesize one large and one small SIP. The Boc group on **8** was deprotected using standard TFA conditions to form **13**, which was subsequently polymerized under two separate conditions. To form the short polymer, 5 mol % of the end cap **12** was added with the monomer at the beginning of the polymerization so that any growing chains would be capped early on in the reaction. This would limit the number of possible growing chains. To form the long polymer, the polymerization was conducted under the same conditions, however the end-cap wasn't introduced to the reaction flask until after the polymerization had run for 5 hours. The latter polymerization conditions ensured that the polymer chains had significant time to grow to a large length, followed by the final end-capping later on (**Scheme 26**). The polymers were dialyzed using a 6-8kg MWCO membrane in DMF to remove smaller molecules and oligomers from the polymer sample. This afforded two distinct polymers, a small one with an M_n of ~2,500 g/mol (**S**) and the other with an M_n = ~8,500 g/mol (**L**) by DMF SEC relative to PMMA.
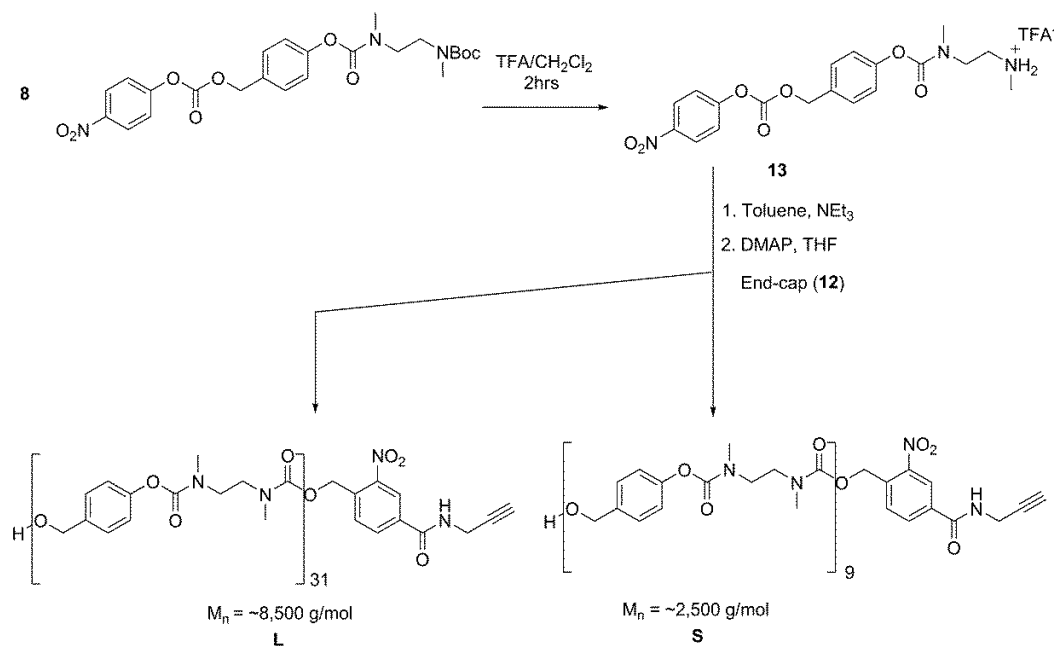
Scheme 26: Synthesis of large and small polymer chains.

In poly-condensation reactions involving monomers like the one used above, complete end-capping is typically difficult to achieve. Therefore it was important to ensure the polymer was mostly end-capped so their depolymerization is truly stimuli-responsve. The ^{1}H-NMR spectra revealed sharp end-cap peaks together with the broad polymer peaks, which integrated relatively higher. The integration ratio concerning the end-cap alkynyl proton, and that of the benzyl methylene protons (present in the backbone) were calculated, and produced a rough approximation of the M_n. A spectrum of the short (**S**) polymer is shown below to exhibit the important peaks involved (**Figure 1**):
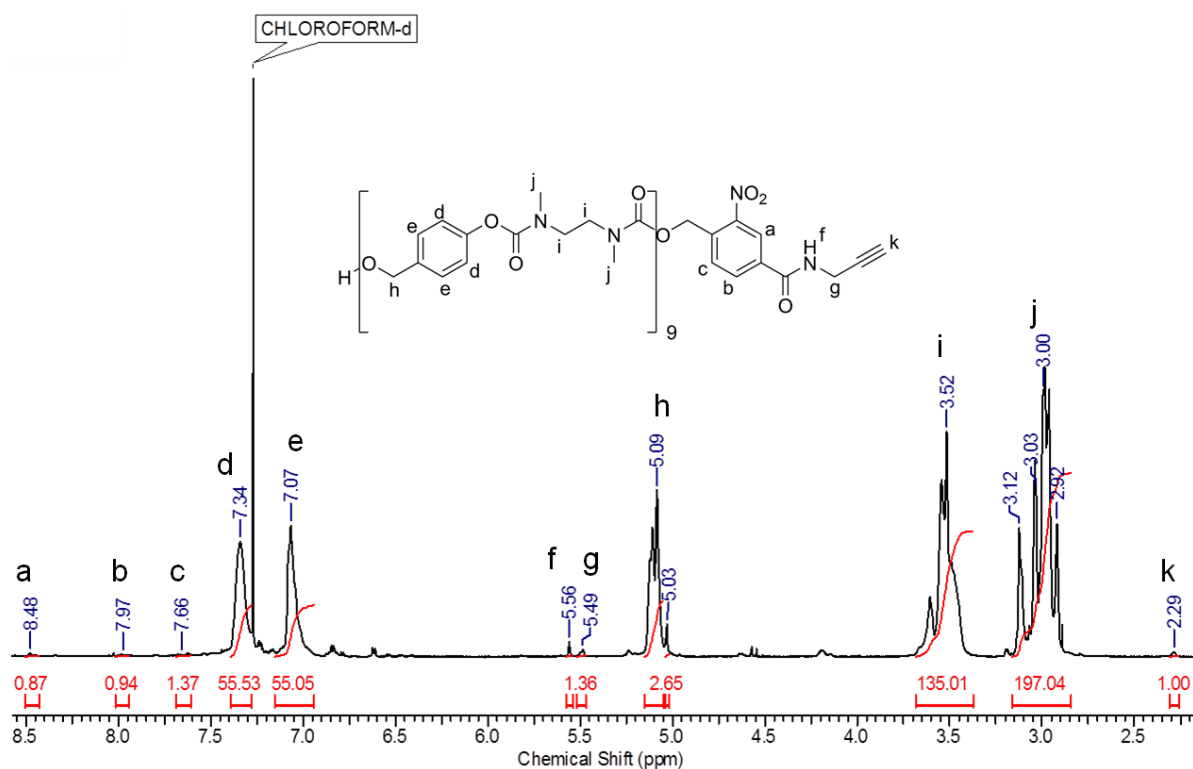
Figure 1: The Large (**S**) SIP with a broad benzyl peak around 5.1ppm and the alkynyl peak around 2.3ppm

M_ns gathered from the SEC analysis could be compared to the M_ns determined from the NMR spectra. Ideally, the polymer length and end-capping determined by NMR spectra and the SEC traces would coincide. Both the SEC and ^{1}H-NMR data is summarized in **Table 1**:

Organic SIP	SEC M_n	Dispersity ($Đ$)	^{1}H-NMR M_n
Small Polymer (**S**)	~ 2,500 g/mol	1.6	~ 8,000 g/mol
Large Polymer (**L**)	~ 8,500 g/mol	1.7	~15,000 g/mol

Table 1: Comparing the M_n retrieved from SEC and ^{1}H-NMR analysis. The ^{1}H-NMR M_ns are calculated by determining the repeat units (n) from the ratio of the alkynyl proton to the polymeric benzyl protons.

The SEC M_ns are significantly smaller than those calculated from the NMR spectra. Initially, it is easiest to explain this data by suggesting that there are un-end-capped polymers. But, it must be noted that the M_ns calculated from the NMR spectra are approximate, and bring with them significant error. When the peaks integrate very low in the case of the end-cap peaks, error can lead to misrepresentative ratios in the number of repeat units. Additionally, when measuring the molecular weights of these polymers relative to polystyrene standards, the ^{1}H-NMR and SEC results are much closer.

With the organic (hydrophobic block) now prepared, amphiphilic co-polymers were the next goal. Polymer termini, relative to small molecules, are difficult to access for a reaction due to the random coil nature of the linear polymer. With this in mind, the copper-mediated azide-alkyne cycloaddition click reaction (CuAAC) was chosen to link them, because it is high yielding, robust, and fast. Polyethylene glycol monomethyl ether (PEG) is a hydrophilic polymer consisting of ether linkages throughout the chain, and was chosen as the hydrophilic block because it is a cheap, commercially available polymer with a dispersity ($Đ$) below 1.10. Two sizes of PEG were chosen: 750 g/mol (**750**) and 2,000 g/mol (**2,000**). The hydroxyl group on these polymers was transformed into the mesylate, followed by S_N2 conditions to attach an azide group to form two differently sized azide-terminated polyethylene glycol hydrophilic blocks (PEG-N$_3$) (**Scheme 27**).
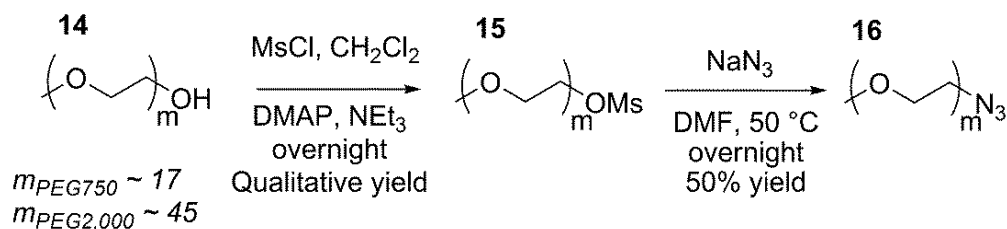
Scheme 27: The synthetic route used to produce both 750 and 2,000 g/mol PEG-azides.

The small (**S**) and large (**L**) hydrophobic polymers were each clicked under copper-mediated conditions to 750 and 2,000 PEG-N$_3$ respectively. The polymers were dialyzed using a 6-8kg MWCO membrane in DMF to remove free PEG species, followed by water as the dialysate to precipitate the copolymer. Centrifugation in water was used to remove residual PEG. Four co-polymer amphiphiles were produced: short organic block coupled to 750 g/mol PEG (**S-750**), short organic block coupled to 2,000 g/mol PEG (**S-2,000**), long organic block coupled to 750 PEG (**L-750**), and long organic block coupled to 2,000 g/mol PEG (**L-2,000**). These reactions are organized in **Scheme 28**:
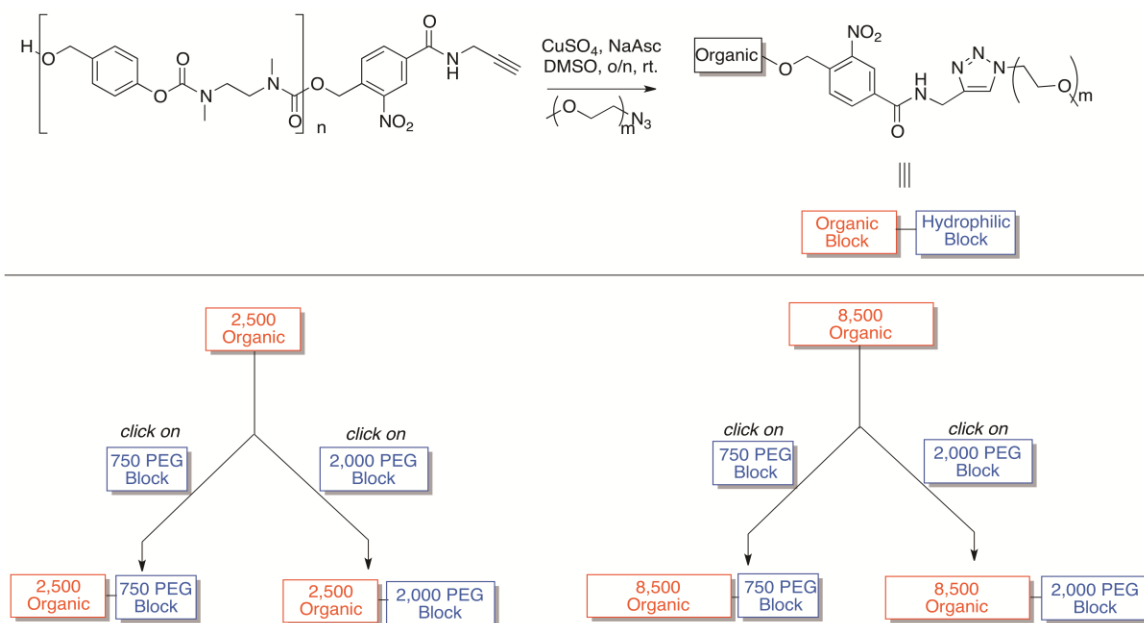
Scheme 28: Amphiphilic block co-polymers, from left to right: **S-750, S-2,000, L-750, and L-2,000.**

^{1}H-NMR spectroscopy and SEC analysis were used to characterize the block copolymers. In the NMR spectra, the initial organic block contained a proton peak

located at approximately at 2.29 ppm, corresponding to the terminal alkyne proton attached to the end-cap. The integration of this alkyne proton depended on the length of the polymer attached, and was shown to integrate to less than the larger polymer relative to the small polymer. However, after coupling what used to be an alkynyl proton was subsequently attached to a triazole ring, whose δ would shift significantly downfield, and thus no longer exist at 2.29ppm in the spectra. This kind of analysis is represented using just one of the amphiphiles (**Figure 2**).
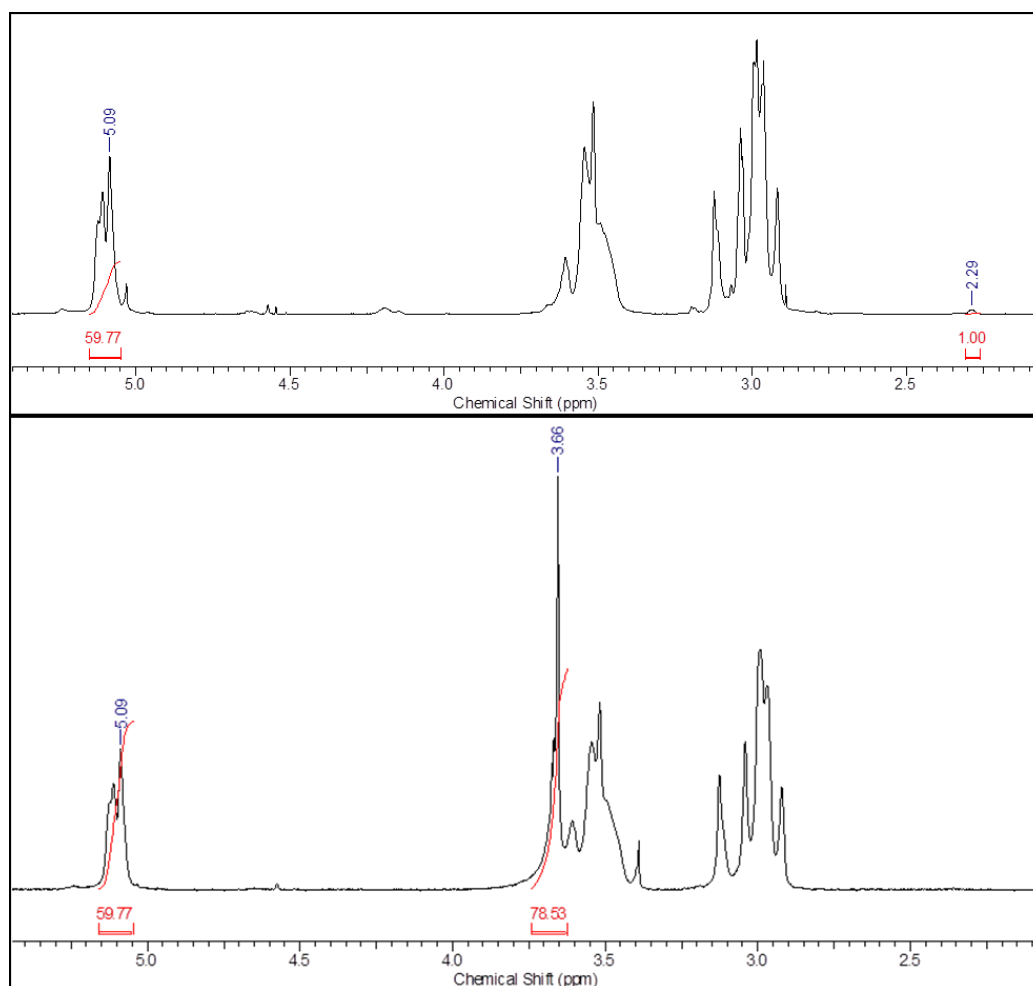
Figure 2: Top: small polymer **S** showing its alkynyl proton peak, Bottom: **S-750** co-polymer without an alkynyl peak and the additional broad PEG methylene peak.

After coupling the hydrophilic PEG to the organic block, each co-polymer shows no sign of a peak around 2.29 ppm in the ^{1}H-NMRs confirming the completion of the click reactions in all four cases. The methylene groups within the PEG polymer appear in

the ^{1}H-NMR spectra around 3.7 ppm as a broad singlet following the coupling reaction. The relative integration between the organic SIP peaks and the PEG peaks approximately correspond to the expected ratio (**Table 2**).

Copolymer	Expected PEG proton/Organic SIP proton Ratio	Observed PEG proton/Organic SIP proton Ratio
S-750	3.8	2.5
S-2,000	10	15
L-750	1.1	0.70
L-2,000	3.0	5.0

Table 2: The relative integrations between the PEG block and the polycarbamate block. These were calculated by comparing the methylene PEG protons and benzyl protons on the organic SIP.

SEC analysis was used to determine the change in molecular weight (M_n) after the hydrophilic PEG blocks were coupled relative the initial organic blocks. Free PEG-N$_3$ 2,000 has a SEC peak at approximately 15.5 minutes, but PEG-N$_3$ 750's SEC peak is within the solvent peaks after 18 minutes and cannot be used to confirm the lack of free PEG. The co-polymers' M_ns should theoretically increase after the coupling reactions, but only one of the four samples (**S-2,000**) showed appreciable increase in M_n in the SEC trace (**Figure 3a-d**).
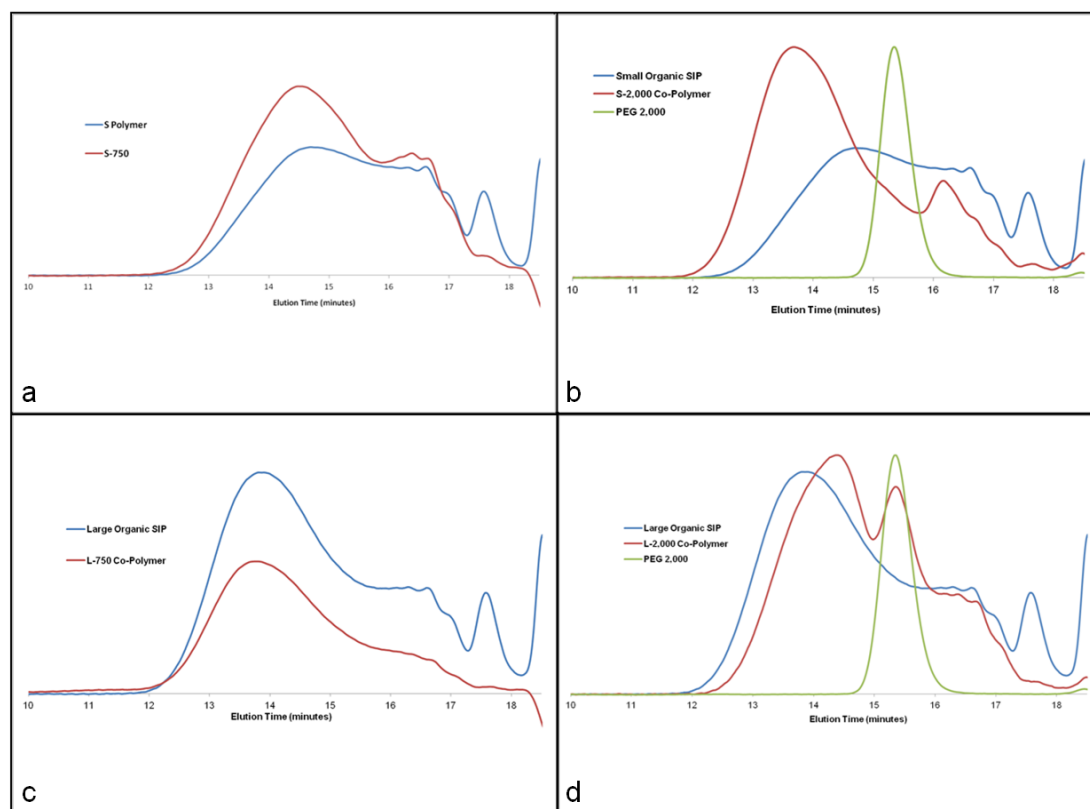
Figure 3: SEC traces before (blue) and after coupling reactions (red), and PEG 2,000 in green. a) **S-750**, b) **S-2,000**, c) **L-750**, d) **L-2,000.** PEG 750 shows up in the solvent peak after 18 minutes.

This result can be attributed to the relative increase in molecular weight of the initial organic block. **S-2,000** undergoes the greatest percent increase in the theoretical molecular weight, an 80% increase from ~2,500 g/mol to 4,500 g/mol. The other three co-polymers underwent relatively smaller changes in molecular weight (<30%) which may not be easily detected using SEC analysis.

2.3   Synthesis of a Control Copolymer

The synthesis of an unresponsive control copolymer was begun to support future degradation studies necessitating a copolymer that does not depolymerize following UV irradiation. This control copolymer shared the same polymer backbones as the hydrophobic and hydrophilic blocks of the four copolymers above, but contained a non-cleavable end-cap. The end-cap used for this control polymer was a glycine-derived

moiety that does not cleave following irradiation. This unresponsive end-cap's synthesis begins with an esterification of glycine affording propargyl ester **17.** The propargyl ester **17** was subsequently coupled to phenol **2** using triphosgene, yielding **18** in an 80% yield. The TBS group was removed under acidic conditions to yield alcohol **19**, followed by its activation using 4-nitrophenyl chloroformate affording the unresponsive control end-cap **20** in a 79% yield over two steps (**Scheme 29**).
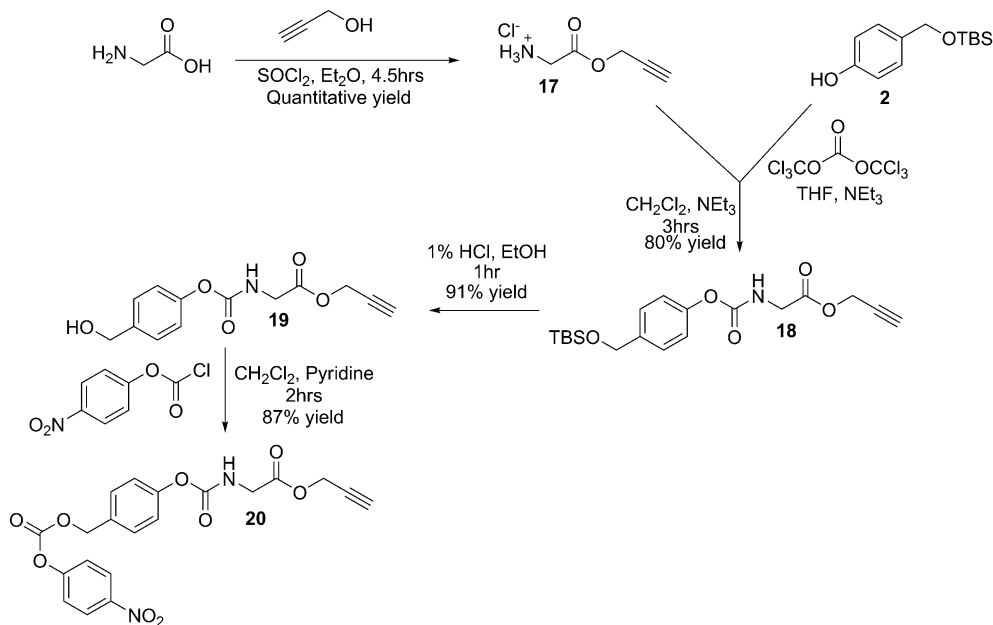
Scheme 29: The synthesis of the unresponsive end-cap for the control polymer.

The end-cap **13** was polymerized with the deprotected activated monomer **20** under basic conditions to afford control polymer **C** having an M_n = 6,500 g/mol and a $Đ$ = 1.5 by DMF SEC. The end-cap was confirmed to be attached to the polymer by finding the terminal alkyne proton in the ^{1}H-NMR appearing at 2.53 ppm This organic polymer was subsequently coupled to PEG-N$_3$ 750 to yield the control copolymer **C-750** (**Scheme 30**).
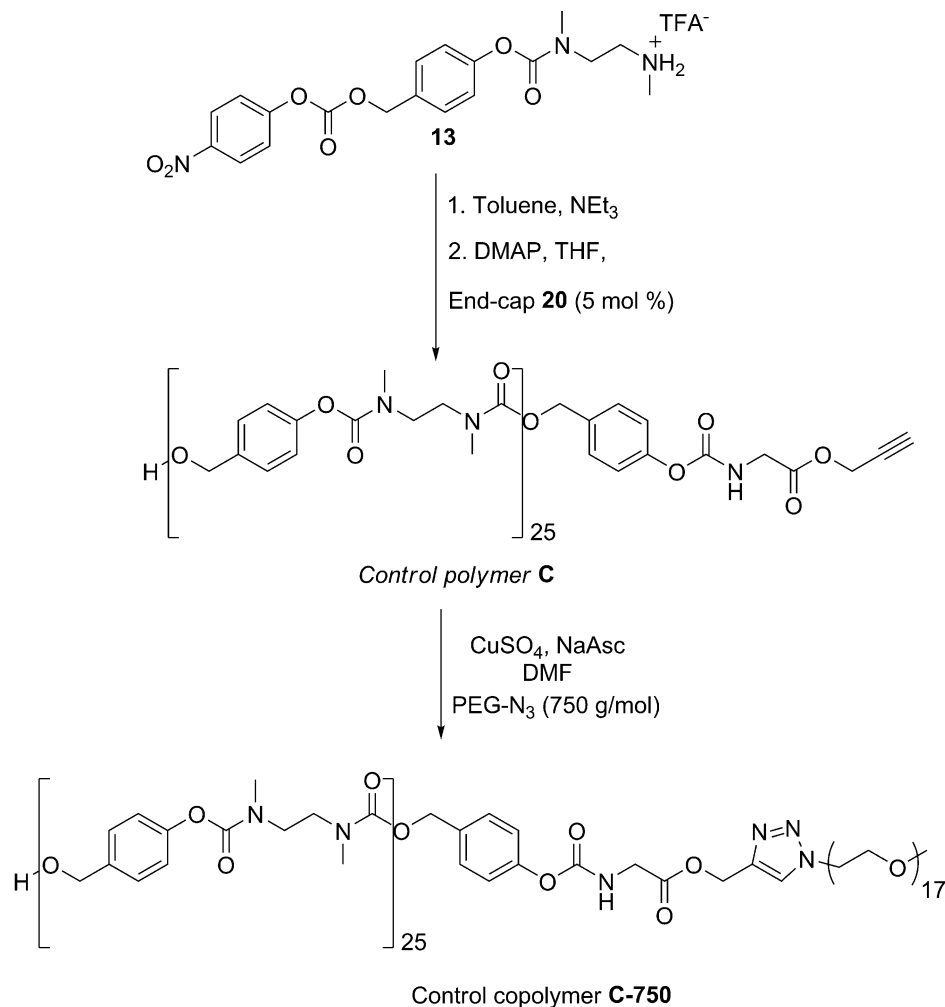
Scheme 30: The polymerization of control polymer **C** incorporating unresponsive end-cap **20**, followed by its coupling to PEG-N$_3$ 750 to form the control copolymer **C-750**.

2.4 Self-Assembly in Aqueous Media

The PEG block of each co-polymer is soluble in aqueous media, and the covalently bonded poly(carbamate) block is not. This imparts amphiphilic characteristics to the resulting co-polymers whose properties were probed using aqueous self-assembly. The aqueous medium was a 100mM phosphate-buffered solution with pH 7.4, chosen to resemble biological conditions. Nano-precipitation of these co-polymers was performed by dissolving each co-polymer in 0.1mL of THF and combining this organic solution it with 0.9mL of the above described buffered water. This was achieved in one of two ways: the THF solution was quickly added to the aqueous solution (denoted "fast"), or

the aqueous solution was slowly added to the THF solution (denoted "slow"). Ultimately, one method was chosen for each co-polymer, and this was determined by the quality of particles formed by the chosen method, ie monodispersity of particles and a lack of aggregates. To give a sense of the optimization performed to determine which method produced the most desirable particles, the first four TEM images shown below (**Figure 4**) represent the undesirable characteristics.
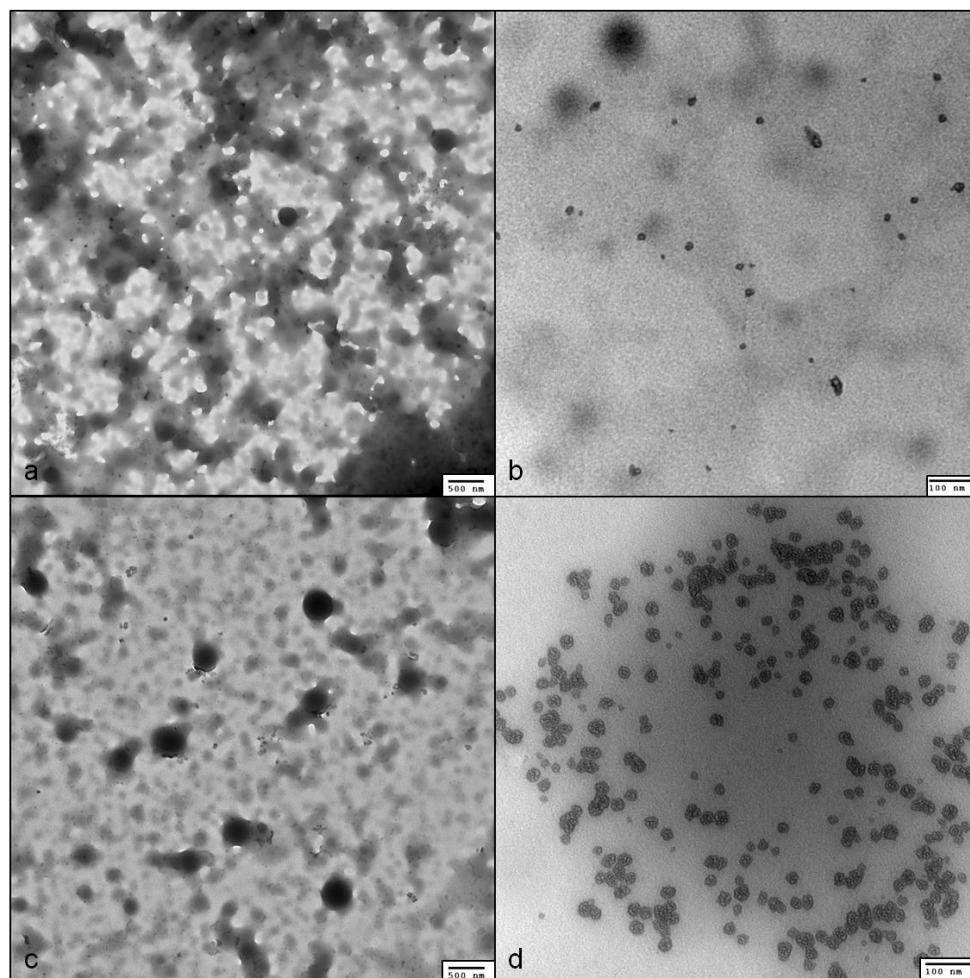
Figure 4: Undesirable self-assembled nanoparticles. a) **S-750** (slow), b) **S-2,000** (fast),c) **L-750** (slow), d) **L-2,000** (slow).

These undesirable characteristics include aggregation and "washiness" (**Figure 4a and 4c**) and inconsistent nanoparticular morphologies throughout the TEM grid (**Figure 4b and 4d**). For these reasons, these particular nano-precipitation techniques were discarded for these co-polymers.

Ultimately however, the most consistent and desirable nanoparticles were formed by fast addition of organic solvent to an aqueous solution for **S-750**, **L-750**, and **L-2,000**, and slow addition for **S-2,000**. After removal of organic solvent via dialysis, these particles were characterized using both dynamic light scattering (DLS) and transmission electron microscopy (TEM). The DLS self-assembly data is summarized in **Table 3**:

Copolymer	DLS Z-Ave.	Nanoparticle Morphology
S-750	179 nm	Vesicles
S-2,000	75 nm	Micelles
L-750	130 nm	Inverted Micelles
L-2,000	66 nm	Micelles

Table 3: **Self-Assembly Data.**

An array of nanoparticles was formed, forming micellar aggregates, micelles, and vesicular assemblies. The DLS data is comparable to the approximate size of the assemblies seen in the TEM images. The TEM images showing these morphologies is summarized in **Figure 5** (below).

Figure 5: Self-assembled nanoparticles. a) **S-750** (fast), b) **S-2,000** (slow), c) **L-750** (fast), d) **L-2,000** (slow).

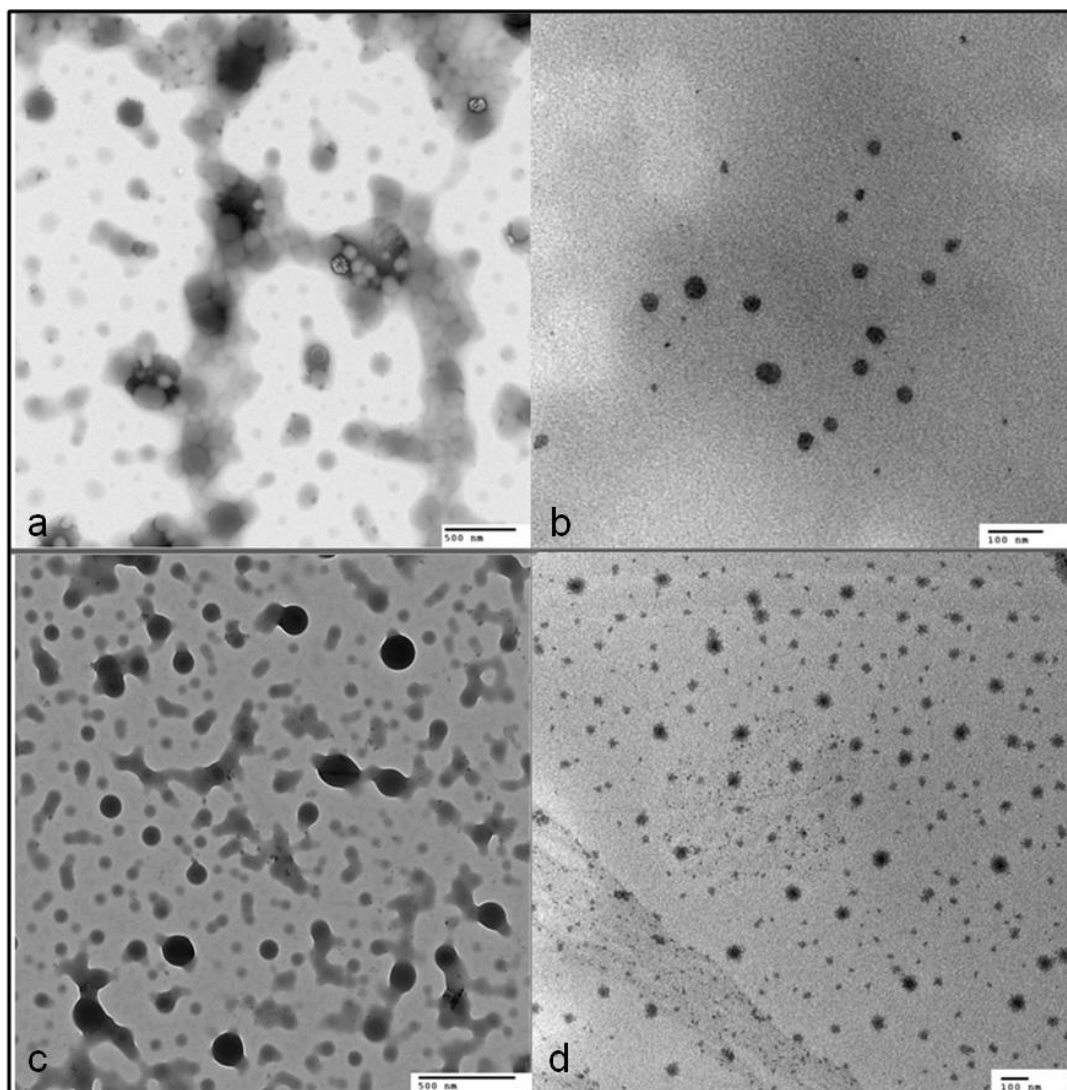**Figure 5** show images that are representative of the nanoparticles plated throughout the grids on the TEM plate. It is clear that the relative lengths of hydrophilic/hydrophobic blocks in each co-polymer has a strong effect on the characteristics of the assembled nanoparticle. It has been previously shown that the $f_{hydrophilic}$ of amphiphilic block co-polymers has a direct effect on the size and morphology of the nanoparticles formed in aqueous solution. A general guideline predicting what any given amphiphile would form in aqueous solution is as follows: hydrophilic volume fraction ($f_{hydrophilic}$) of 25% of below form inverted microstructures,

$f_{hydrophilic}$ of $35 \pm 10\%$ form vesicles (polymersomes), and $f_{hydrophilic}$ of 45% and above form spherical micelles. The hydrophilic weight ratio (the weight of the hydrophilic block divided by the weight of the copolymer) is a good approximation of the hydrophilic volume ratio. These are rough guidelines because of the various other factors that can contribute to which morphology a nanoparticle may take, namely the hydrophobicity of the organic block and the hydrophilicity of the aqueous block. Other factors include the random coil nature of the respective blocks, controlling the rigidity of the block when assembled as a nanoparticle. The guideline works well if the respective blocks remain constant, but in this work, the organic block is a polymer that has not been incorporated into block co-polymers.

Sample Name	Calculated approximate $f_{hydrophilic}$	Expected Morphology	Observed Morphology
S-750	23%	Vesicles/inverted micelles	Vesicular assemblies
S-2,000	44%	Micelles	Micelles
L-750	9%	Inverted micelles	Inverted micelles
L-2,000	20%	Inverted micelles	Micellar aggregates

Table 4: Hydrophilic weight ratios and morphologies of amphiphiles.

The morphologies follow the guidelines of $f_{hydrophilic}$ ratios to some degree, but as expected, do not perfectly follow these established guidelines. The **S-750**, **S-2,000, and L-750** co-polymers follow the guideline more closely, forming vesicles and micelles, respectively. On the other hand **L-2,000** is predicted to be forming inverted micellar structures, but is observed to form micellar aggregates based on the TEM images. The factors leading to the lack of consistency between observed and theoretical morphologies are: how hydrophobic/hydrophilic each block is, and the rigidity of each block. In the assemblies above, the observed morphologies would result from having a $f_{hydrophilic}$ ratio of about 15% higher than the calculated $f_{hydrophilic}$ ratios of these co-polymers. Thus, the organic block is acting less hydrophobic than expected. This can be attributed to the repeat unit containing a polar carbamate group, giving the polymer chain a more polar nature, thus reducing its hydrophobicity. Ultimately, four amphiphilic block self-

immolative copolymers were successfully synthesized and self-assembled to form morphologies very closely to the rough guidelines previously reported.

2.5   Degradation and Release Studies

Due to the self-immolative nature of the organic block, the responsiveness of the co-polymer assemblies can be characterized.The aqueous portion of the nano-precipitation procedure was a pH=7.4 100mM phosphate buffer solution to mimic biological conditions. Upon end-cap triggering with UV light, the PEG chains were expected to be cleaved from the depolymerizing SIP, causing destabilization of the nanoparticles. Therefore the kind of nanoparticles couls be measured over time as the depolymerization progresses. Additionally, these assemblies could be loaded with a fluorescent cargo and following nanoparticle breakdown, will be released into solution. Nile red is a suitable cargo because it is fluorescent when surrounded in a hydrophobic environment (ie, in the interior of a micelle, or bi-layer of vesicle), but photo-chemically quenched when in an aqueous environment[73].
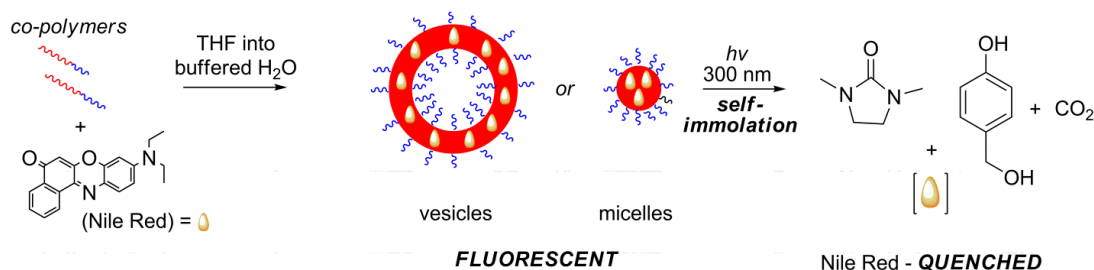
Scheme 31: A representation of the Nile Red release study monitored by fluorescence. Two studies were designed to monitor the degradation of these assemblies: the first using DLS and TEM to measure the size and light-scattering characteristics of the assemblies over time, and the second using fluorescence spectroscopy to measure the release of Nile red over time. Only two of the four co-polymers synthesized will be used in the degradation study: **L-750** and **L-2,000**.

The Nile red release study was conducted using the same nano-precipitation method implemented for the self-assembly characterization. Additionally, Nile red is pre-dissolved in the THF co-polymer solution at 2 wt% (relative to the co-polymer). An

additional dialysis in buffered water ensures that the assemblies are in a fully buffered aqueous medium. In addition to **L-750** and **L-2,000**, a control co-polymer was incorporated into this release study. This control polymer is identical to **L-2,000** except that it did not have a UV-triggerable moiety. Prior to the application of UV light, a fluorescence spectrum of the Nile red-loaded nanoparticles was taken to standardize the count rate of the three samples, corresponding to their initial fluorescence (100%). After the application of 20 minutes of UV light, subsequent fluorescence spectra were routinely measured over the period of approximately 7 days. The data is presented in **Graph 6**:
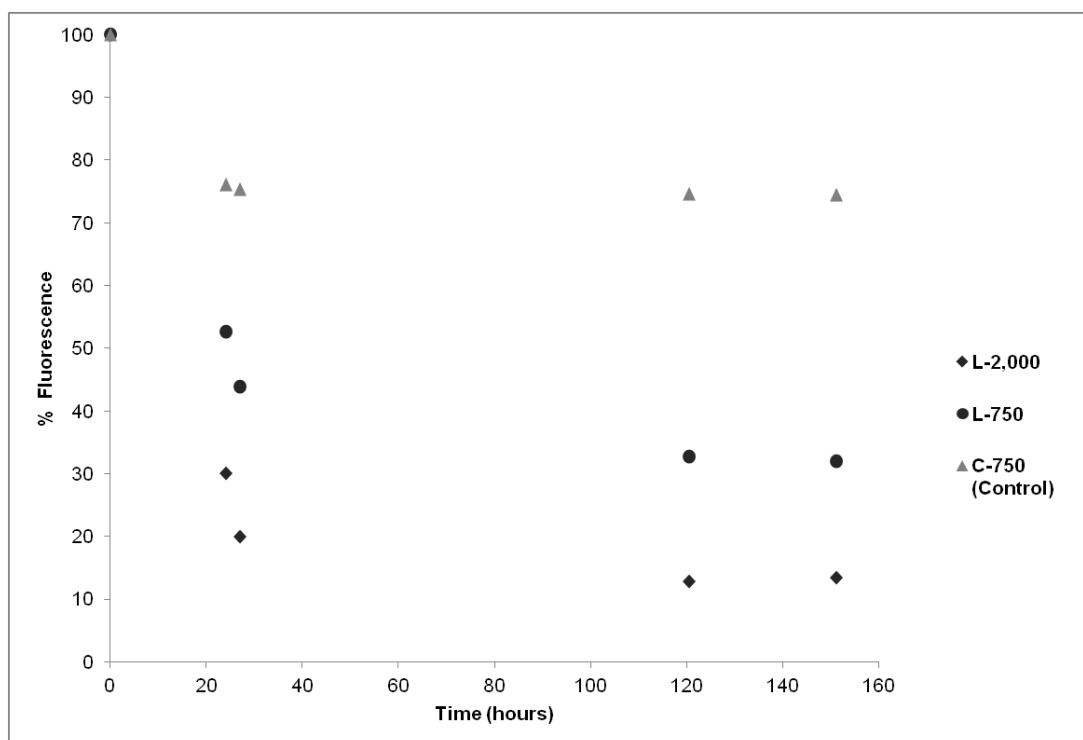
Figure 6: Nile red release over time.

The decrease in fluorescence is directly proportional to the release of Nile red into the aqueous medium surrounding the nanoparticles. Nile red is a hydrophobic dye, and is thus photo-chemically quenched in water, and does not fluoresce. Upon UV irradiation, the triggerable nanoparticles burst-release their cargo; at least half of the Nile red is released in 20 hours, followed by a plateau. The control polymer (using control copolymer **C-750** discussed previously) does release some of its cargo, and this can be attributed to Nile red diffusing out of the control nanoparticles. This seems to plateau around 80%, whereas the **L-750** and **L-2,000** plateau at 30% and 10% , respectively.

Although diffusion accounts for a small amount decrease in fluorescence, the majority of this release must be attributed to the self-immolation of the stimuli-responsive co-polymers, triggered by UV-light.

In the second degradation study, the morphologies are formed using the same nano-precipitation procedure that was employed to characterize the self-assembly behaviour described earlier. DLS measurement are taken of both samples, and subsequently applied with 20 minutes of UV light in a quartz cuvette to ensure all UV light reaches the assemblies in solution. From here, DLS measurements are taken routinely to monitor any changes in count rate. The count rate measures the degree to which the photons are scattered in the sample. Count rate is a value that depends on both the number of particles in the solution, and their size. As the number of particles increases, the more photons are scattered; as the size of any given particle increases, the more likely it is to scatter light. **Figure 7** summarizes the data retrieved in this study :
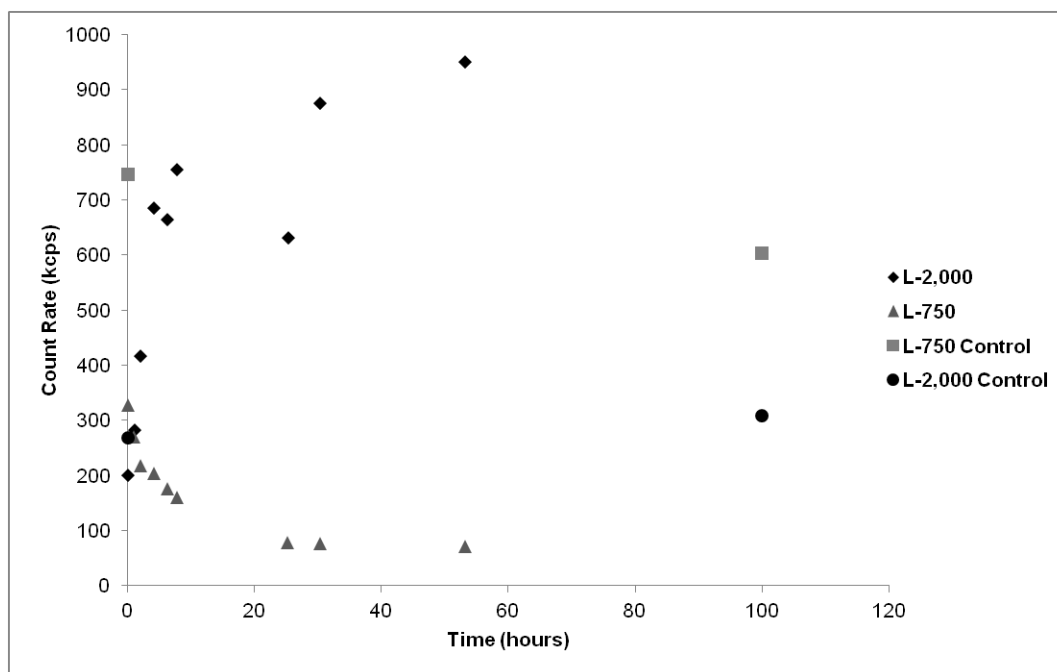
Figure 7: Degradation of nanoparticles. DLS count rate upon UV triggering with the control polymers included. The two co-polymers used were not applied with UV light, and their DLS behaviour was measured over the period of 100 hours.

Both co-polymers have significant changes in their count rate. Unexpectedly, the assemblies **L-2,000** exhibited a ~5-fold increase in count rate from 200 to 950 kcps, and the **L-750** has ~4-fold decrease from 328 to 71 kcps. This data seems counter-intuitive because they are nanoparticles that ultimately destabilize into very similar products. This may be due to how readily each nanoparticle sample is transformed into aggregates. **L-750** produces solid particles whereas **L-2,000** are collections of micelles (micellar aggregates), and it seems that the latter more readily formed aggregates upon depolymerization, explaining the increase in count rate. Additionally, a control study was completed to determine the degree to which the UV-light trigger is responsive for the change in light-scattering. To do this, the nanoparticles were formed as normal, but no UV light was applied to the samples. The count rate was measured over a period of four days did not change significantly (<20%): **L-750** went from 747 to 603 kcps, and **L-2,000** went from 269 to 309 kcps (**Figure 7**).This shows that the application of UV light is essential to the marked changes observed in the degradation study where the nanoparticles were irradiated with UV light. To confirm the disappearance of the parent nanoparticles after depolymerization, TEM images were taken of the degraded self-assemblies used in this study (**Figure 9**).
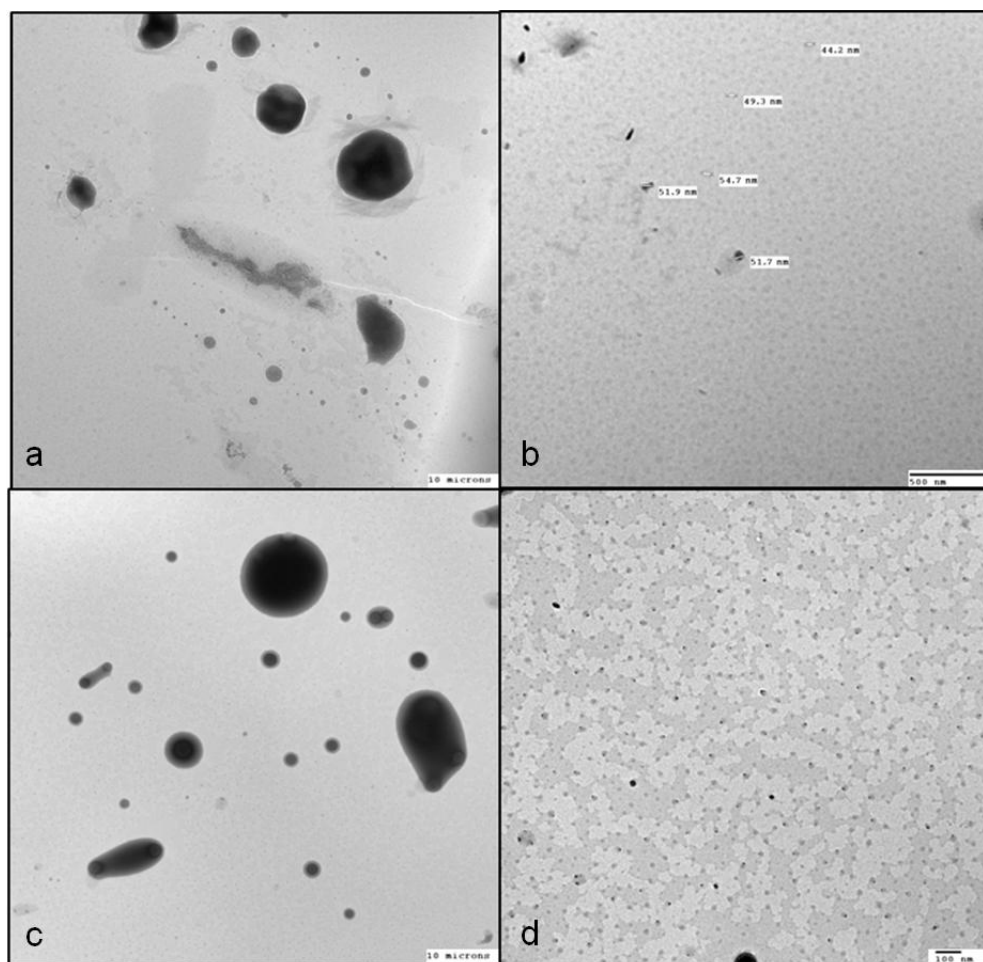
Figure 8: Post-degradation TEM images of the assemblies. a) and b) are **L-2,000**, c) and d) are **L-750**.

The images of both **L-750** and **L-2,000** consisted of a uniform background with small aggregates, interrupted with relatively massive aggregates (~ 5μm). Nothing of the original micellar assemblies remained after depolymerization.

2.6   Incorporation of PDMAEMA as a Hydrophilic Block

So far this research has been limited to the use of the hydrophilic block PEG for the amphiphiles, justified by its commercial availability and low dispersity. Even with these convenient characteristics, there are other reported hydrophilic polymers which have more interesting properties, namely multi-responsiveness. Poly(2-dimethylaminoethyl methacrylate) (PDMAEMA) has been gaining interest in many fields

recently, due to its thermal and pH sensitivities. The pendant tertiary amine groups on each repeat unit can be protonated and positively charged or neutral, giving the polymer the ability to have varying degrees of protonation and therefore charge. Additionally, PDMAEMA has been shown to have unique thermo-responsiveness; as the temperature is increased from 30 to 50 °C, the polymer chains undergoes a "chain collapse" phenomenon whereby its hydrodynamic volume significantly decreases. This polymer could be incorporated onto the SIPs prepared above and would theoretically give the resulting amphiphiles responsiveness to light, pH, and temperature all of which could be varied to control the morphology in the resulting nanoparticles.

Reversible addition-fragmentation chain transfer (RAFT) was the method employed to polymerize the 2-(dimethylamino)ethyl methacrylate into PDMAEMA using an initiator with a pendant azide attached. 3-bromo-propanol was combined with sodium azide under S_N2 conditions to afford 3-azido -propanol (**21**) in a 77% yield. This azido-alcohol was coupled to acid **22** under EDC conditions to afford the RAFT initiator **23**. 2-(dimethylamino)ethyl methacrylate and initiator **23** were polymerized under typical RAFT conditions using AIBN to produce PDMAEMA **24** with an M_n = 3,500 g/mol and $Đ$ = 1.35 by DMF SEC. Additionally, an IR spectrum of this polymer was taken and the peak located at approximately 2,100 cm^{-1} confirmed the presence of the azide functionality at the terminus. The presence of an azide at its terminus is critical so that PDMAEMA can be successfully clicked onto the alkyne-terminated organic block of the polycarbamate SIP to form a di-block amphiphile. Under the same conditions employed to couple PEG-azide blocks to the organic block mentioned previously, it was observed that PDMAEMA did not undergo coupling at all. The ^{1}H-NMR spectrum was identical to the initial organic block, suggesting that after purification using dialysis the uncoupled PDMAEMA polymer was dialyzed out. Due to the numerous pendant amines along the PDMAEMA chain, the copper employed in the traditional azide-alkyne click reaction may be ligated throughout the length of this hydrophilic block. This would significantly hinder copper's ability to mediate the cycloaddition reaction necessary to covalently link the azide with the alkyne, and may be a significant factor concerning the failure of this reaction.
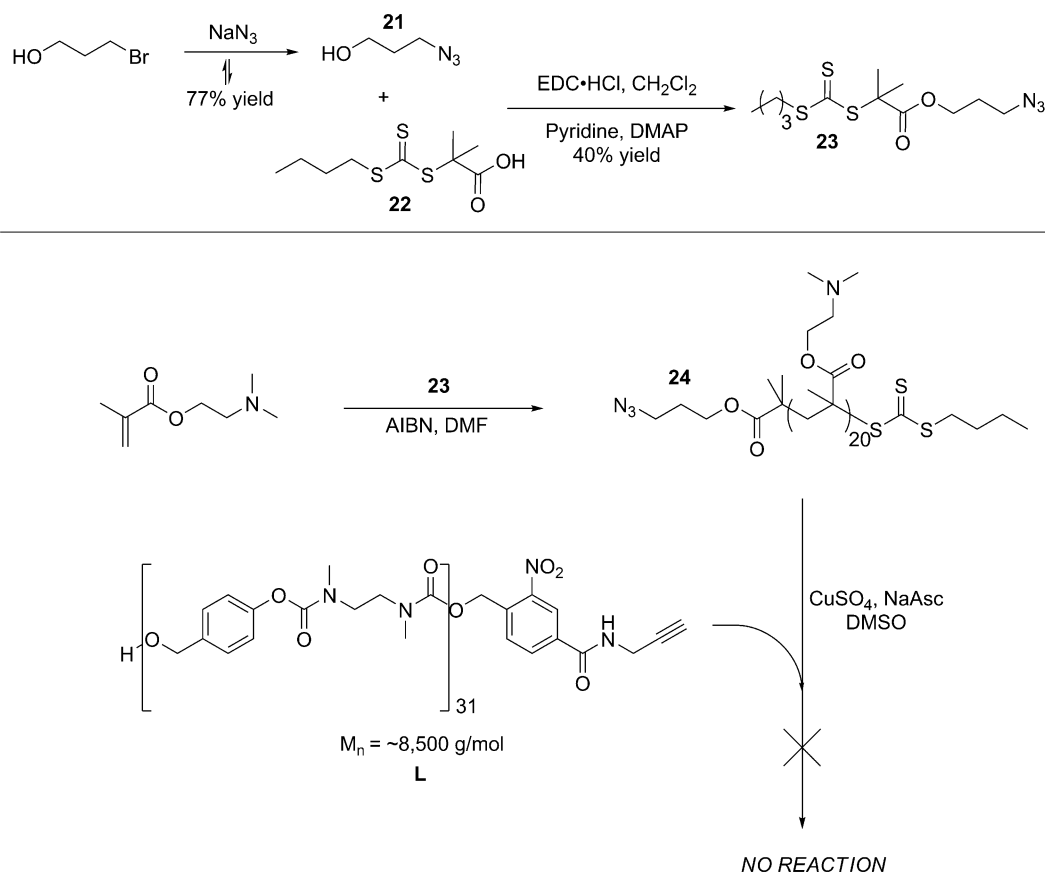
Scheme 32: The synthesis of the RAFT initiator (top) and the synthesis of PDMAEMA, and its unsuccessful coupling to the long (**L**) organic SIP (bottom).

2.7   Conclusions and Future Work

In conclusion, the copper-mediated azide-alkyne click reaction was demonstrated to be an effective method to covalently link two polymers with the aim of carefully producing block copolymers with the desired hydrophilic volume ratio. Additionally, the self-assembly nature of the block copolymers was shown to adhere closely with the previously reported guidelines to form morphologies such as compound micelles, vesicles, and micellar aggregates. The self-immolative nature of this system was studied by irradiating a set of nanoparticles with UV light and monitoring their degradation using techniques including DLS and TEM. Depolymerization was shown to vastly change the morphological and properties of these nanoparticles. The nanoparticles were also shown

to have the ability to be loaded with the hydrophobic fluorescent cargo Nile red, which upon UV irradiation was released slowly at physiological pH. The release of Nile red was monitored using fluorimetry, demonstrating the system's drug-delivery potential

In the future, an additional release study will be performed on the vesicle nanoparticles by loading their interior with a hydrophilic cargo (such as fluorescein) to confirm their vesicular properties and the versatility of this system. PDMAEMA was not successfully coupled to the photo-responsive organic block, but efforts to this end are ongoing. Following successful coupling of these two blocks into a copolymer, its self-assembly properties will be probed while varying conditions including pH, light, and temperature to demonstrate the multi-responsive nature of a copolymeric system composed of PDMAEMA coupled to a photo-responsive SIP.

3 Experimental

General

All reagents were purchased from commercial suppliers and were used without further purification. Triethylamine (Et$_3$N), pyridine, and dichloromethane were distilled from calcium hydride before use. Anhydrous tetrahydrofuran (THF) and N,N-dimethylformamide (DMF) were obtained from a solvent purification system using aluminum oxide columns. ^{1}H NMR spectra were obtained in CDCl$_3$ at 400 MHz or 600 MHz on Varian Inova instruments. NMR chemical shifts (δ) are reported in ppm and are calibrated against residual solvent signals of CDCl$_3$ (δ 7.27), (CD$_3$)$_2$SO (δ 2.50) or D$_2$O (δ 4.75). High resolution mass spectrometry(HRMS) was performed on either a Finnigan MAT 8400 or a PE-Sciex API 365 mass spectrometer using electron impact (EI) ionization. Size exclusion chromatography (SEC) was carried out at a flow rate of 1 mL/min in N,N-dimethylformamide (DMF) with 10 mM LiBr and 1% (v/v) NEt$_3$ at 85 °C using a Waters 2695 separations module equipped with a Waters 2414 differential refractometer and two PLgel 5 μm mixed-D (300 mm × 7.5 mm) columns from Polymer

Laboratories connected in series. SEC calibrations were performed using poly(methyl methacrylate) (PMMA) standards. Dialyses were performed using Spectra/Por® regenerated cellulose membranes with either a 6000-8000 g/mol or 50,000 g/mol molecular weight cutoff (MWCO). Products only characterized using ^{1}H-NMR spectroscopy are previously reported molecules.

Synthesis of 4-((tert-butyldimethylsilyloxy)methyl)phenol **2**

tert-Butyl chloride (6.66g, 44mmol, 1.1eq.) followed by imidazole (6.04g, 89mmol, 2.2eq.) were dissolved in 30mL of dry N,N-dimethylformamide (DMF) and stirred for 10 minutes. 4-hydroxybenzyl alcohol (5.00g, 40mmol, 1.0eq.) was added to this solution, and it was stirred overnight. The solvent was removed and the resulting residue was partitioned between an aqueous solution of 0.1M HCl (100mL) and 100mL of CH_2Cl_2, and the aqueous layer was extracted with three further additions of CH_2Cl_2 (3x30mL). The organic layers were combined and dried using $MgSO_4$, and this was filtered off to afford a crude residue. The crude residue was purified via column chromatography with an eluent 10/90 EtOAc/hexanes to yield a clear and colourless oil **2** in an 97% yield (9.34g). ^{1}H-NMR data (400 MHz, $CDCl_3$): δ 7.20-7.25 (m, 2H), 6.80-6.85 (m, 2H), 4.67 (s, 3H), 0.94 (s, 10H), 0.09 (s, 6H). ^{1}H-NMR matched with previously reported molecule[37].

Synthesis of tert-butyl methyl(2-(methylamino)ethyl)carbamate **5**

The diamine **4** (2.86g, 32mmol, 1.0eq) was dissolved in 12.5% by volume triethylamine in methanol (92mL) and cooled to 0 °C. Boc-anhydride (Boc₂O) (7.07g, 32mmol, 1.0eq) was dissolved in methanol (12mL) and added to the stirring diamine solution dropwise over 1 hour at 0 °C. The resulting solution was stirred at room

temperature overnight. The solvent was removed and the resulting residue was purified via column chromatography using a [10:3:87] [MeOH:Net$_3$:EtOAc] eluent to afford **5** in a 53% yield (3.27g). ^{1}H-NMR data (400 MHz, CDCl$_3$): δ 3.20-3.40 (m, 2H), 2.88 (s, 3H), 2.70-2.80 (m, 1H), 2.46 (s, 2H), 1.55-1.60 (m, 1H), 1.46 (s, 9H). ^{1}H-NMR matched with previously reported molecule[37].

Synthesis of **6**

Triphosgene (1.50g, 5.1 mmol, 0.33 eq.) was dissolved in freshly distilled CH$_2$Cl$_2$ (150mL), and in another flask, the TBS-phenol **2** (3.62g, 15mmol, 1.0eq) was dissolved in THF (50mL) and triethylamine (2.1mL, 15 mmol, 1 eq.) The solution of **2** was added dropwise into the triphosgene solution, and stirred for 15 minutes to form the appropriate chloroformate. In a separate flask, diamine **5** (2.86g, 15mmol, 1eq.) was dissolved in CH$_2$Cl$_2$ in addition to triethylamine (2.1mL, 15 mmol, 1.0 eq.). This solution was dropped into the solution of the TBS-chloroformate, and stirred for 3hrs at room temperature. The reaction mixture was partitioned between a sat. NH$_4$Cl solution and CH$_2$Cl$_2$ and the aqueous layer was extracted three times (3 x 30mL). The combined organic layers were washed once more with a small amount of sat. NH$_4$Cl, followed by the drying of the organic layers using MgSO$_4$. The drying agent was filtered off, and the solvent removed in vacuo. The crude residue was purified via column chromatography with an eluent 35/65 EtOAc/hexanes to yield a clear and colourless oil **6** in an 70% yield (4.01g). ^{1}H-NMR data (600 MHz, CDCl$_3$) δ 7.25-7.35 (m, 2H), δ 7.00-7.10 (m, 2H), δ 4.72 (s, 2H), δ 3.50-3.55 (m, 1H), δ 3.30-3.45 (m, 3H), δ 3.04-3.13 (m, 3H), δ 2.80-2.94 (m, 3H), δ 0.94 (s, 9H), δ 0.10 (s, 6H). ^{1}H-NMR matched with previously reported molecule[37].

Synthesis of **7**

37% HCl (0.40mL) was dissolved in EtOH (38mL) to form a 1% HCl in EtOH solution. Protected monomer **6** (5.46g, 12 mmol, 1.00 eq.) was added to this solution, and stirred at room temperature for 1hr. The reaction mixture was diluted with CH$_2$Cl$_2$, washed with a sat. NaHCO$_3$ solution, and extracted out of the aqueous layer three times with CH$_2$Cl$_2$ (3 x 10mL). The combined organic layers were dried using MgSO$_4$, the

drying agent was filtered off, and the solvent removed in vacuo. The crude residue was purified via column chromatography with an eluent of 70/30 EtOAc/hexanes to yield clear and colourless oil **7** in a 97% yield (4.08g). ^{1}H-NMR data (600 MHz, CDCl$_3$): δ 7.31-7.39 (m, 2H), 7.05-7.15 (m, 2H), 4.67 (s, 2H), 3.55-3.65 (m, 1H), 3.51-3.45 (m, 3H), 3.13 (s, 2H), 3.04 (s, 2H), 2.93 (s, 3H), 1.68-1.82 (m, 1H), 1.45 (s, 10H). ^{1}H-NMR matched with previously reported molecule[37].

Synthesis of **8**

The alcohol **7** (0.60g, 1.8 mmol, 1.0 eq) was dissolved in CH$_2$Cl$_2$ (6mL), followed by the addition of pyridine (0.45 mL, 5.5 mmol, 3.1 eq). Para-nitro chloroformate (0.72g, 3.6 mmol, 2.0 eq.) was dropped into this solution, which was stirred for 2hrs at room temperature. The reaction mixture was diluted with CH$_2$Cl$_2$ and washed with a 1 M HCl solution, then the aqueous phase was extracted three times with CH$_2$Cl$_2$ (3 x 20mL). The combined organic layers were dried using MgSO$_4$, the drying agent was filtered off, and the solvent removed in vacuo. The crude residue was purified via column chromatography with a gradient eluent of CH$_2$Cl$_2$ → 50/50 CH$_2$Cl$_2$/EtOAc to yield a slightly yellow viscous liquid in an 89% yield (0.79g). ^{1}H-NMR data (600 MHz, CDCl$_3$): δ 8.23 - 8.32 (m, 1H), 8.10 - 8.18 (m, 1H), 7.45 (d, J = 8.59 Hz, 1H), 7.39 (d, J = 8.98 Hz, 1H), 5.28 (s, 1H), 3.42 - 3.55 (m, 2H), 3.15 (s, 1H), 3.06 (s, 1H), 2.95 (s, 2H), 1.44 - 1.53 (m, 5H). ^{1}H-NMR matched with previously reported monomer[37].

Synthesis of 4-(hydroxymethyl)-3-nitrobenzoic acid **10**

Benzyl bromide 9 (1.50g, 5.8mmol, 1.0 eq.) was added to a solution of Na$_2$CO$_3$ (3.0g, 28mmol, 5eq.) in 60mL of 50/50 H2O:acetone. This solution was brought to reflux and stirred overnight. The solvents were evapourated and the resulting residue was acidified using aqueous1M HCl to a pH of 1. Ethyl acetate (100mL) was added and the aqueous layer was extracted with additional ethyl acetate (3x20mL). The combined organic layers were dried using MgSO$_4$, the drying agent was filtered off, and the solvent removed in vacuo to afford a crude **10** (1.14g). ^{1}H-NMR data (600 MHz, CDCl$_3$): δ 13.40-13.65 (m, 1H), 8.48 (s, 1H), 8.27 (s, 1H), 8.00 (s, 1H), 5.65-5.75 (m, 1H), 4.75-4.98 (m, 2H). ^{1}H-NMR matched with previously reported molecule[61].

Synthesis of 4-(hydroxymethyl)-3-nitro-N-(prop-2-ynyl)benzamide **11**

Crude **10** (1.14g, 5.8mmol, 1.0 eq.) and pyridine (4.0mL, 50mmol, 8.6 eq.) were dissolved in CH_2Cl_2 (20mL), followed by EDC•HCl (1.33g, 7.0mmol, 1.2eq.) and stirred for 15 minutes. Propargyl amine (2.22mL, 35mmol, 6.0eq.) and DMAP (0.85g, 7.0mmol, 1.2 eq.) were added and this solution stirred overnight at room temperature. This solution was diluted with ethyl acetate and washed with a saturated aqueous $NaHCO_3$ solution (30mL), followed by an aqueous 1M HCl solution (20mL), and distilled water. The organic fraction was collected and was dried using $MgSO_4$, the drying agent was filtered off, and the solvent removed in vacuo to afford pure residue **11**in a 72% yield (0.98g). ^{1}H-NMR data (600 MHz, $CDCl_3$): δ 8.45 (s, 1H), 8.07-8.11 (m, 1H), 7.90-7.95 (m, 1H), 7.45-7.65 (m, 1H), 4.96 (s, 2H), 4.12-4.17 (m, 2H), 3.45-3.80 (m, 1H) 2.46-2.50 (m, 1H). ^{1}H-NMR matched with previously reported molecule[61].

Synthesis of 2-nitro-4-(prop-2-ynylcarbamoyl)benzyl 4-nitrophenyl carbonate **12**

The alcohol **11** (0.74g, 3.2 mmol, 1.00 eq) was dissolved in THF (10mL), followed by the addition of pyridine (0.80 mL, 10 mmol, 3.10 eq). Para-nitro chloroformate (1.27 g, 6.3 mmol, 2.00 eq.) was dropped into this solution, which was stirred for 2hrs at room temperature. The reaction mixture was diluted with CH_2Cl_2 and washed with a 1 M HCl solution, then the aqueous phase was extracted three times with CH_2Cl_2 (3 x 30mL). The combined organic layers were dried using $MgSO_4$, the drying agent was filtered off, and the solvent removed in vacuo. The crude residue was purified via column chromatography with an eluent of 50/50 EtOAc:hexanes to yield a slightly yellow solid in an 59% yield (0.75g). ^{1}H-NMR data (600 MHz, $CDCl_3$): δ 8.52-8.57 (m, 1H), 7.84 (s, 1H), 7.52-7.56 (m, 2H), 7.46-7.50 (m, 1H), 7.07-7.12 (m, 1H), 6.82 (s, 2H), 4.93 (s, 2H), 2.35-2.40 (m, 1H), 1.70 (s, 2H). ^{13}C NMR data (DMSO -d_6, 100 MHz): δ 163.46, 155.11, 151.65, 146.94, 145.28, 134.65, 133.46, 132.76, 129.45, 125.45, 80.72, 73.30, 66.73, 28.74. MS calc'd for **12** 399.0703; found, 399.0815.

Synthesis of Small Polycarbamate (**S**)

The activated monomer **8** (1.28g, 2.5 mmol, 1.00 eq.) was dissolved in a 1:1 mixture of CH_2Cl_2/TFA (13 mL) and stirred at room temperature for 2hrs. The TFA and CH_2Cl_2 were removed by a stream of argon, followed by in vacuo conditions. The deprotected residue **13** was dissolved in toluene (13mL), followed by the end-cap **12** (50mg, 0.13mmol, 0.05eq.) dissolved in THF (2mL)**.** DMAP (68mg, 0.56 mmol, 0.22 eq.), and triethylamine (4.4mL, 31 mmol, 12.5 eq.) and stirred at room temperature for 24 hours. The reaction mixture was diluted in CH_2Cl_2 and washed with a solution of 1 M HCl (1 x 30mL), and twice with sat. Na_2CO_3 (2 x 50mL). The combined organic layers were dried using $MgSO_4$, the drying agent was filtered off, and the solvent removed in vacuo. The polymer was then dissolved in 3mL DMF, and dialyzed with a 6-8K membrane with DMF as the dialysate (2 x 200mL). The last solvent used in this dialysis is water, which precipitates the polymer. Water is removed in a lyophilizer to afford pure polymer **S** (200mg). ^{1}H-NMR data (600 MHz, $CDCl_3$): δ 7.30-7.40 (m, 55H), δ 7.02-7.10 (m, 55H), δ 5.05-5.15 (m, 60H), δ 3.39-3.68 (m, 135H), δ 2.88-3.15 (m, 197H), δ 2.29 (m, 1H). M_n = 2,500 g/mol, **Đ** = 1.6.

Synthesis of Large Polycarbamate (**L**)

The activated monomer **8** (1.28g, 2.5 mmol, 1.00 eq.) was dissolved in a 1:1 mixture of CH_2Cl_2/TFA (13 mL) and stirred at room temperature for 2hrs. The TFA and CH_2Cl_2 were removed by a stream of argon, followed by in vacuo conditions. The deprotected residue **13** was dissolved in toluene (13mL), followed by DMAP (68mg, 0.56 mmol, 0.22 eq.), and triethylamine (4.4mL, 31 mmol, 12.5 eq.) and stirred at room temperature for 5 hours. The end-cap **12** (50mg, 0.13mmol, 0.05eq.) was dissolved in minimal THF (1mL) and this solution was added to the polymerization vessel, and the resulting solution was stirred overnight. The reaction mixture was diluted in CH_2Cl_2 and washed with a solution of 1 M HCl (1 x 30mL), and twice with sat. Na_2CO_3 (2 x 50mL). The combined organic layers were dried using $MgSO_4$, the drying agent was filtered off, and the solvent removed in vacuo. The polymer was then dissolved in 3mL DMF, and dialyzed with a 6-8K membrane with DMF as the dialysate (2 x 200mL). The last solvent used in this dialysis is water, which precipitates the polymer. Water is removed in a lyophilizer to afford pure polymer **L** (265mg). ^{1}H-NMR data (600 MHz, $CDCl_3$): δ

7.30-7.40 (m, 86H), δ 7.02-7.10 (m, 78H), δ 5.05-5.15 (m, 97H), δ 3.39-3.68 (m, 195H), δ 2.88-3.15 (m, 286H), δ 2.29 (m, 1H). M_n = 8,500 g/mol, Đ = 1.7.

Synthesis of Poly(ethylene gylocol) Monomesylate (**PEG-OMs 750)**

Poly(ethylene glycol) monomethyl ether (PEG-OH, 750 g/mol) (1.0g, 1.3mmol, 1.0eq.) was dissolved in CH_2Cl_2 (5mL), and DMAP (50mg, 0.40mmol, 0.3eq.) and trimethylamine (0.56mL, 4.0 mmol, 3.0eq.) were added to this solution. MsCl (0.28mL, 3.6mmol, 2.7eq.) was added dropwise over a period of 30 minutes, and the reaction vessel was stirred overnight at room temperature. The reaction solution was diluted with CH_2Cl_2 and washed with minimal 6M HCl (2 x 1mL). The CH_2Cl_2 was separated from the aqueous layer and slow added to diethyl ether at 0 °C to precipitate out the polymer. The solid polymer was filtered off to afford pure PEG-OMs (750 g/mol) (980mg). ^{1}H-NMR matched with previously reported molecule[61].

Synthesis of Poly(ethylene gylocol) Monoazide (**PEG-N₃ 750**)

PEG-OMs (750 g/mol) (830mg, 1.1mmol, 1.0eq.) was dissolved in DMF (10mL), followed by NaN_3 (0.72g, 11mmol, 10.0eq.). This solution was heated to 90 °C overnight. This reaction solution was precipitated in cold diethyl ether and the polymer was filtered off. This polymer was dissolved in distilled water and extracted with minimal CH_2Cl_2 (3 x 1mL). The CH_2Cl_2 was removed in vacuo and the polymeric residue was precipitated again in cold ether and the polymer was filtered off to afford pure PEG-N₃ (750 g/mol) (375mg). ^{1}H-NMR data (600 MHz, $CDCl_3$): δ 3.64-3.72 (77H, m), 3.37 (3H, s). ^{1}H-NMR matched with previously reported molecule[61].

Synthesis of Poly(ethylene gylocol) Monomesylate **(PEG-OMs 2,000)**

Poly(ethylene glycol) monomethyl ether (PEG-OH, 2,000 g/mol) (2.5g, 1.25mmol, 1.0eq.) was dissolved in CH_2Cl_2 (10mL), and DMAP (46mg, 0.38mmol, 0.3eq.) and trimethylamine (0.52mL, 3.75 mmol, 3.0eq.) were added to this solution. MsCl (0.26mL, 3.38mmol, 2.7eq.) was added dropwise over a period of 30 minutes, and the reaction vessel was stirred overnight at room temperature. The reaction solution was diluted with CH_2Cl_2 and washed with minimal 6M HCl (2 x 1mL). The CH_2Cl_2 was

separated from the aqueous layer and slow added to diethyl ether at 0 °C to precipitate out the polymer. The solid polymer was filtered off to afford pure PEG-OMs (2,000 g/mol) (2.1mg). ^{1}H-NMR data (600 MHz, CDCl$_3$): δ 4.35-4.40 (2H, m), 3.45-3.87 (184H, m), 3.38 (3H, s), 2.09 (3H, s). ^{1}H-NMR matched with previously reported molecule[61].

Synthesis of Poly(ethylene gylocol) Monoazide (**PEG-N$_3$ 2,000)**

PEG-OMs (2,000 g/mol) (1.5mg, 0.75mmol, 1.0eq.) was dissolved in DMF (15mL), followed by NaN$_3$ (0.50g, 0.80mmol, 10.0eq.). This solution was heated to 90 °C overnight. This reaction solution was precipitated in cold diethyl ether and the polymer was filtered off. This polymer was dissolved in distilled water and extracted with minimal CH$_2$Cl$_2$ (3 x 1mL). The CH$_2$Cl$_2$ was removed in vacuo and the polymeric residue was precipitated again in cold ether and the polymer was filtered off to afford pure PEG-N$_3$ (2,000 g/mol) (670mg). ^{1}H-NMR data (600 MHz, CDCl$_3$): δ 3.64-3.72 (181H, m), 3.37 (3H, s). ^{1}H-NMR matched with previously reported molecule[61].

Synthesis of Copolymer **S-750**

Polymer **S** (100mg, 1.00 eq.) was dissolved in dry DMSO (3mL) followed by the 750 g/mol PEG-azide (36mg, 1.00 eq.). CuSO$_4$ (19mg, 0.12 mmol, 3.0 eq.) and sodium ascorbate (24g, 0.12 mmol, 3.0 eq.) were added to this solution, and the reaction mixture was put under a high-vacuum and flushed with Argon gas. This process was repeated twice, and the solution was stirred overnight at room temperature. The DMSO reaction was dialyzed in a 50K membrane with water as the dialysate (3 x 200mL). The resulting emulsion was shaken, followed by centrifugation at 6000 RPM for 10 minutes. The aqueous mother liquor was discarded, and the sample was dried using the lyophilizer to remove residual water to afford a white solid **S-750** (150mg). ^{1}H NMR (600 MHz, CDCl$_3$) δ 7.30-7.40 (m, 60H), 7.02-7.10 (m, 55H), 5.05-5.15 (m, 61H), 3.62-3.72 (s, 80H), 3.35-3.59 (m, 137H), 2.85-3.20 (m, 190). M$_n$ = 4,400 g/mol, Đ = 1.9.

Synthesis of Copolymer **S-2,000**

Polymer **S** (97mg, 1.00 eq.) was dissolved in dry DMSO (3mL) followed by the 2,000 g/mol PEG-azide (80mg, 1.00 eq.). CuSO$_4$ (19mg, 0.12 mmol, 3.0 eq.) and sodium

ascorbate (24g, 0.12 mmol, 3.0 eq.) were added to this solution, and the reaction mixture was put under a high-vacuum and flushed with Argon gas. This process was repeated twice, and the solution was stirred overnight at room temperature. The DMSO reaction was dialyzed in a 50K membrane with water as the dialysate (3 x 200mL). The resulting emulsion was shaken, followed by centrifugation at 6000 RPM for 10 minutes. The aqueous mother liquor was discarded, and the sample was dried using the lyophilizer to remove residual water to afford a white solid **S-2,000** (120mg). ^{1}H NMR (600 MHz, CDCl$_3$) δ 7.30-7.40 (m, 62H), 7.02-7.10 (m, 59H), 5.05-5.15 (m, 60H), 3.62-3.72 (s, 456H), 3.35-3.59 (m, 152H), 2.85-3.20 (m, 201H). M_n = 4,600 g/mol, Đ = 2.0.

Synthesis of Copolymer **L-750**

Polymer **L** (165mg, 1.00 eq.) was dissolved in dry DMSO (4mL) followed by the 750 g/mol PEG-azide (15mg, 1.00 eq.). CuSO$_4$ (13mg, 0.08 mmol, 3.0 eq.) and sodium ascorbate (15g, 0.08 mmol, 3.0 eq.) were added to this solution, and the reaction mixture was put under a high-vacuum and flushed with Argon gas. This process was repeated twice, and the solution was stirred overnight at room temperature. The DMSO reaction was dialyzed in a 50K membrane with water as the dialysate (3 x 200mL). The resulting emulsion was shaken, followed by centrifugation at 6000 RPM for 10 minutes. The aqueous mother liquor was discarded, and the sample was dried using the lyophilizer to remove residual water to afford a white solid **L-750** (160mg). ^{1}H NMR (600 MHz, CDCl$_3$) δ 7.30-7.40 (m, 102H), 7.02-7.10 (m, 94H), 5.05-5.15 (m, 97H), 3.62-3.72 (s, 64H), 3.35-3.59 (m, 209H), 2.85-3.20 (m, 293H). M_n = 9,500 g/mol, Đ = 1.5.

Synthesis of Copolymer **L-2,000**

Polymer **L** (100mg, 1.00 eq.) was dissolved in dry DMSO (4mL) followed by the 2,000 g/mol PEG-azide (23mg, 1.00 eq.). CuSO$_4$ (9mg, 0.06 mmol, 3.0 eq.) and sodium ascorbate (9g, 0.05 mmol, 3.0 eq.) were added to this solution, and the reaction mixture was put under a high-vacuum and flushed with Argon gas. This process was repeated twice, and the solution was stirred overnight at room temperature. The DMSO reaction was dialyzed in a 50K membrane with water as the dialysate (3 x 200mL). The resulting emulsion was shaken, followed by centrifugation at 6000 RPM for 10 minutes. The

aqueous mother liquor was discarded, and the sample was dried using the lyophilizer to remove residual water to afford a white solid **L-2,000** (90mg). [^1]H NMR (600 MHz, CDCl$_3$) δ 7.30-7.40 (m, 62H), 7.02-7.10 (m, 59H), 5.05-5.15 (m, 60H), 3.62-3.72 (s, 456H), 3.35-3.59 (m, 152H), 2.85-3.20 (m, 201H). M_n = 10,500 g/mol, Đ = 1.8.

Synthesis of TBS protected end-cap **18**

Triphosgene (0.6124g, 2.10 mmol, 0.33 eq.) was dissolved in freshly distilled CH$_2$Cl$_2$ (60mL), and in another flask, the TBS-phenol **2** was dissolved in THF (50mL) and triethylamine (0.88mL, 2.10 mmol, 1 eq.) The solution of **2** was added dropwise into the triphosgene solution, and stirred for 15 minutes to form the appropriate chloroformate. In a separate flask, the ammonium salt **17** was dissolved in CH$_2$Cl$_2$ in addition to triethylamine (1.32mL, 9.453 mmol, 1.5 eq.). This solution was dropped into the solution of the TBS-chloroformate, and stirred for 3hrs at room temperature. The reaction mixture was partitioned between a sat. NH$_4$Cl solution and CH$_2$Cl$_2$ and the aqueous layer was extracted three times (3 x 30mL). The combined organic layers were washed once more with a small amount of sat. NH$_4$Cl, followed by the drying of the organic layers using MgSO$_4$. The drying agent was filtered off, and the solvent removed in vacuo. The crude residue was purified via column chromatography with an eluent 35/65 EtOAc/hexanes to yield a clear and colourless oil **18** in an 80% yield (4.812g). [^1]H-NMR data (600 MHz, CDCl$_3$): δ 7.34 (m, 2H), δ 7.13 (m, 2H), δ 5.53 (m, 1H), δ 4.81 (m, 2H), δ 4.73 (m, 2H), δ 4.15 (m, 2H), δ 1.60 (m, 1H), δ 0.94 (s, 9H), δ 0.10 (s, 6H). MS calc'd for **11** 377.5069; found, 377.5155.

Synthesis of **19**

37% HCl (0.35mL) was dissolved in EtOH (12.6mL) to form a 1% HCl in EtOH solution. The TBS end-cap **18** (0.5026g, 1.33 mmol, 1.00 eq.) was added to this solution, and stirred at room temperature for 1hr. The reaction mixture was diluted with CH$_2$Cl$_2$, washed with a sat. NaHCO$_3$ solution, and extracted out of the aqueous layer three times with CH$_2$Cl$_2$ (3 x 10mL). The combined organic layers were dried using MgSO$_4$, the drying agent was filtered off, and the solvent removed in vacuo. The crude residue was purified via column chromatography with an eluent of 70/30 EtOAc/hexanes to yield a

clear and colourless oil **19** in a 91% yield (0.3203g). ^{1}H-NMR data (600 MHz, CDCl$_3$): δ 7.32-7.40 (m, 2H), δ 7.13-7.18 (m, 2H), δ 5.50-5.65 (m, 1H), δ 4.78-4.83 (m, 2H), δ 4.64-4.68 (m, 2H), δ 4.13-4.19 (m, 2H), δ 2.52-2.58 (m, 1H). MS calc'd for **12** 263.2613; found, 263.2573.

Synthesis of activated end-cap **20**

The alcohol **19** (0.3016g, 1.15 mmol, 1.00 eq) was dissolved in CH$_2$Cl$_2$ (5mL), followed by the addition of pyridine (0.30 mL, 2.91 mmol, 3.10 eq). Para-nitro chloroformate (0.4610 g, 2.30 mmol, 2.00 eq.) was dropped into this solution, which was stirred for 2hrs at room temperature. The reaction mixture was diluted with CH$_2$Cl$_2$ and washed with a 1 M HCl solution, then the aqueous phase was extracted three times with CH$_2$Cl$_2$ (3 x 20mL). The combined organic layers were dried using MgSO$_4$, the drying agent was filtered off, and the solvent removed in vacuo. The crude residue was purified via column chromatography with an gradient eluent of CH$_2$Cl$_2$ → 50/50 CH$_2$Cl$_2$/EtOAc to yield a slightly yellow solid in an 87% yield (0.4246g). ^{1}H-NMR data (600 MHz, CDCl$_3$): δ 8.24-8.30 (m, 2H), 7.43-7.49 (m, 2H), δ 7.32-7.40 (m, 2H), δ 7.14-7.20 (m, 2H), δ 5.50-5.57 (m, 1H), δ 5.25-5.31 (m, 2H), δ 4.77-4.83 (m, 2H), δ 4.10-4.18 (m, 2H), δ 2.54 (m, 1H). MS calc'd for **20** 428.3490; found, 428.3539.

Synthesis of control polymer **C**

The monomer **8** (1.099g, 2.18 mmol, 1.00 eq.) was dissolved in a 1:1 mixture of CH$_2$Cl$_2$/TFA (11.9 mL) and stirred at room temperature for 2hrs. The TFA and CH$_2$Cl$_2$ were removed by a stream of argon, followed by in vacuo conditions. Dissolve **13** in toluene (12mL), followed by the end-cap **20**, DMAP (0.058g, 0.47 mmol, 0.22 eq.), and triethylamine (3.8mL, 27 mmol, 12.0 eq.) and stirred at room temperature for 24 hours. The reaction mixture was diluted in CH$_2$Cl$_2$ and washed with a solution of 1 M HCl (1 x 30mL), and twice with sat. Na$_2$CO$_3$ (2 x 50mL). The combined organic layers were dried using MgSO$_4$, the drying agent was filtered off, and the solvent removed in vacuo. The polymer was then dissolved in 3mL DMF, and dialyzed with a 6-8K membrane with DMF as the dialysate (2 x 200mL). The last solvent used in this dialysis is water, which precipitates the polymer. Water is removed in a lyophilizer to afford pure **C** (400mg). ^{1}H-

NMR data (600 MHz, CDCl$_3$): δ 7.30-7.40 (m, 46H), δ 7.02-7.10 (m, 44H), δ 5.05-5.15 (m, 47H), δ 3.58-3.65 (m, 12H), δ 3.42-3.57 (m, 86H), δ 3.10-3.15 (m, 18H), δ 3.02-3.06 (m, 19H), δ 2.95-3.01 (m, 119H), 2.91-2.94 (m, 16H), 2.88-2.90 (m, 34H), 2.53 (t, 1H). M_n = 6500 g/mol, $Đ$ = 1.418.

Synthesis of control copolymer **C-750**

Polymer **C** (0.15g, 1.00 eq.) was dissolved in dry DMF (5mL) followed by the 750 PEG-azide (0.020g, 0.027 mmol, 1.00 eq.). CuSO$_4$ (0.007g, 0.0438 mmol, 2.00 eq.) and sodium ascorbate (0.023g, 0.116 mmol, 5.00 eq.) were added to this solution, and the reaction mixture was put under a high-vacuum and flushed with Argon gas. This was repeated twice more, and the solution was then heated to 50 ^{o}C and stirred overnight. The DMF reaction was dialyzed in a 50K membrane with water as the dialysate (3 x 200mL). The resulting emulsion was shaken, then centrifuged at 6000 RPM for 10 minutes. The aqueous mother liquor was discarded, and the sample was put on the lyophilizer to remove residual water to afford a purple solid **C-750** (81mg). ^{1}H-NMR data (600 MHz, CDCl$_3$): δ 7.30-7.40 (m, 46H), δ 7.02-7.10 (m, 46H), δ 5.05-5.15 (m, 50H), δ 3.63-3.67 (m, 68H), δ 3.58-3.63 (m, 18H), δ 3.42-3.57 (m, 95H), δ 3.10-3.15 (m, 23H), δ 3.02-3.07 (m, 22H), δ 2.95-3.01 (m, 90H), 2.89-2.94 (m, 18H). M_n = 7,000 g/mol, $Đ$ = 1.5.

Synthesis of 3-azidopropan-1-ol **21**

NaN$_3$ (3.04g, 47mmol, 1.3eq.) was dissolved in 3-bromo-1-propanol (3.2mL, 35mmol, 1.0eq.), and this mixture was stirred at 100 °C overnight. The reaction mixture was diluted with diethyl ether, and the insoluble salts were removed using filtration. The ether was removed in vacuo to afford crude **21** in a 77% yield (2.71g). ^{1}H NMR (599 MHz, CDCl$_3$) δ 3.75-3.77 (m, 2H), 3.45-3.47 (m, 2H), 1.83-1.86 (m, 2H), 1.65 (s, 1H).

Synthesis of 3-azidopropyl 2-(butylthiocarbonothioylthio)-2-methylpropanoate **23**

Acid **22** (2.83g, 12mmol, 1.0eq.) was dissolved in 40mL of CH$_2$Cl$_2$ followed by 9mL of pyridine. EDC•HCl (2.98g, 15mmol, 1.2eq.) was dropped into this solution and stirred at

room temperature for 20 minutes. Alcohol **21** (1.65g, 16mmol, 1.2eq.) was added and this reaction was stirred overnight. The reaction solution was dilluted with CH_2Cl_2 and washed with saturated aqueous $NaHCO_3$, aqueous 1M HCl and distilled water. The combined organic layers were dried using $MgSO_4$, the drying agent was filtered off, and the solvent removed in vacuo. This crude residue was purified using column chromatography using an eluent of 10/90 EtOAc/hexanes to afored pure **23** in a 40% yield (1.73g). ^{1}H NMR (600 MHz, $CDCl_3$) δ 4.17-4.20 (m, 2H), 3.35-3.38 (m, 2H), 3.29-3.33 (m, 2H), 1.89-1.93 (m, 2H), 1.70 (s, 6H), 1.66 (s, 2H), 1.41-1.45 (m, 2H), 0.93-0.95 (m, 3H). ^{13}C NMR data ($CDCl_3$, 100 MHz): δ 172.80, 62.73, 55.88, 48.19, 36.63, 29.91, 28.00, 23.35, 22.06, 13.57. MS calc'd for **23** 335.0796; found, 335.0459.

Synthesis of PDMAEMA **24**

RAFT initiator **23** (0.18g, 0.53mmol, 1.0eq.) was dissolved in DMF (1.25mL), followed by the methyl methacrylate monomer (0.56mL, 3.2mmol, 6.0eq.) and AIBN (29mg, 0.18mmol, 0.33eq.). Argon was flushed into this solution for 30 minutes to remove oxygen gas, and the reaction was subsquently heated to 65 °C and stirred at this temperature for 4 hours. This reaction was cooled to room temperature and inserted into a dialysis bag (MWCO ~ 6,000 – 8,000) with water as the dialysate (3 x 1L). The sample was frozen and subsequently dried using the lyophilizer to remove residual water to afford a yellow viscous gel **24** (490mg). ^{1}H NMR (600 MHz, DMSO-d_6) δ 3.95-4.06 (m, 2H), 2.55-2.65 (m, 2H), 2.17-2.34 (m, 7H), 1.66-1.85 (m, 2H), 0.70-1.10 (m, 3H). M_n = 3,500 g/mol, Đ = 1.35.

Nanoprecipitation Procedure

The co-polymer was dissolved into dry THF at a concentration of 8mg/mL. 0.1mL of this THF-copolymer solution and 0.9mL of water were combined using two methods to nanoprecipitate the co-polymer: the THF-copolymer solution was quickly added to 0.9mL of 100mM phosphate buffered water at pH 7.4, **or** the buffered water was slowly added to the THF-copolymer solution. The resulting emulsion was stirred for one hour, and then dialyzed overnight using a 1,000 MW cut-off membrane with the same phosphate buffered water (2 x 2L) as the dialysate to remove THF. This emlusion was

taken for measurements using dynamic light scattering (DLS). For TEM imaging, these nanoparticles in water were diluted 10 times using the buffered water solution. 10μL of this diluted nanoparticle emulsion was added to a TEM copper grid using a micropipette. The water evapourated, and left the nanoparticles on the grid for imaging.

Nile Red Release Study

The copolymer is dissolved into dry THF at a concentration of 8mg/mL, and Nile Red is added to this solution at a concentration of 2 wt % relative to the co-polymer. This THF-copolymer-Nile Red solution was combined with 0.9mL of 100mM phosphate buffered water at pH 7.4 using one of the control outlined in the nanoprecipitation proecdure above. The resulting emulsion was stirred for one hour, and then dialyzed overnight using a 1,000 MW cut-off membrane with the same phosphate buffered water (2 x 2L) as the dialysate to remove THF and Nile Red. This emulsion was diluted 10 times with buffered water and added to a quartz cuvette so that a initial fluorescence spectrum was taken, as a control. The nanoparticles were irradiated with UV lamp (wavelength: 300-350 nm, $23mWcm^{-2}$) for 20 minutes, and a fluorescence spectrum was taken immediately after irradiation. Subsequent measurements were taken to form a release profile with fluorimeter count rate as the dependant parameter.

DLS Degradation Study

The copolymer is dissolved into dry THF at a concentration of 8mg/mL, and the THF-copolymer solution was combined with 0.9mL of 100mM phosphate buffered water at pH 7.4 using one of the control outlined in the nanoprecipitation proecdure above. The resulting emulsion was stirred for one hour, and then dialyzed overnight using a 1,000 MW cut-off membrane with the same phosphate buffered water (2 x 2L) as the dialysate to remove THF. This emulsion was diluted 10 times with buffered water and added to a quartz cuvette so that a initial DLS measurement can be taken. The nanoparticles were irradiated with UV lamp (wavelength: 300-350 nm, $23mWcm^{-2}$) for 20 minutes, and a DLS measurement was taken immediately after irradiation. Subsequent measurements were taken to form a light-scattering profile using the DLS count rate as the dependant parameter.

4   References

1. Tschan, M. J. L.; Brulé, E.; Haquette, P.; Thomas, C. M. *Polym. Chem.* **2012**, *3*, 836.

2. Tian, H.; Tang, Z.; Zhuang, X.; Chen, X.; Jing, X. Prog. *Polym. Sci*. **2012**, *37*, 237.

3. Gross, R. A.; Kalra, B. *Science* **2002**, *297*, 803.

4. Sisson, A. L.; Schroeter, M.; Lendlein, A. *In Handbook of Biodegradable Polymers; Wiley-VCH Verlag GmbH and Co.* KGaA: **2011**, p 1.

5. Gilding, D. K.; Reed, A. M. *Polymer* **1979**, *20*.

6. Reed, A. M.; Gilding, D. K. *Polymer* **1981**, *22*, 494.

7. Li, Y.; Thouas, G. A.; Chen, *Q.-Z. RSC Advances* **2012**, *2*, 8229.

8. Langer, R.; Vacanti, J. *Science* **1993**, *260*, 920.

9. Jeong, B.; Bae, Y. H.; Lee, D. S.; Kim, S. W. *Nature* **1997**, *388*.

10. Uhrich, K. E.; Cannizzaro, S. M.; Langer, R. S.; Shakesheff, K. M. *Chemical Reviews* **1999**, *99*, 3181.

11. Kataoka, K.; Harada, A.; Nagasaki, Y. *Adv. Drug Delivery Rev*. **2001**, *47*, 113.

12. Yih, T. C.; Al-Fandi, M. J. *Cell. Biochem*. **2006**, *97*, 1184.

13. Kumari, A.; Yadav, S. K.; Yadav, S. C. *Colloids and Surfaces B: Biointerfaces* **2010**, *75*, 1.

14. Gupta, A. P.; Kumar, V. *Eur. Polym. J.* **2007**, *43*, 4053.

15. Vert, M. *Biomacromolecules* **2005**, *6*, 538.

16. Morachis, J. M.; Mahmoud, E. A.; Almutairi, A. *Pharmacol. Rev.***2012**, *64*, 505.

17. Wei, H.; Zhuo, R.-X.; Zhang, X.-Z. *Prog. Polym. Sci.* **2012**, *38*, 503.

18. Bang, E.-K.; Lista, M.; Sforazzini, G.; Sakai, N.; Matile, S. *Chem. Sci*. **2012**, *3*, 1752.

19. Ko, N. R.; Yao, K.; Tang, C.; Oh, J. K. *J. Polym. Sci. A Polym. Chem.* **2012**, n/a.

20. Bauhuber, S.; Hozsa, C.; Breunig, M.; Göpferich, A. *Advanced Materials* **2009**, *21*, 3286.

21. Emilitri, E.; Ranucci, E.; Ferruti, P. *J. Polym. Sci. A Polym. Chem.* **2005**, *43*, 1404.

22. Meng, F.; Hennink, W. E.; Zhong, Z. *Biomaterials* **2009**, *30*, 2180.

23. Wang, Y., et al., *Biomaterials* **2012**, *33*, 6570.

24. Binauld, S.; Stenzel, M. H. *Chem. Commun*. **2013**, *49*, 2082.

25. Zhao, C.; Nie, S.; Tang, M.; Sun, S. *Prog. Polym. Sci.* **2011**, *36*, 1499.

26. Park, I.-K.; Singha, K.; Arote, R. B.; Choi, Y.-J.; Kim, W. J.; Cho, C.-S. *Macromol. Rapid Commun.* **2010**, *31*, 1122.

27. Gao, W.; Chan, J. M.; Farokhzad, O. C. *Mol. Pharm*. **2010**, *7*, 1913.

28. Dai, S.; Ravi, P.; Tam, K. C. *Soft Matter*, **2008**, *4*, 435.

29. Jain, R.; Standley, S. M.; Fréchet, J. M. J. *Macromolecules* **2007**, *40*, 452.

30. Heffernan, M. J.; Murthy, N. *Bioconjugate Chem.* **2005***, 16*, 1340.

31. Zhao, H.; Sterner, E. S.; Coughlin, E. B.; Theato, P. *Macromolecules* **2012**, *45*, 1723.

32. C. deGracia Lux, C. L. McFearin, S. Joshi-Barr, J. Sankaranarayanan, N. Fomina, and A. Almutairi, *ACS Macro. Lett*., **2012**, *1*, 922–926.

33. Blencowe, C. A.; Russell, A. T.; Greco, F.; Hayes, W.; Thornthwaite, D. W. *Polym. Chem.* **2011**, *2*, 773.

34. Wong, A. D.; DeWit, M. A.; Gillies, E. R. *Adv. Drug Delivery Rev.* **2012**, *64*, 1031.

35. Peterson, G. I.; Larsen, M. B.; Boydston, A. J. *Macromolecules* **2012***, 45*, 7317.

36. Fan, B.; Gillies, E. R.* "Self-immolative Polymers." *Encyc. Polym. Sci.* **in press.**

37. McBride, R. A.; Gillies, E. R. *Macromolecules*, **2013**, *46*, 5157–5166.

38. F. M. H. deGroot, C. Albrecht, R. Koekkoek, P. H. Beusker, and H.W. Scheeren, *Angew. Chem., Int. Ed.,* **2003**, *42*, 4490–4494.

39. R. J. Amir, N. Pessah, M. Shamis, and D. Shabat, *Angew. Chem., Int. Ed*., **2003**, *42*, 4494–4499.

40. M. L. Szalai, R. M. Kevwitch, and D. V. McGrath, *J. Am. Chem. Soc.,* **2003**, *125*, 15688–15689.

41. M. Shamis, H. N. Lode, and D. Shabat, *J. Am. Chem. Soc.*, **2004**, *126*, 1726–1731.

42. R. Erez, E. Segal, K. Miller, R. Satchi-Fainaro, and D. Shabat, *Bioorg. Med. Chem*., **2009**, *17*, 4327–4335

43. E. Sella and D. Shabat, *Chem. Commun.* **2008**, 5701–5703

44. E. Sella and D. Shabat*, J. Am. Chem. Soc*., **2009**, *131*, 9934–9936.

45. E. Sella, R. Weinstain, R. Erez, N. Z. Burns, P. S. Baran, and D. Shabat, *Chem. Commun*., **2010**, *46*, 6575–6577

46. A. Sagi, R. Weinstain, N. Karton, and D. Shabat, *J. Am. Chem. Soc.,* **2008**, *130*, 5434–5435.

47. J. S. Robbins, K. M. Schmid, and S. T. Phillips, *J. Org. Chem.,* **2013**, *78*, 3159–3169.

48. R. Weinstain, P. S. Baran, and D. Shabat, *Bioconjugate Chem.,* **2009***, 20*, 1783–1791.

49. O. Vogl*, J. Polym. Sci., A: Polym. Chem*., **2000**, *38*, 2293–2299.

50. S. A. MacDonald, C. G. Willson, and J. M. J. Frechet, *Acc. Chem. Res*., **1994***, 27*, 151–158.

51. H. Ito and C. G. Willson, *Polym. Eng. Sci*., **1983**, *23*, 1012–1018.

52. W. Seo and S. T. Phillips, *J. Am. Chem. Soc.*, **2010**, *132*, 9234–9235.

53. J. A. Kaitz and J. S. Moore, *Macromolecules*, **2013**, *46*, 608–612.

54. S. Köstler, B. Zechner, B. Trathnigg, H. Fasl, W. Kern, and V. Ribitsch, *J. Polym. Sci., Polym. Chem.*, **2009**, *47*, 1499–1509.

55. C.-H. Brachais, R. Duclos, C. Vaugelade, J. Huguet, M. L. Capelle-Hue, and C. Bunel, *Int. J. Pharm.,* **1998***, 169*, 23–31.

56. C. H. Brachais, J. Huguet, and C. Bunel, *Polymer*, **1997**, *38*, 4959–4964.

57. U.S. Pat. 4144226 (to Monsanto Co) (**1979**), M. M. Crutchfield, V. D. Papanu, and C. B. Warren.

58. U.S. Pat. 4140676 (to Monsanto Co) (**1979**), M. M. Crutchfield and C. J. Upton.

59. J. K. Kim, V. K. Garripelli, U. H. Jeong, J. S. Park, M. A. Repka, and S. Jo, *Int. J. Pharm.*, **2010**, *401*, 79–86 .

60. B. Belloncle, C. Bunel, L. Menu-Bouaouiche, O. Lesouhaitier, and F. Burel, *J. Polym. Environ.*, **2012**, *20*, 726–731.

61. B. Fan, J. F. Trant, A. D. Wong, and E. R. Gillies, *J. Am. Chem. Soc.*, **2014**, *136,* 10116–10123.

62. DeWit, M. A.; Gillies, E. R. *J. Am. Chem. Soc*. **2009**, *131*, 18327.

63. Chen, E. K. Y.; McBride, R. A.; Gillies, E. R. *Macromolecules*, **2012**, *45*, 7364.

64. Mai, Y.; Eisenberg, *A. Chem. Soc. Rev*. **2012**, *41*, 5969.

65. Christian, D. A.; Cai, S.; Bowen, D. M.; Kim, Y.; Pajerowski, J. D.; Discher, D. E. *European Journal of Pharmaceutics and Biopharmaceutics* **2009**, *71*, 463.

66. Dennis E. Discher and Adi Eisenberg, *Science*, **2002**, *297*, 967-973.

67. Mikhail, A. S.; Allen, C. *J. Controlled Release* **2009**, *138*, 214.

68. Kataoka, K.; Harada, A.; Nagasaki, Y. *Adv. Drug Delivery Rev*. **2012**, *64*, 37.

69. Tanner, P.; Baumann, P.; Enea, R.; Onaca, O.; Palivan, C.; Meier, W. *Acc. Chem. Res.* **2011**, *44*, 1039.

70. G. Liu, X. Wang, J. Hu, G. Zhang, and S. Liu, *J. Am. Chem. Soc.* **2014**, *136*, 7492−7497.

71. J. Niskanen , C. Wu , M. Ostrowski , G. G. Fuller , S. Hietala , and H. Tenhu , *Macromolecules*, **2013**, *46 (6)*, pp 2331–2340.

72. Q. Yan and Y. Zhao, *Chem. Commun*., **2014**, *50*, 11631-11641.

73. P. Greenspan and S. D. Fowler, *Journal of Lipid Research*, **1985**, *26*, 781-789.

74. F. Ahmed, P. J. Photos, and D. E. Discher, *Drug Dev. Res.,* **2006**, *67*, 4-14.

5   Appendices

Appendix A: NMR Characterization Data
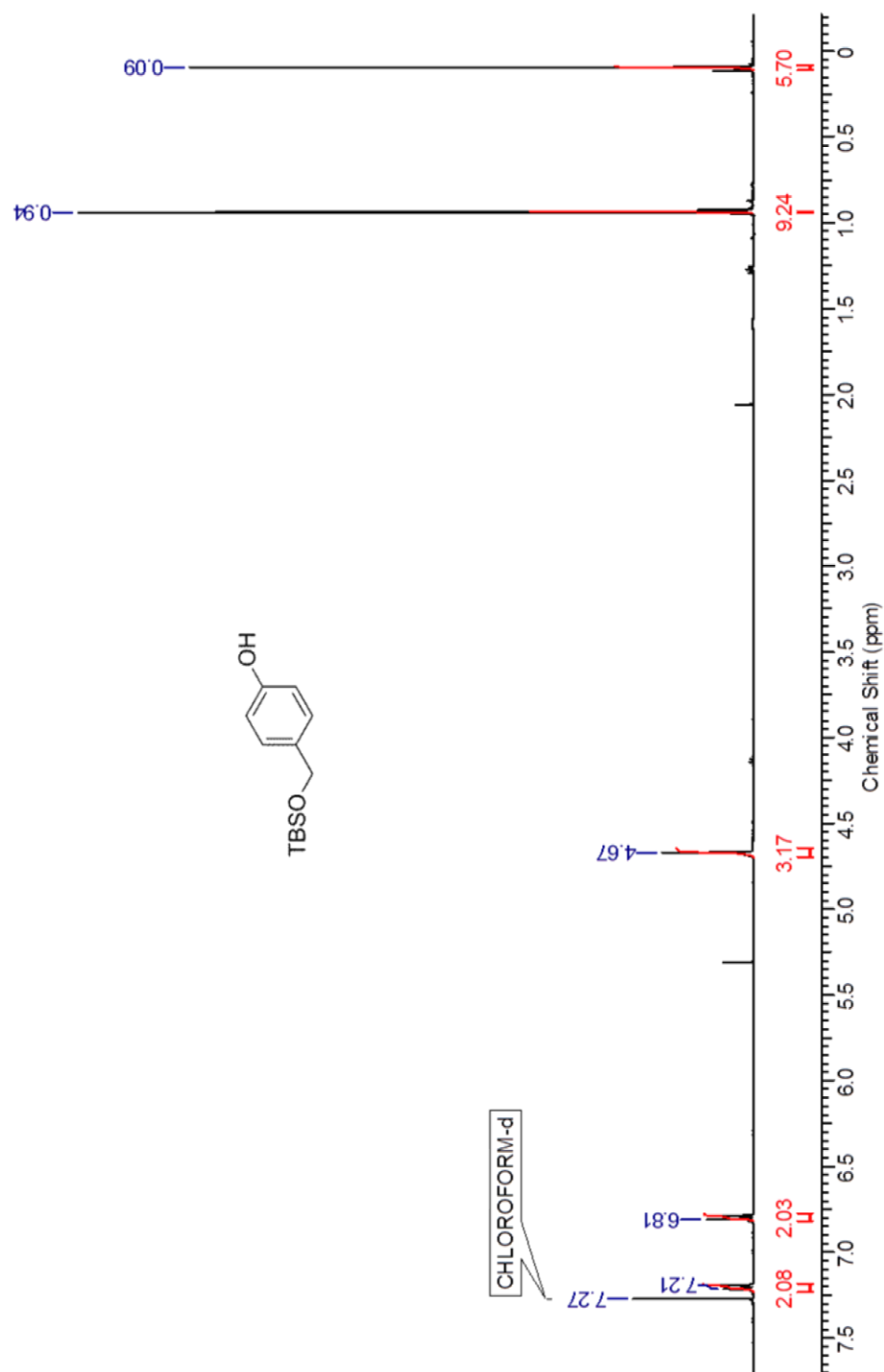
Figure A1: ^{1}H-NMR spectrum of compound **2**.
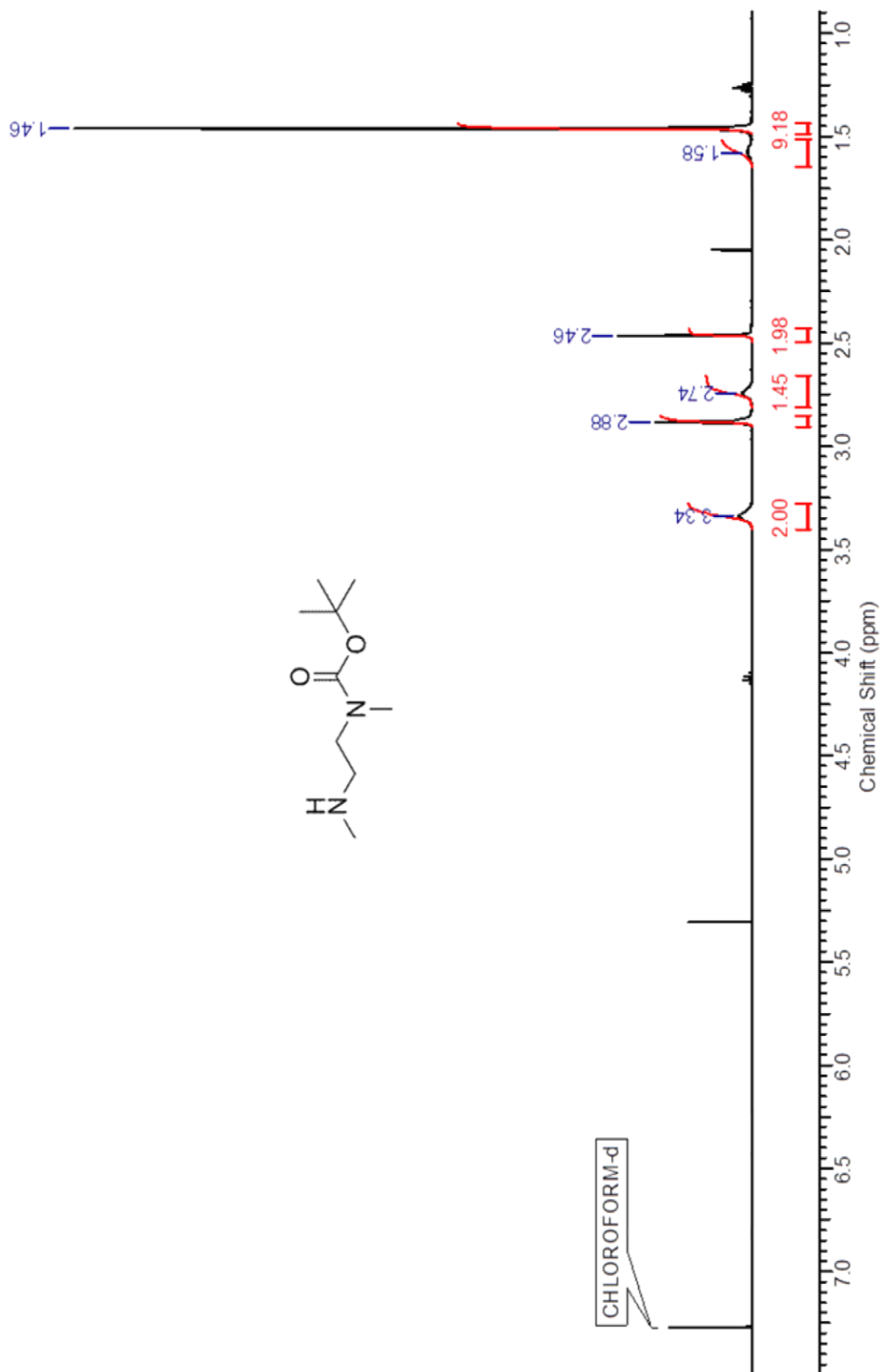
Figure A2: ¹H-NMR spectrum of compound **5**.
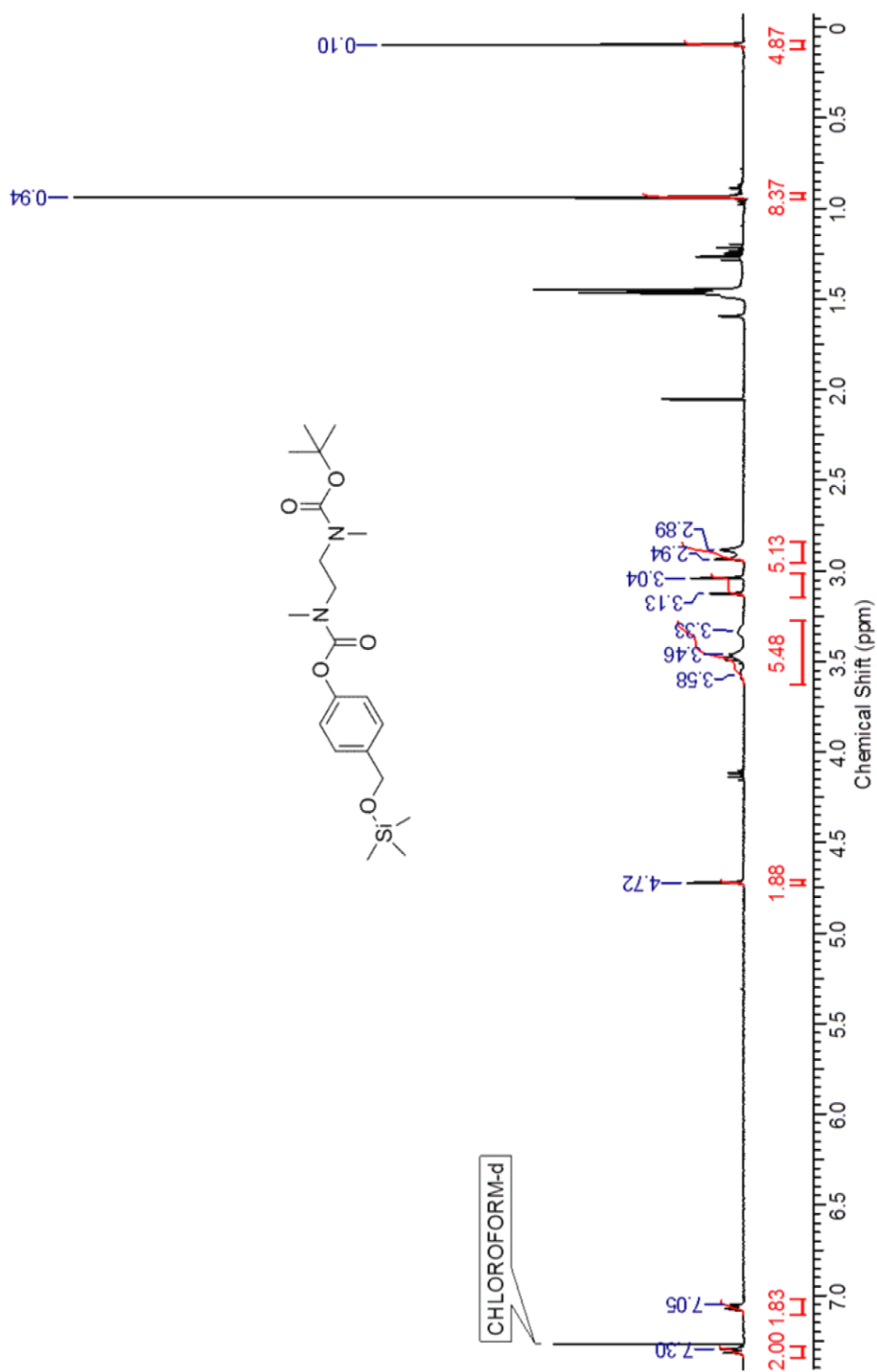
Figure A3: ^{1}H-NMR spectrum of compound **6**.
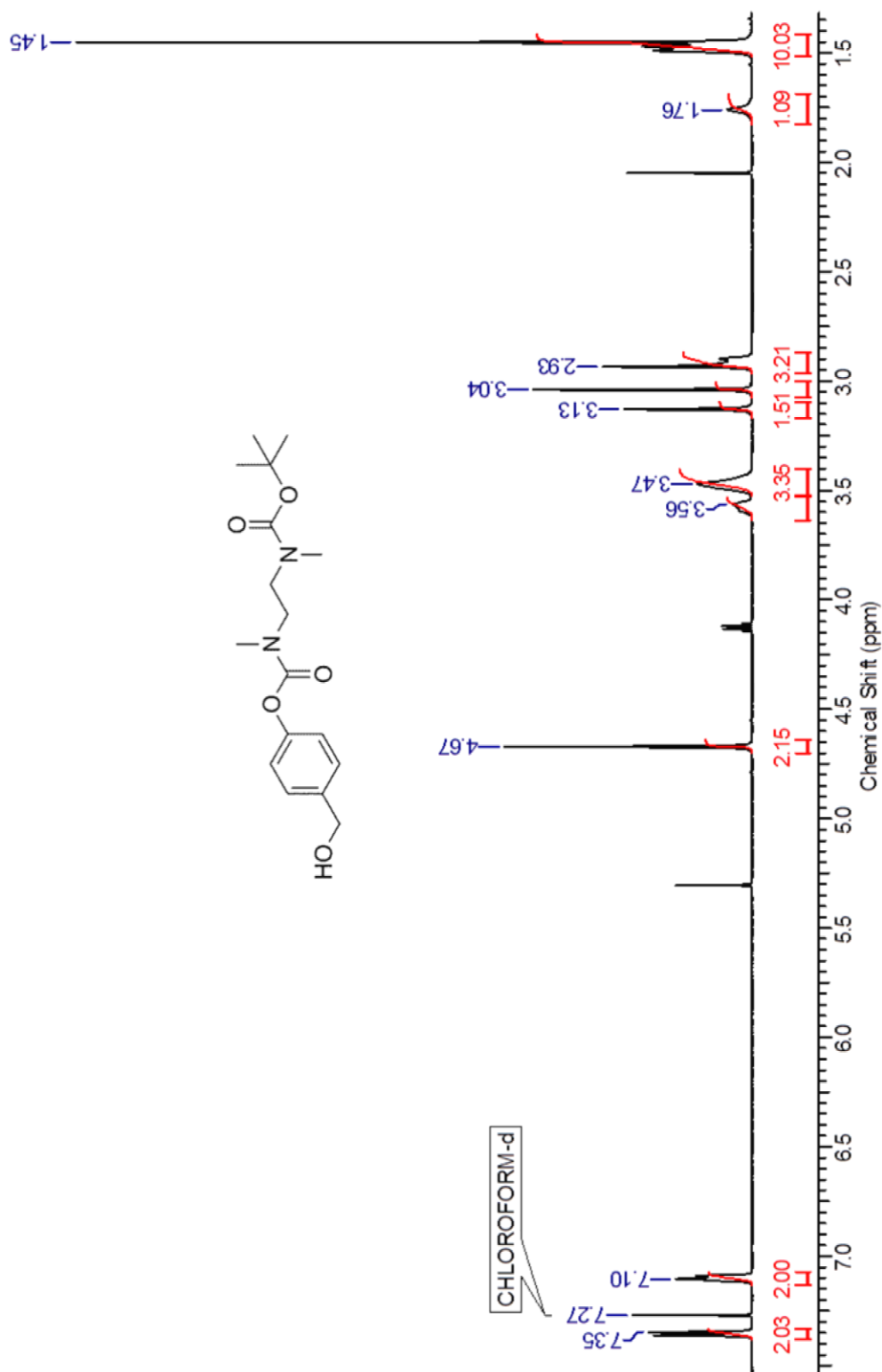
Figure A4: ^{1}H-NMR spectrum of compound **7**.
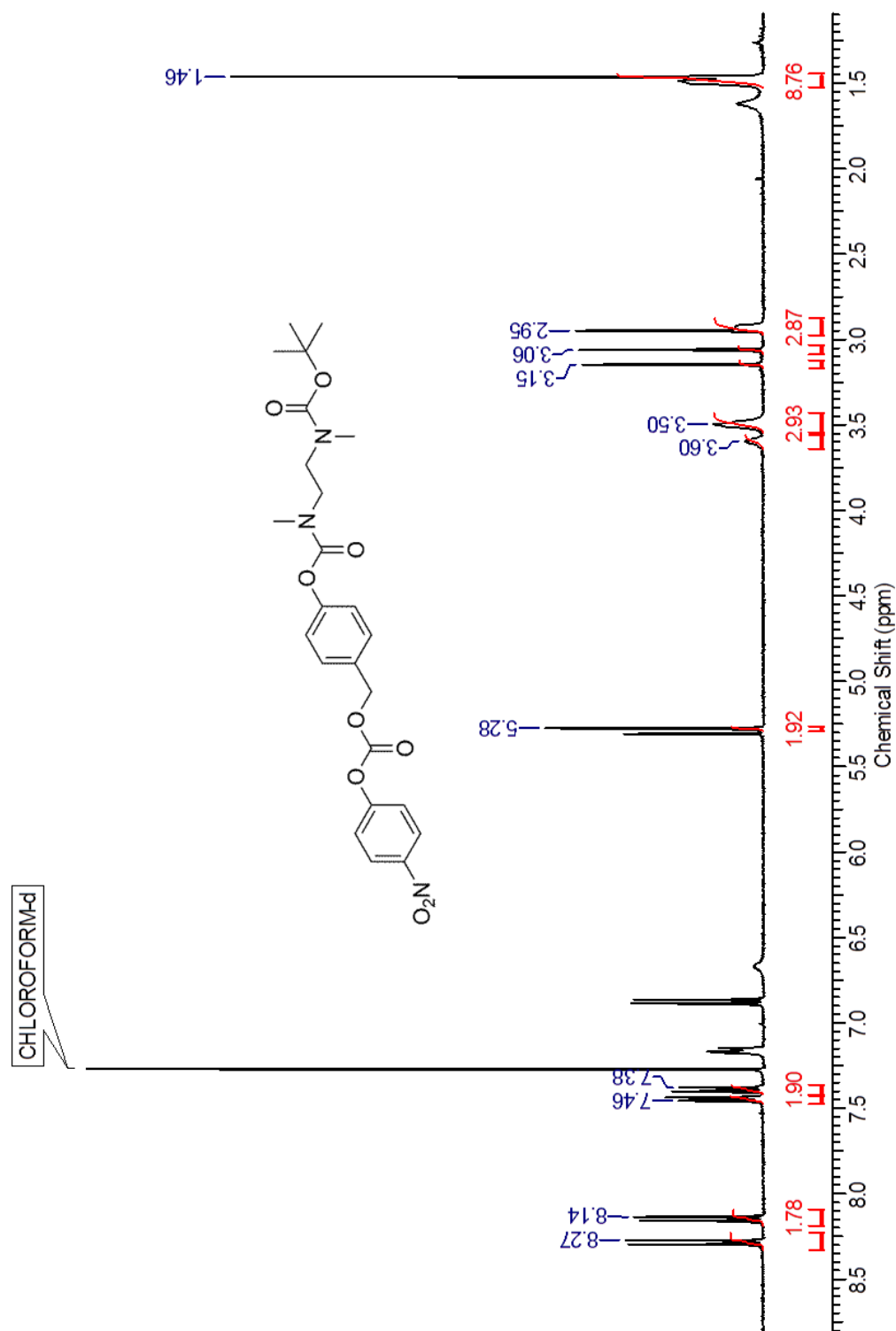
Figure A5: ¹H-NMR spectrum of compound **8**.
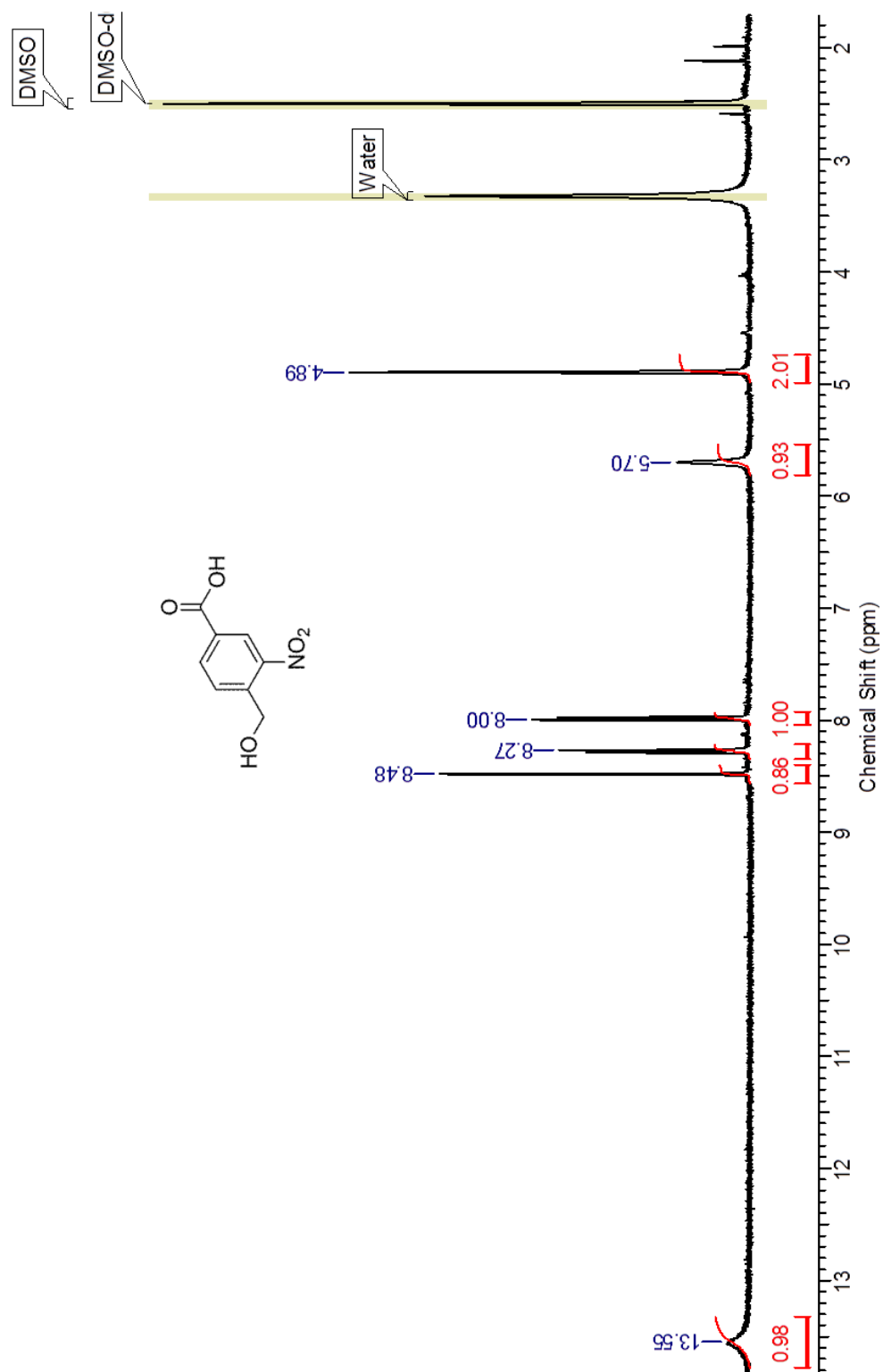
Figure A6: ¹H-NMR spectrum of compound **10**.
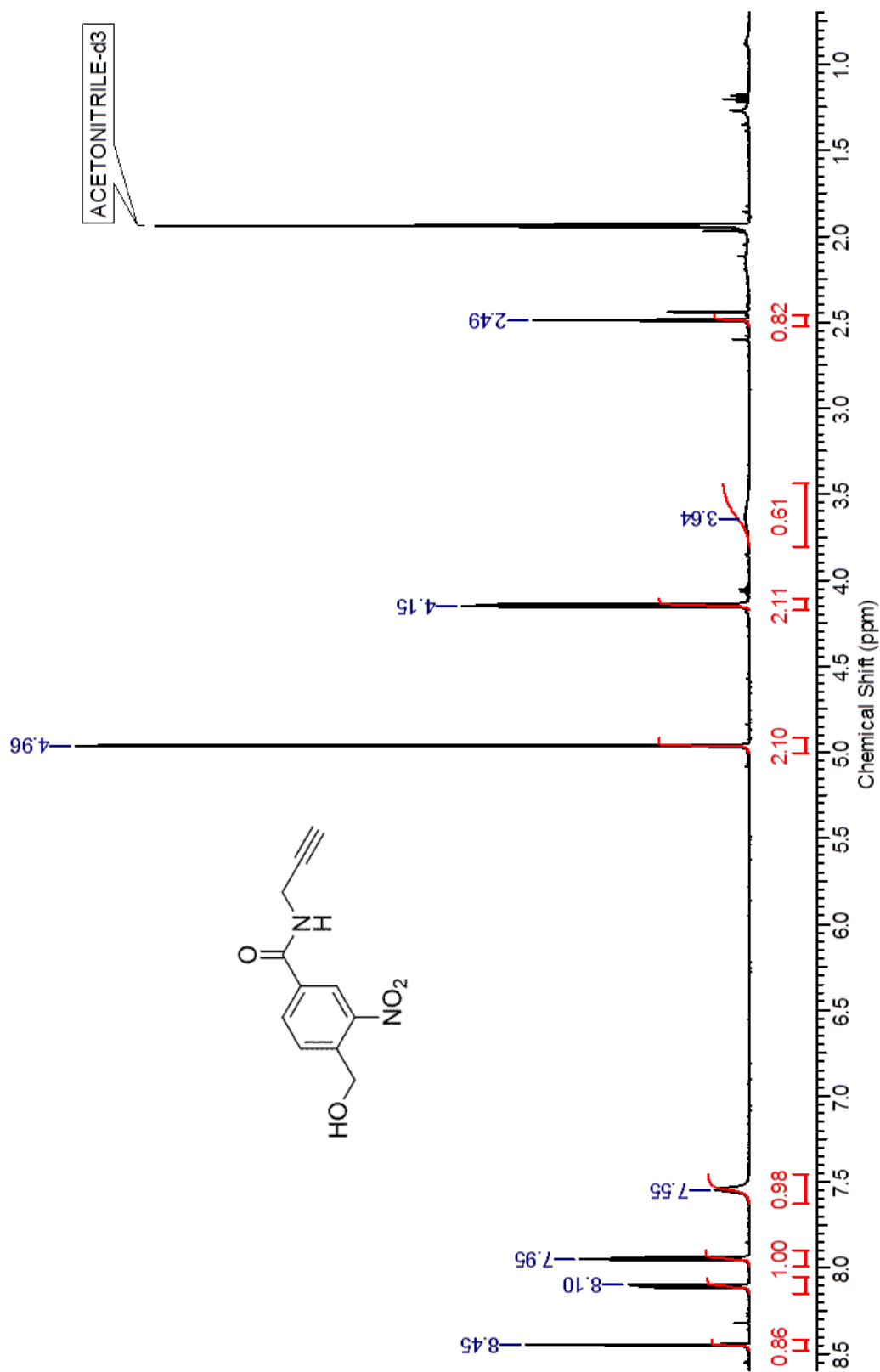
Figure A7: ^{1}H-NMR spectrum of compound **11**.
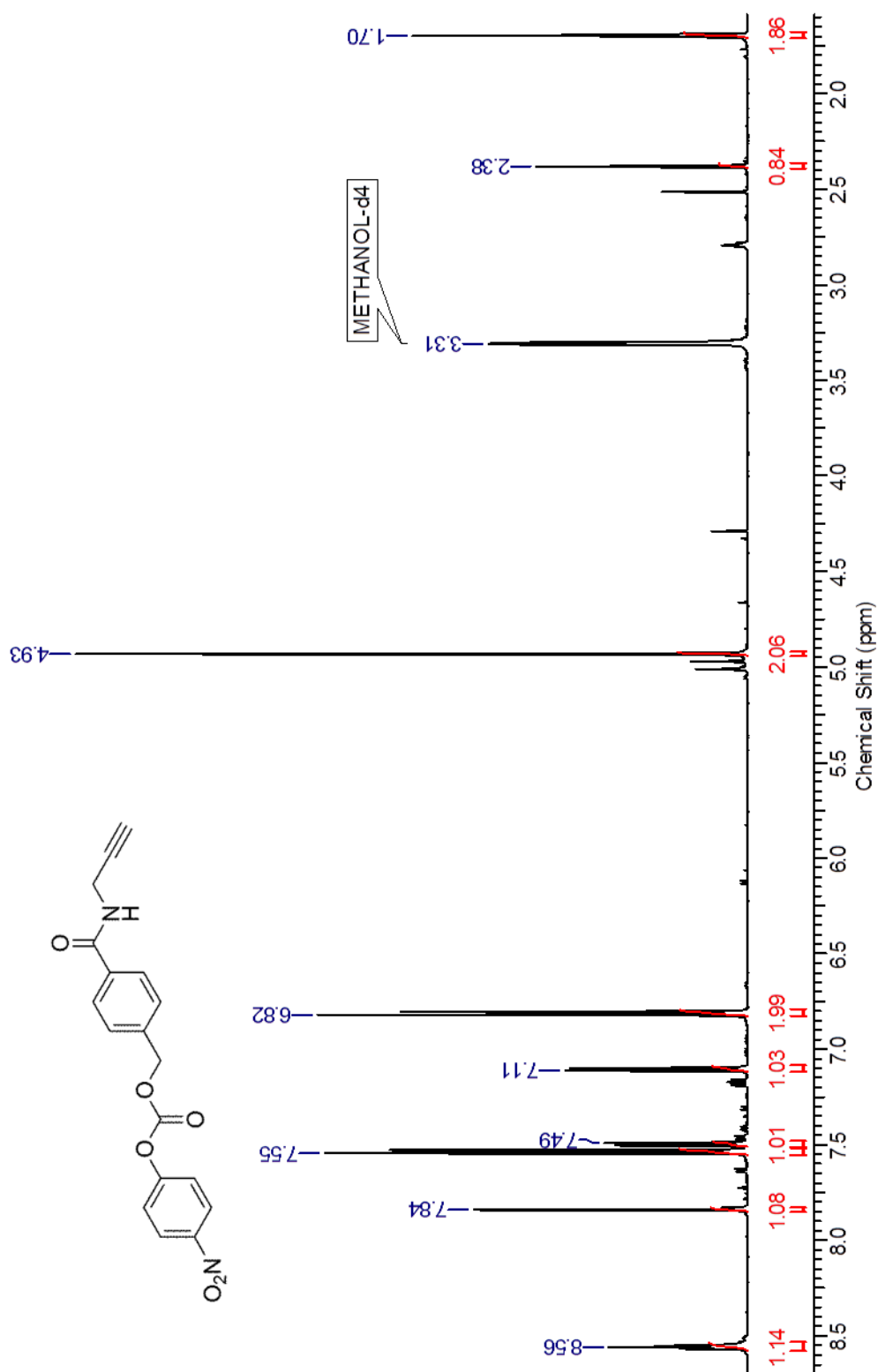
Figure A8: ^{1}H-NMR spectrum of compound **12**.
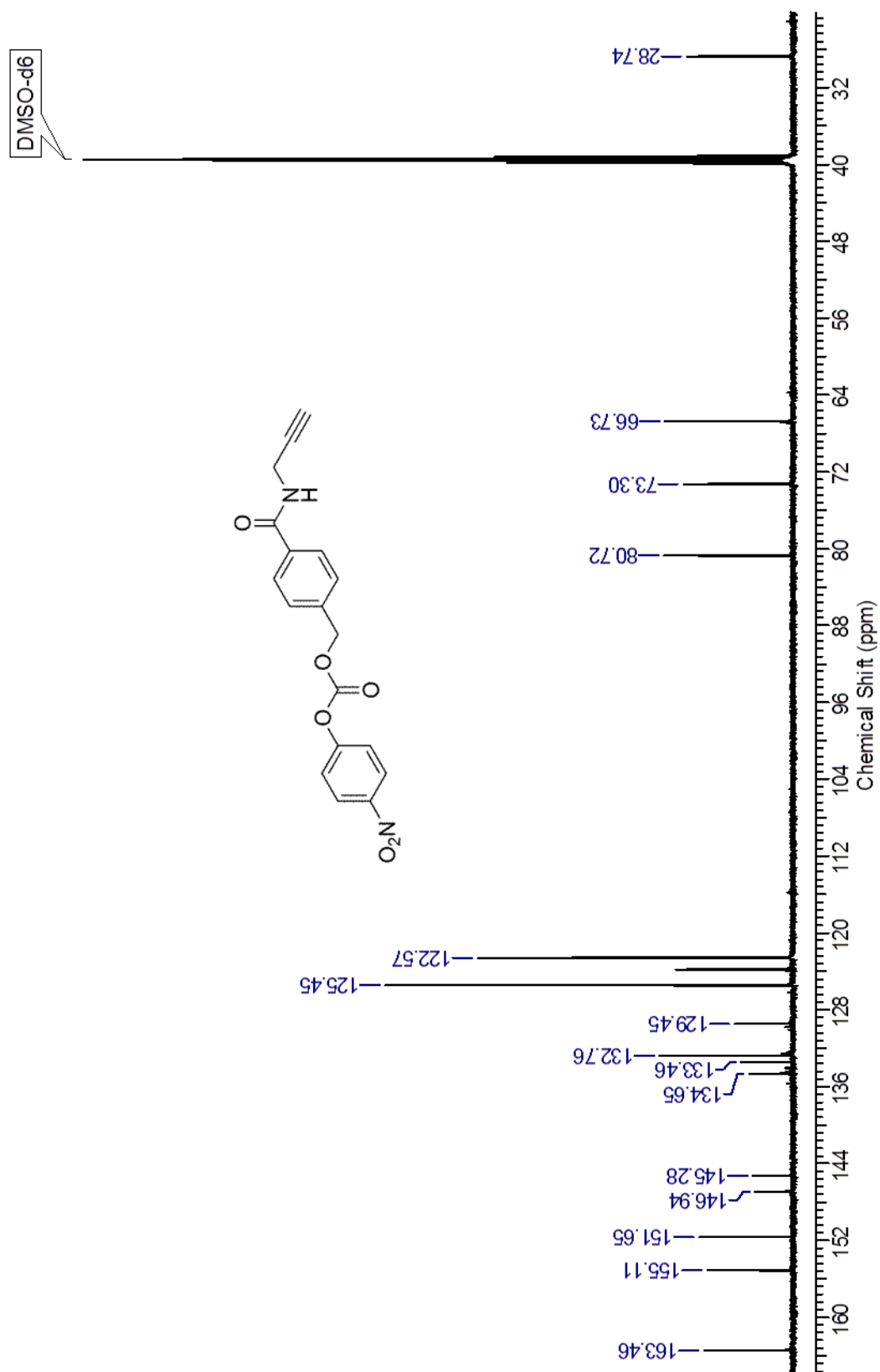
Figure A9: ^{13}C-NMR spectrum of compound **12**.
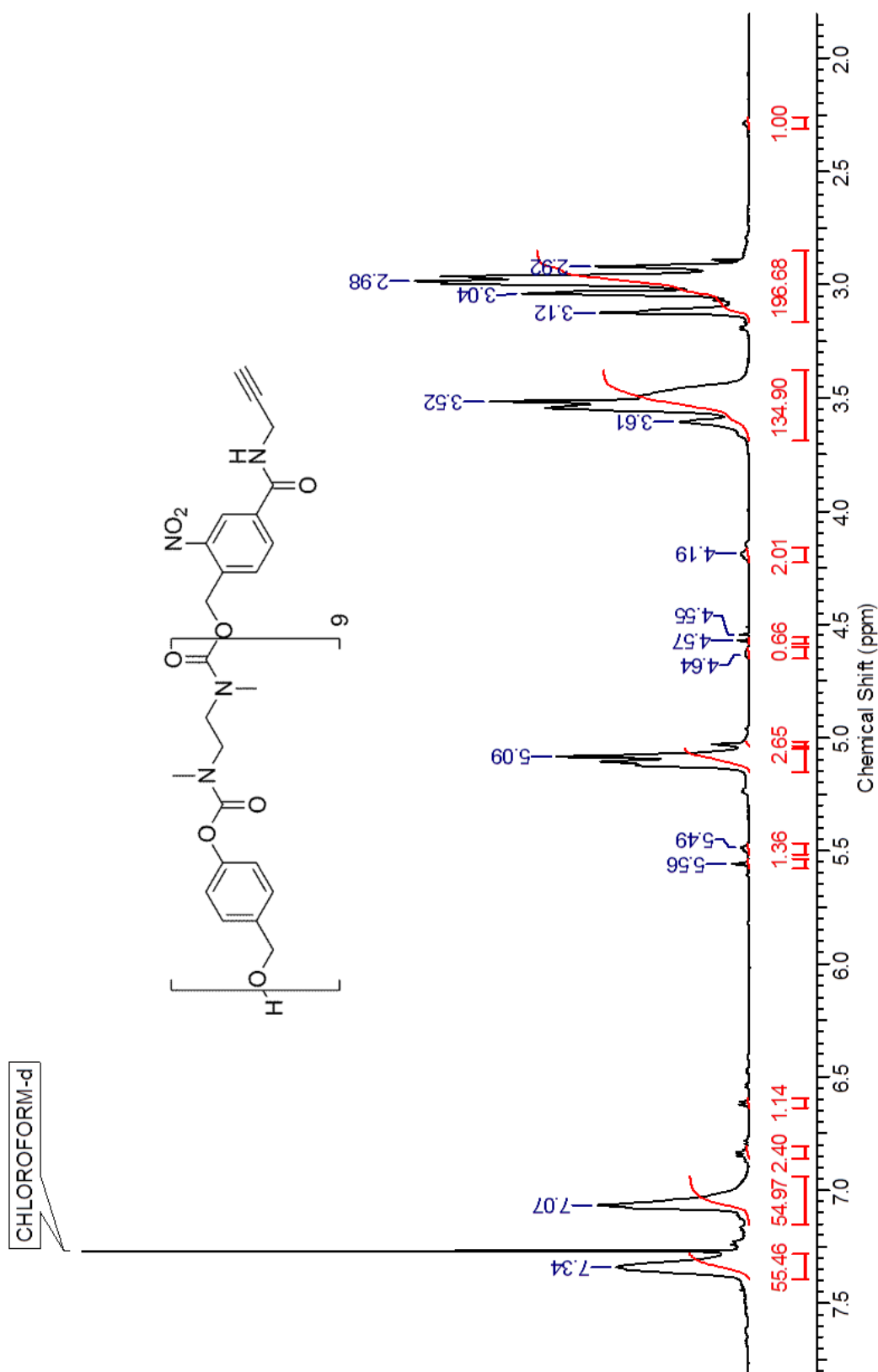
Figure A10: ^{1}H-NMR spectrum of compound polymer **S**.
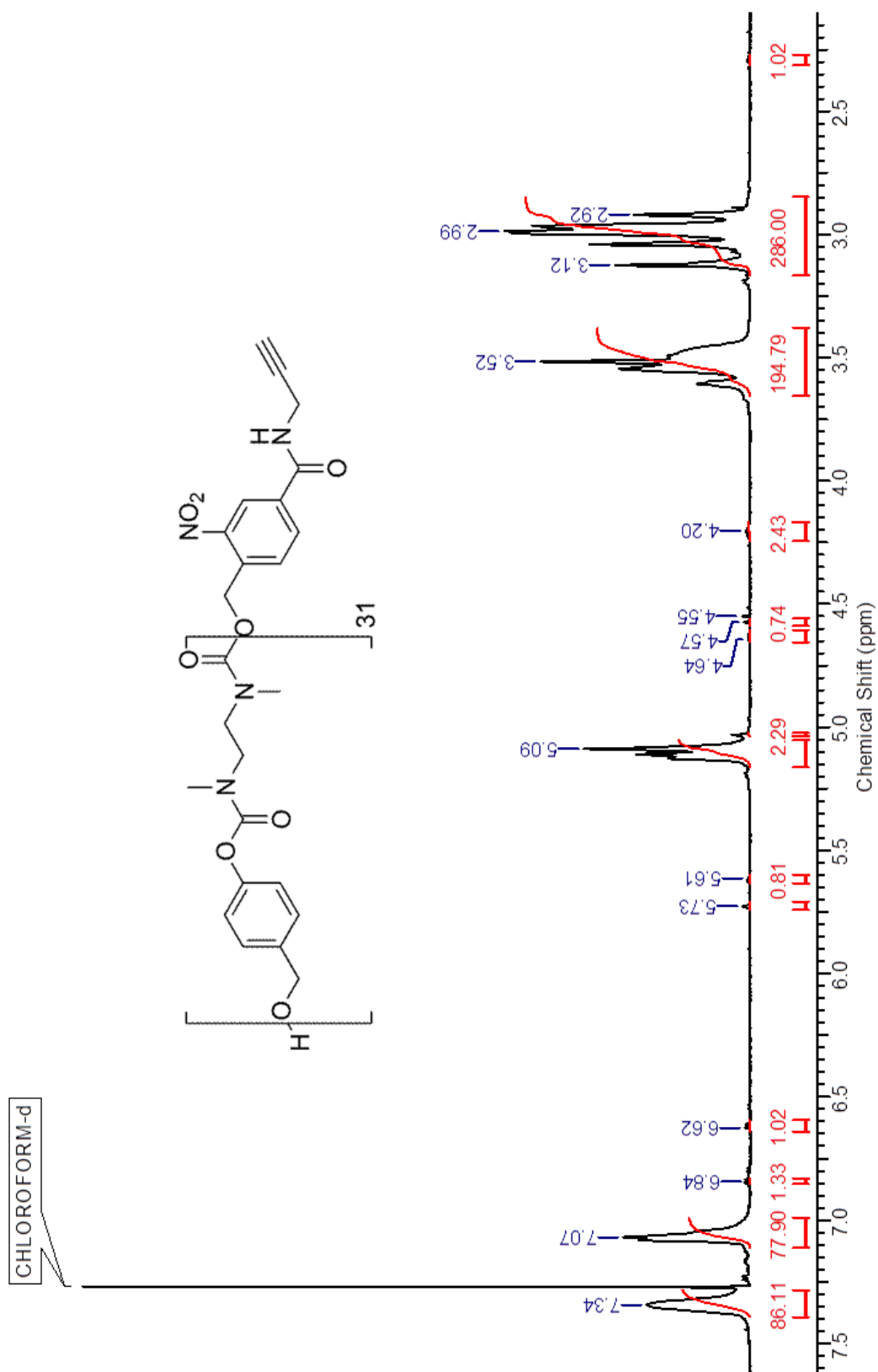
Figure A11: ^{1}H-NMR spectrum of compound polymer **L**.
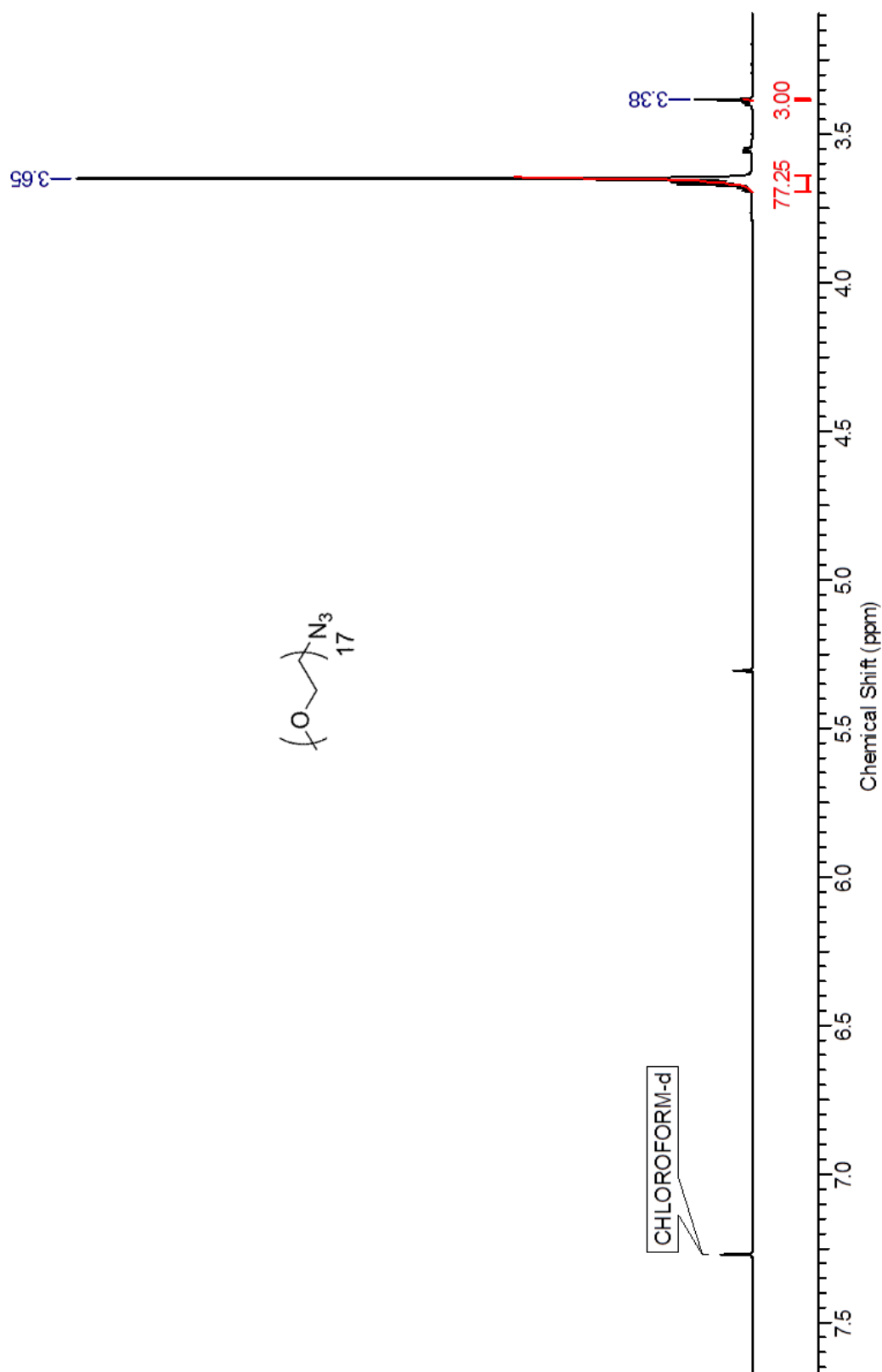
Figure A12: ^{1}H-NMR spectrum of compound **16** (750 g/mol).
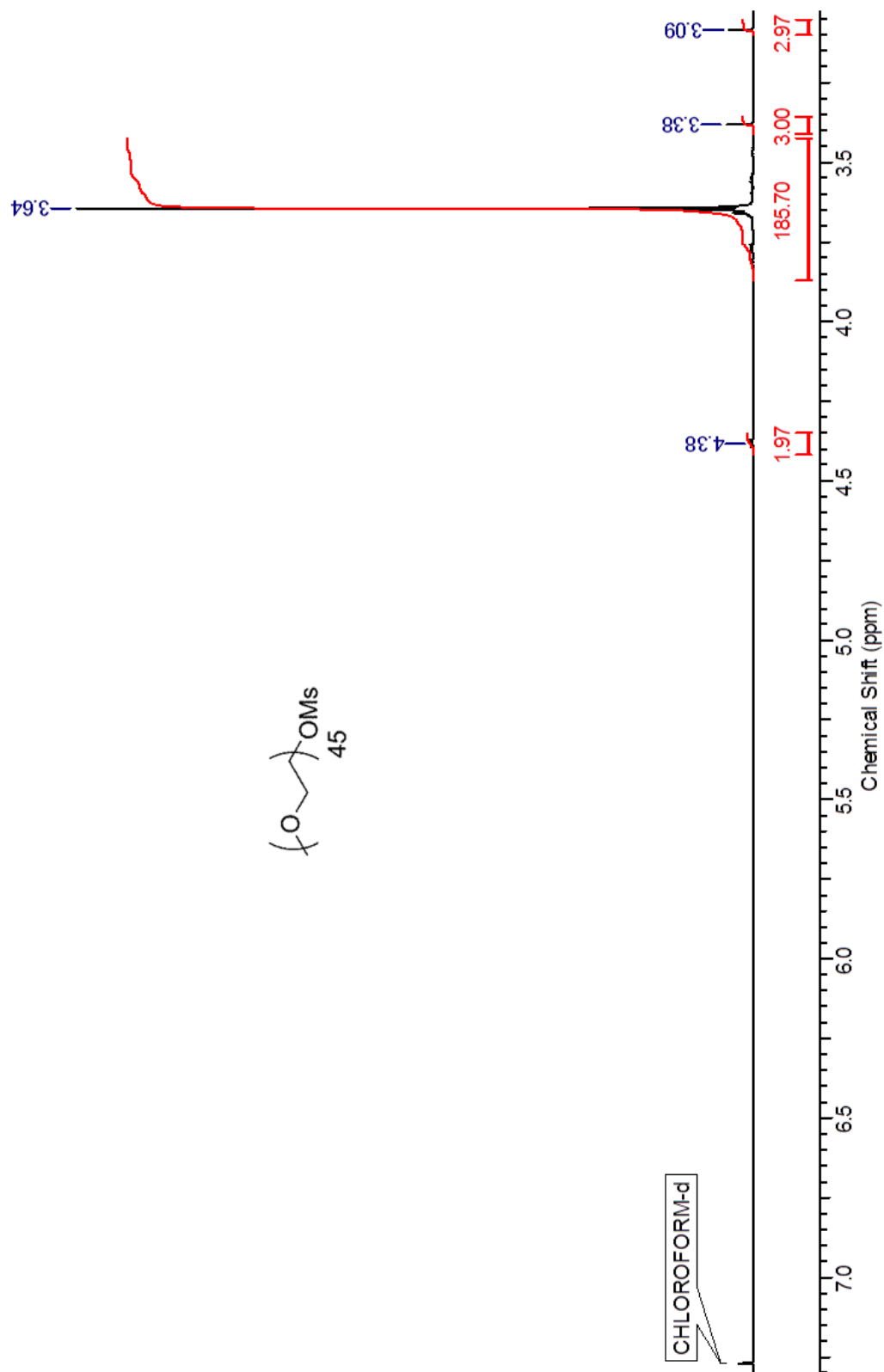
Figure A13: ^{1}H-NMR spectrum of compound **15** (2,000 g/mol).
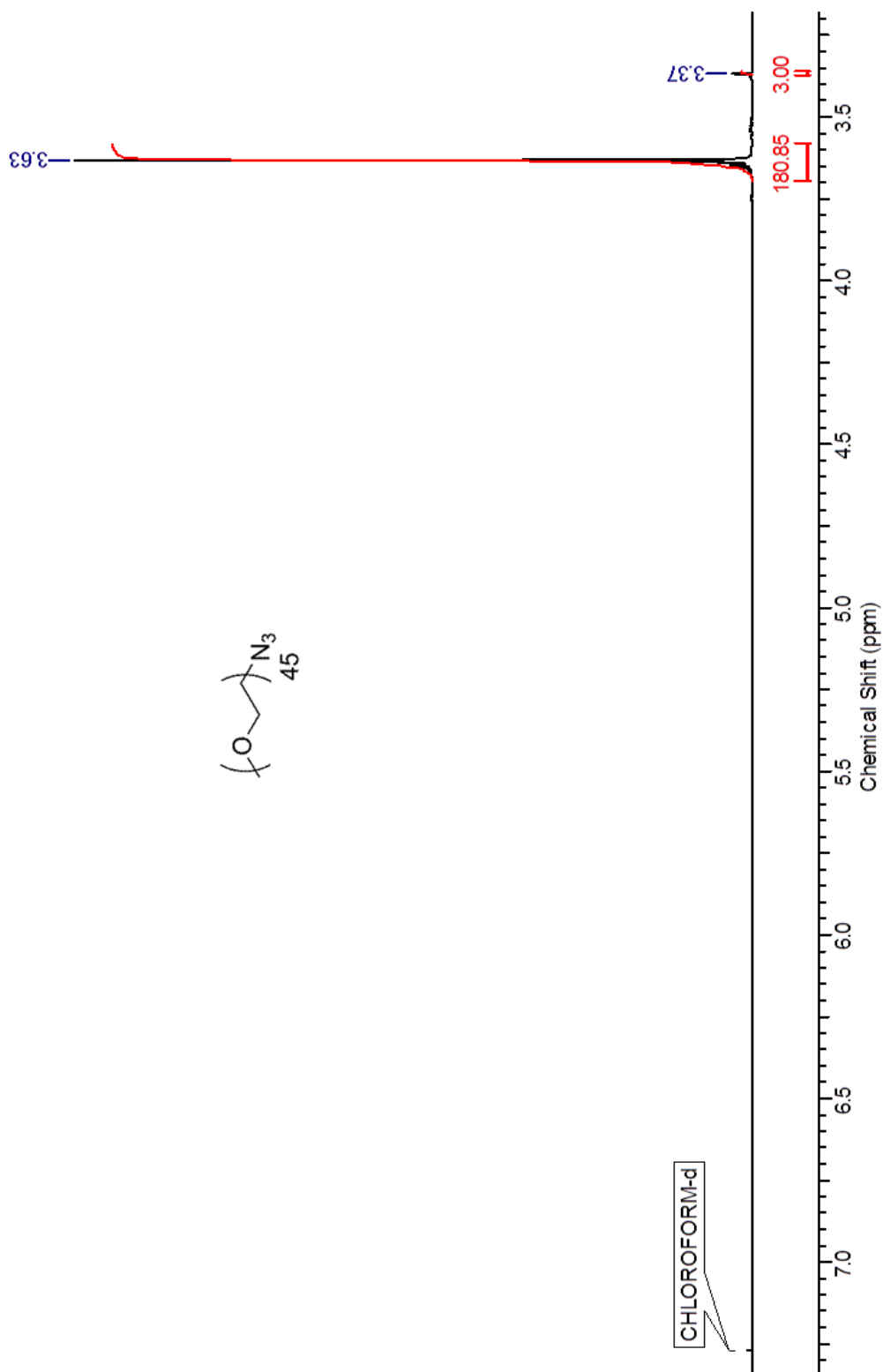
Figure A14: ^{1}H-NMR spectrum of compound **16** (2,000 g/mol).
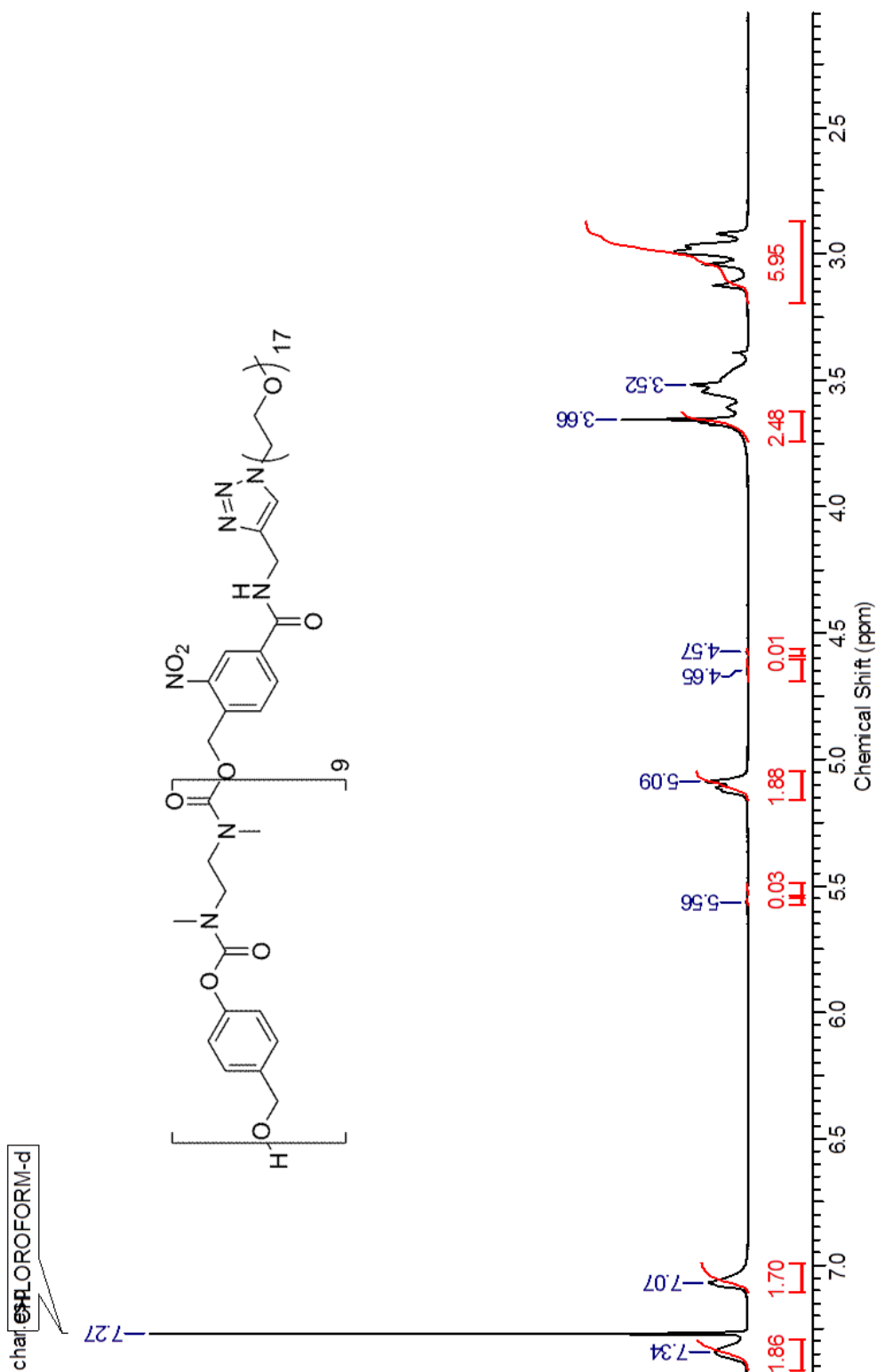
Figure A15: ¹H-NMR spectrum of copolymer **S-750.**
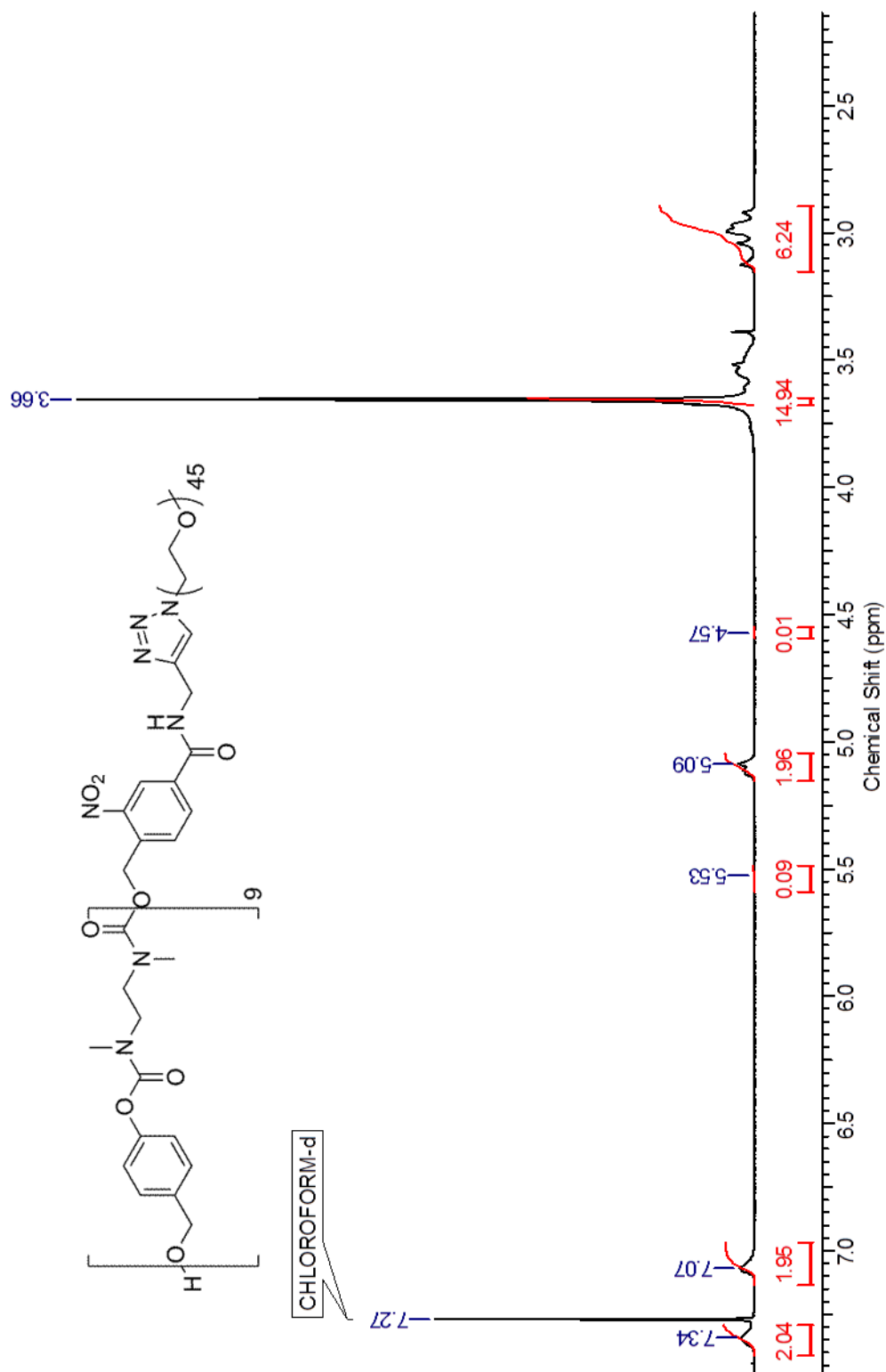
Figure A16: ^{1}H-NMR spectrum of copolymer **S-2,000.**
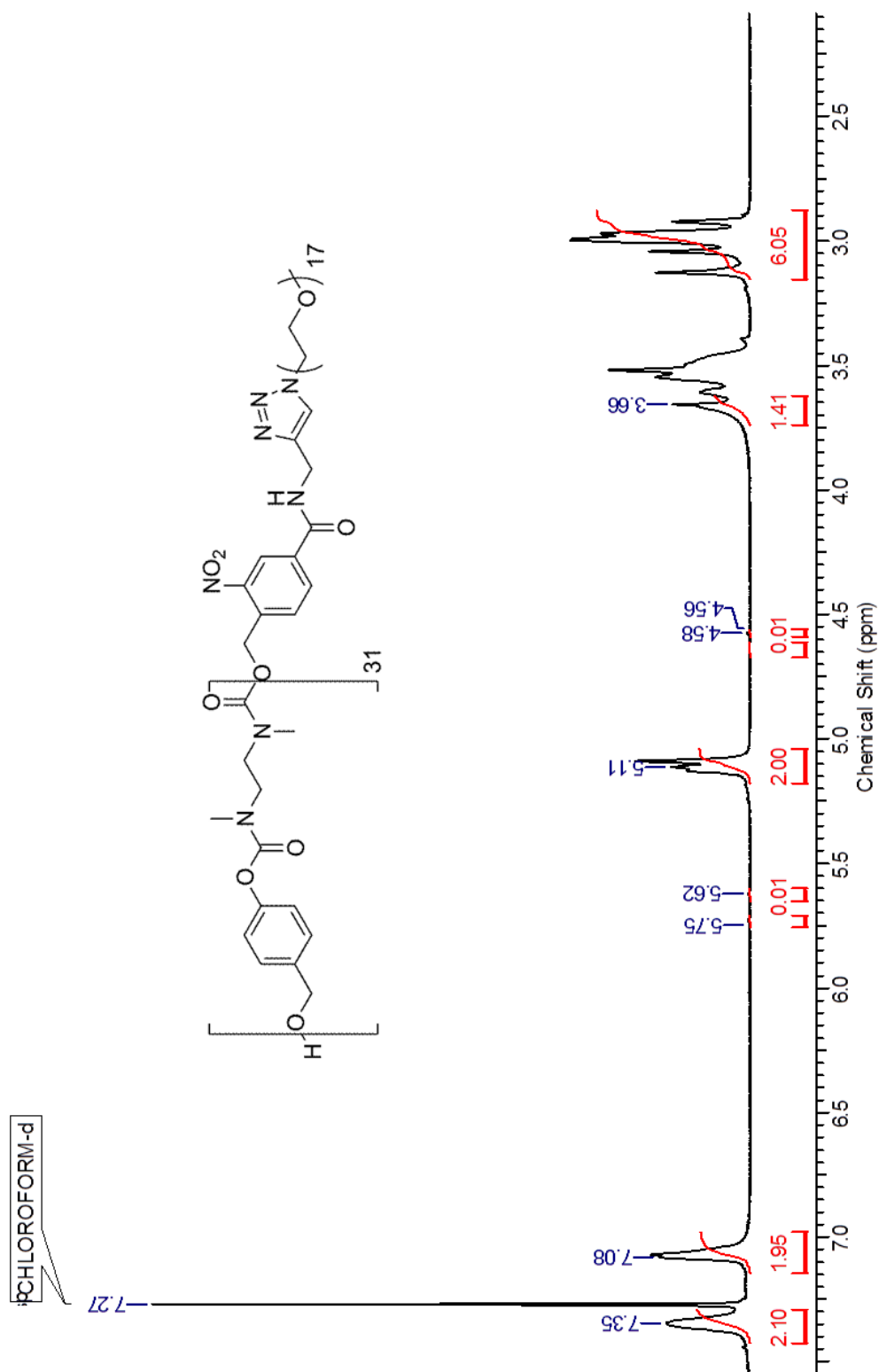
Figure A17: ^{1}H-NMR spectrum of copolymer **L-750.**
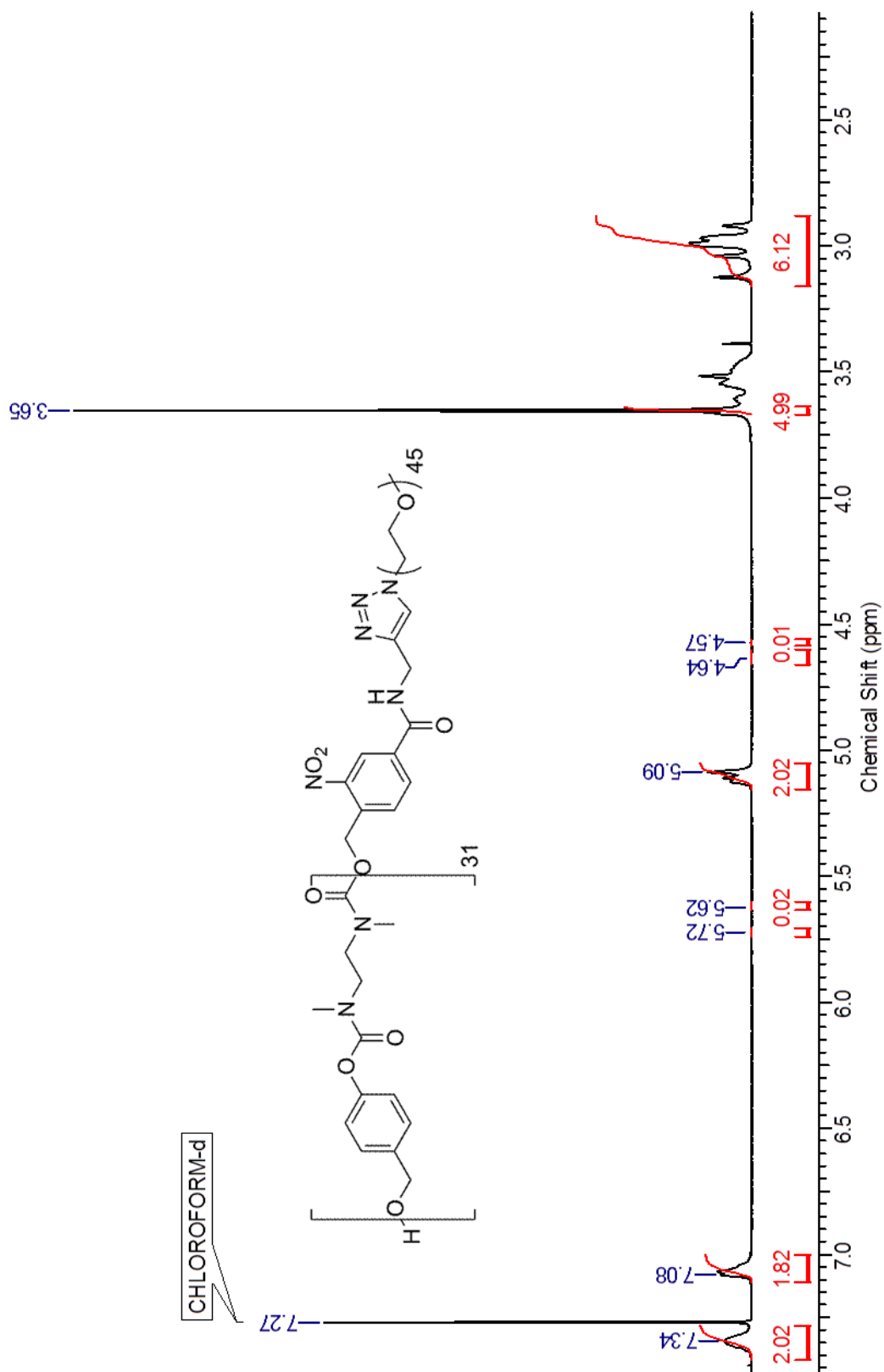
Figure A18: ^{1}H-NMR spectrum of copolymer **L-2,000.**
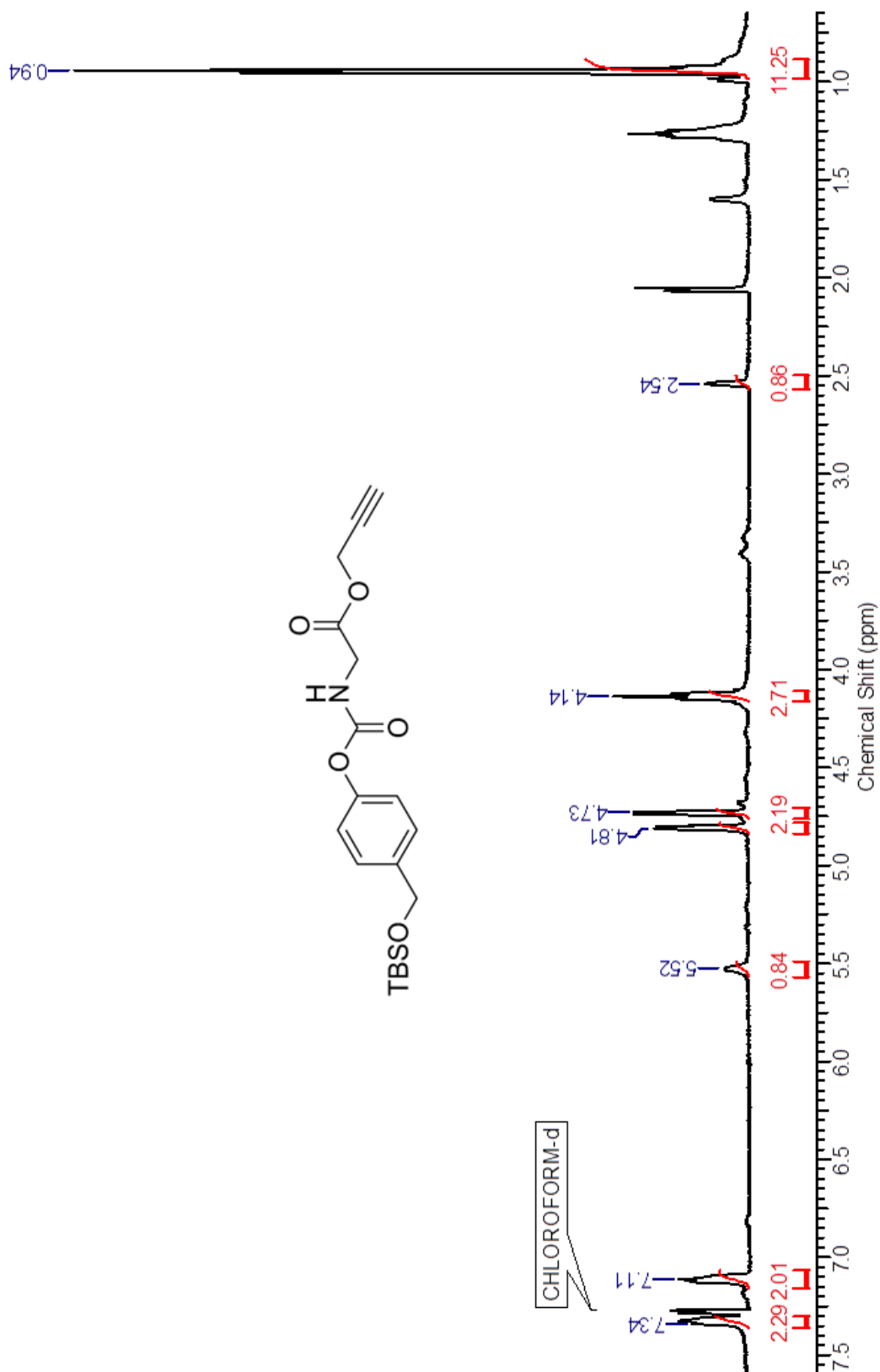
Figure A19: ^{1}H-NMR spectrum of compound **18**.
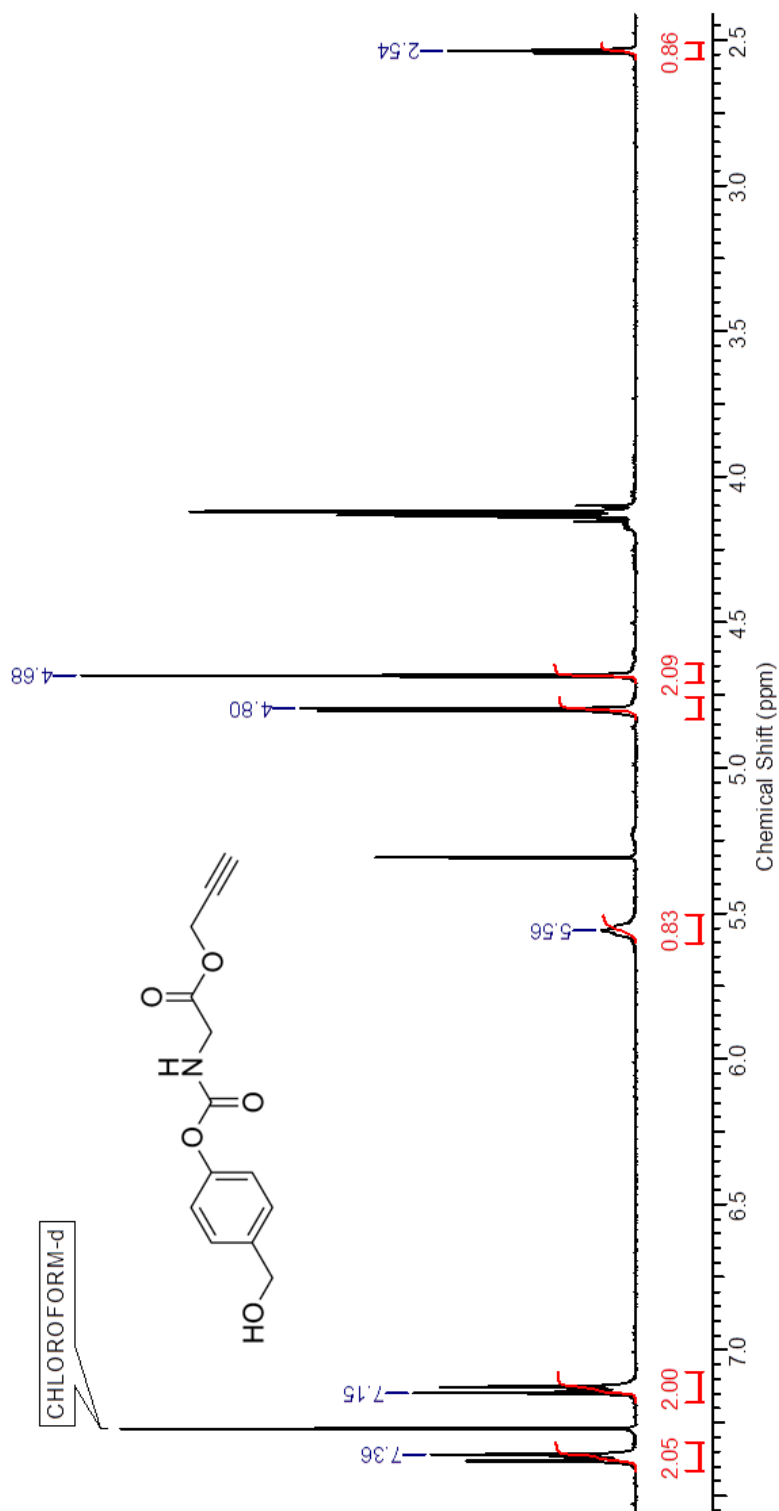
Figure A20: ^{1}H-NMR spectrum of compound **19**.
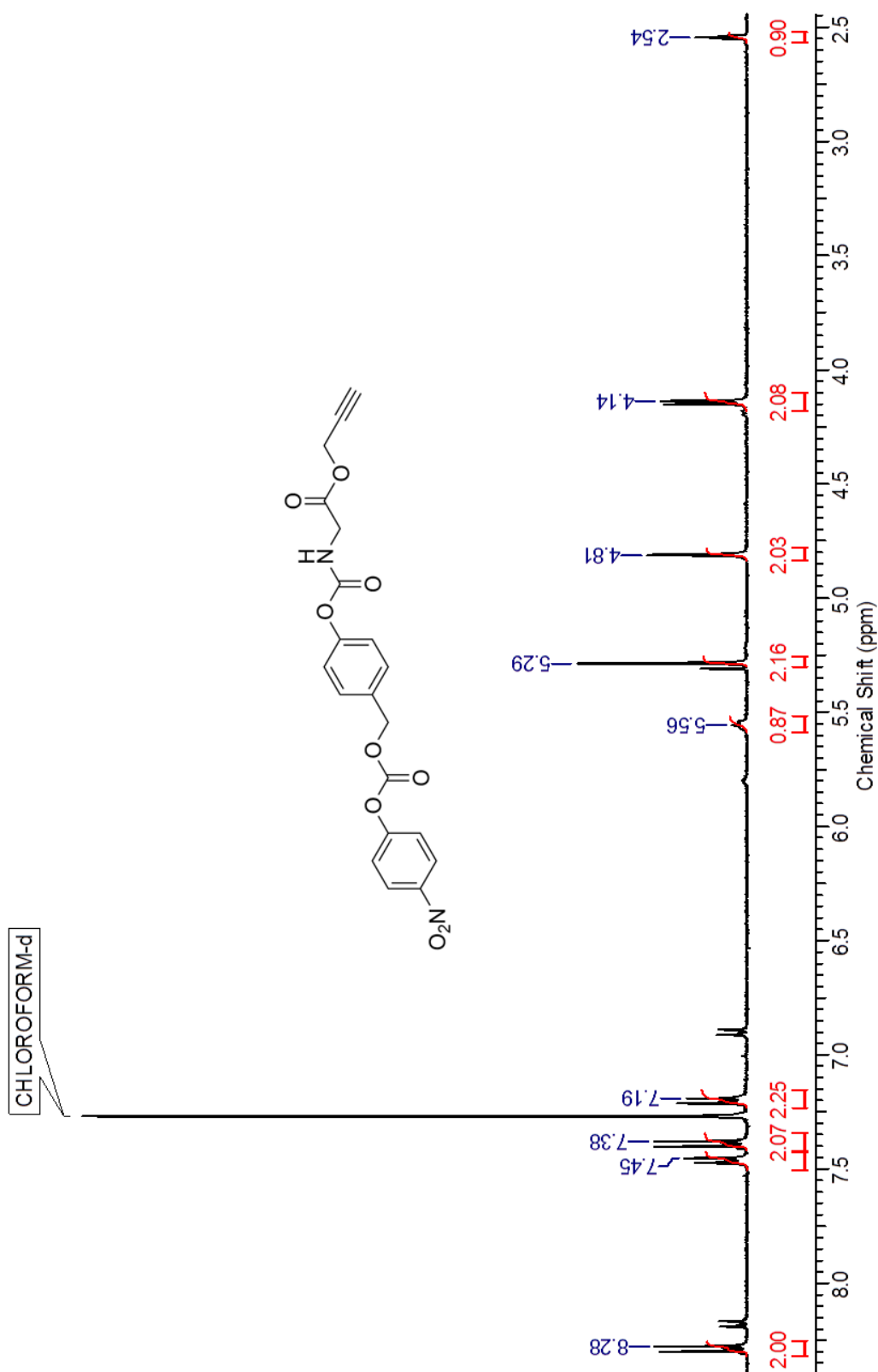
Figure A21: ^{1}H-NMR spectrum of compound **20**.
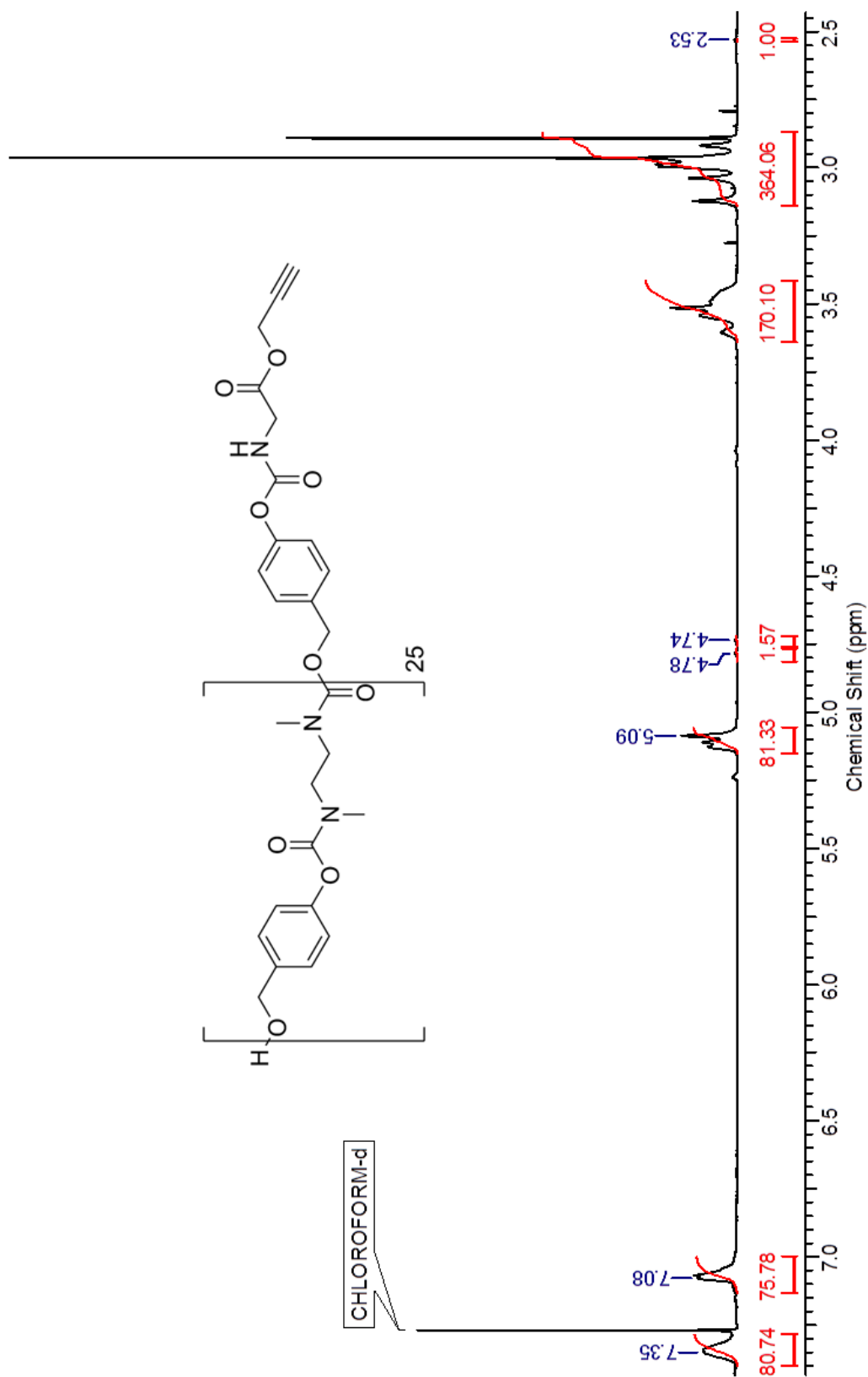
Figure A22: ^{1}H-NMR spectrum of polymer **C**.
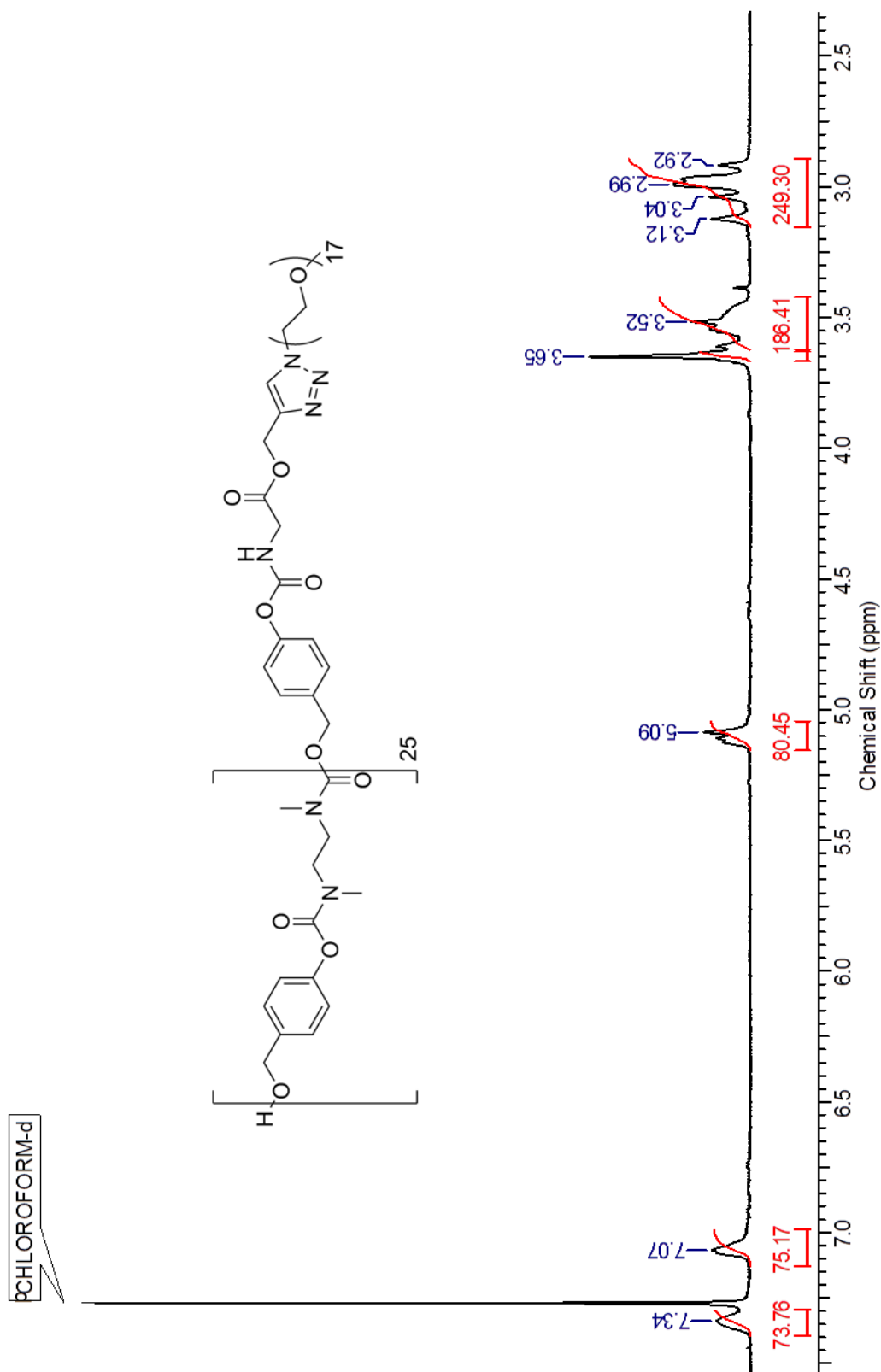
Figure A23: ^{1}H-NMR spectrum of copolymer **C-750**.
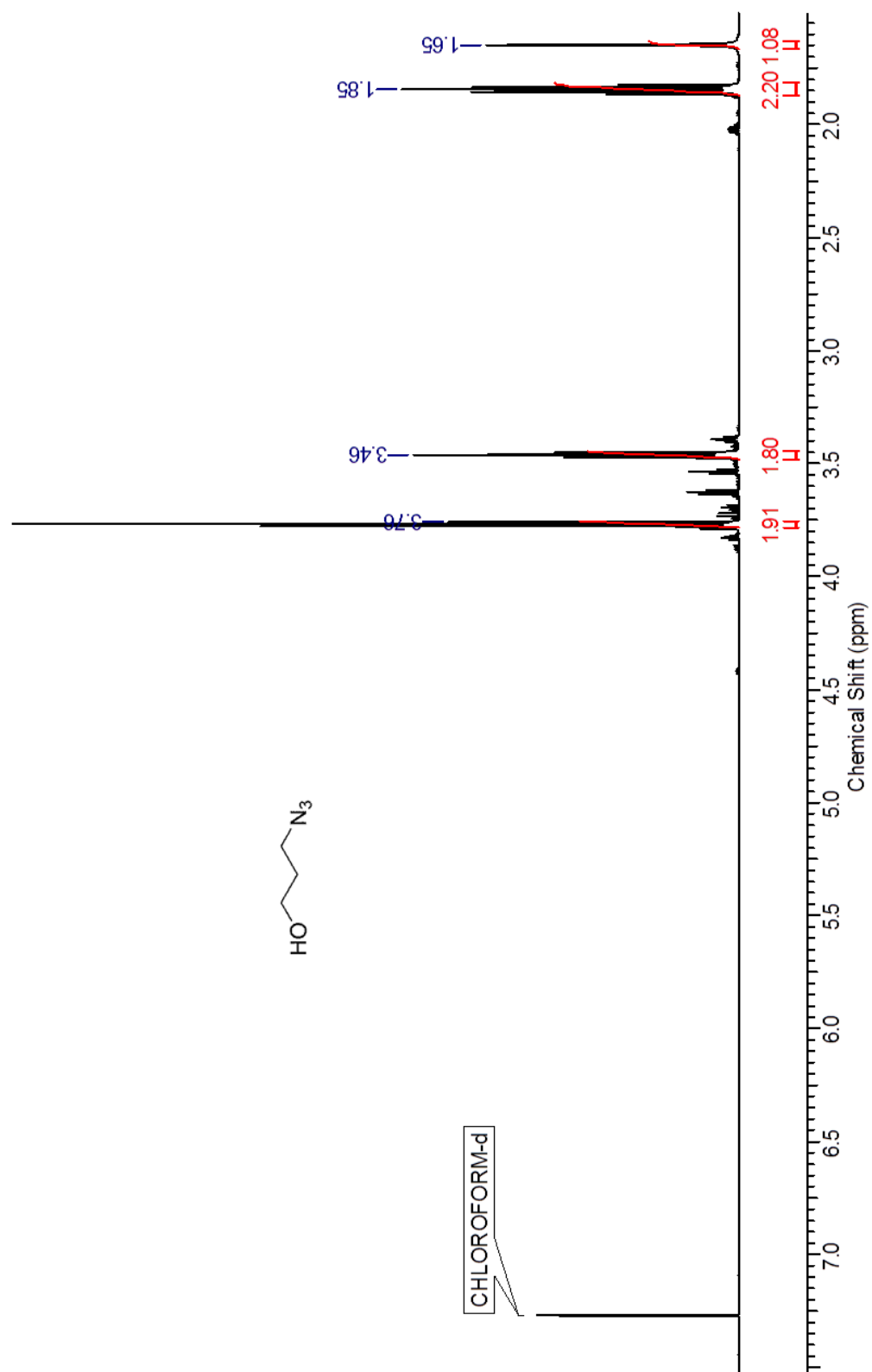
Figure A24: ¹H-NMR spectrum of compound **21**.
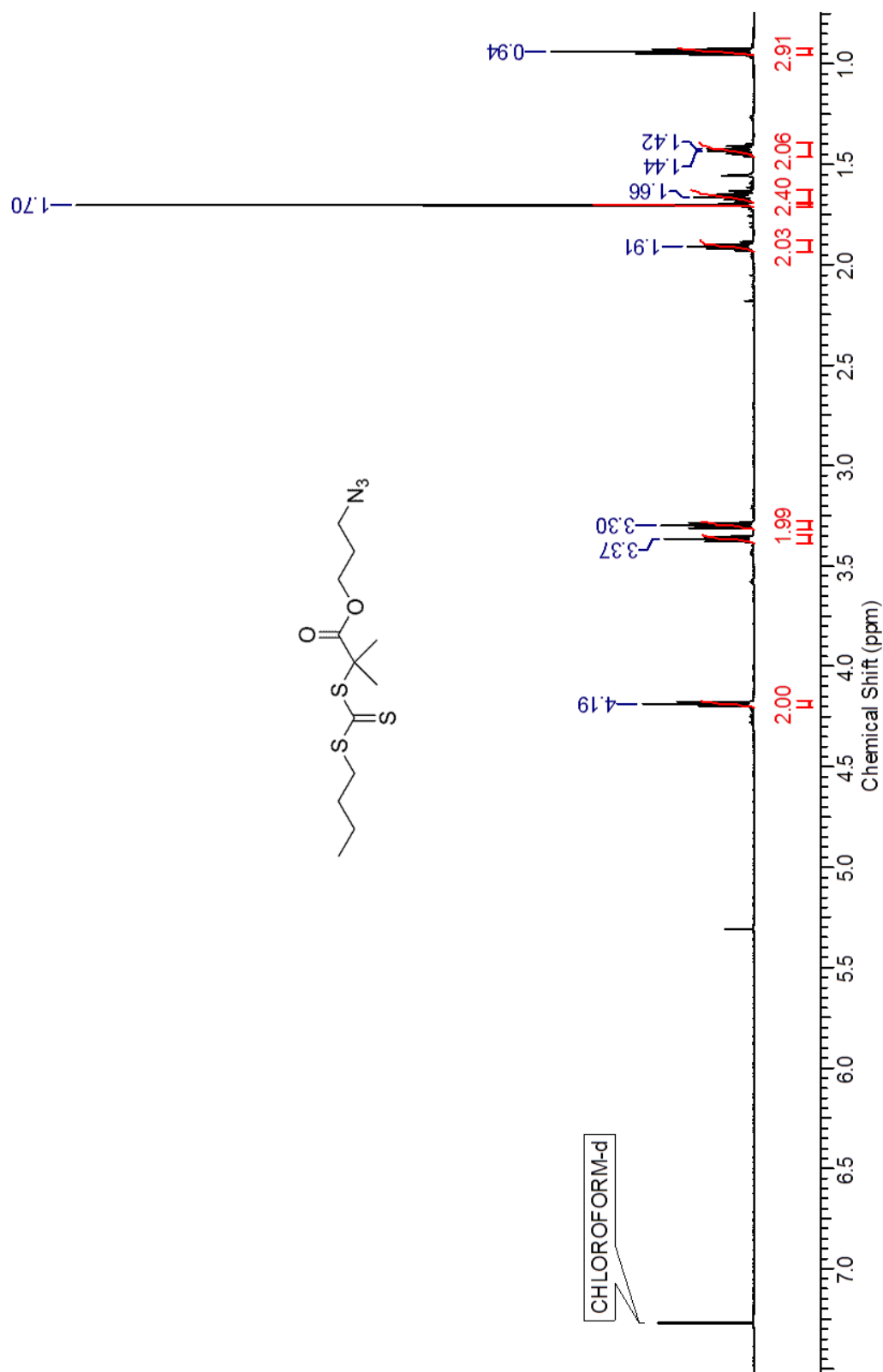
Figure A25: ¹H-NMR spectrum of compound **23**.
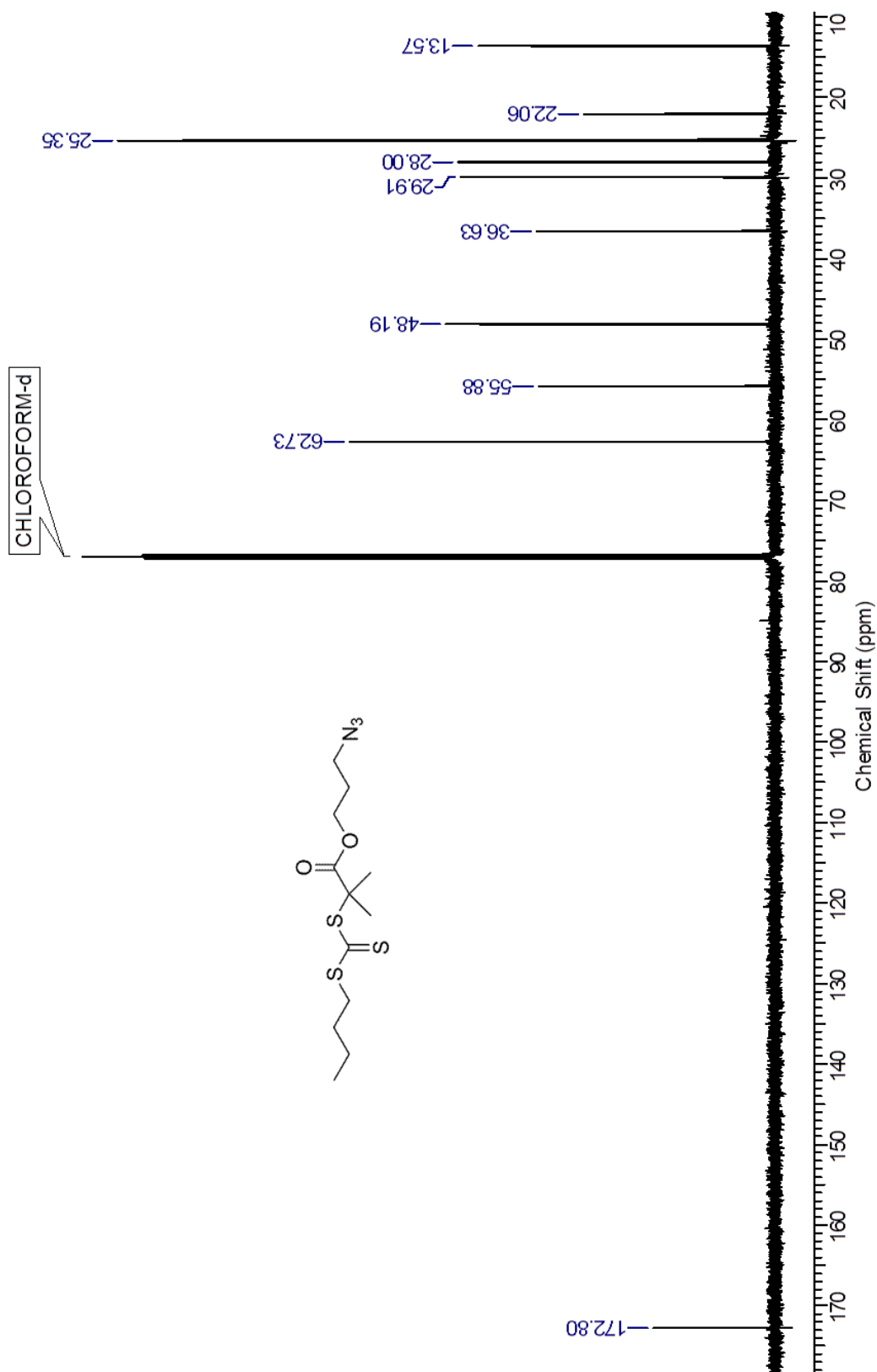
Figure A26: ^{13}C-NMR spectrum of compound **23**.
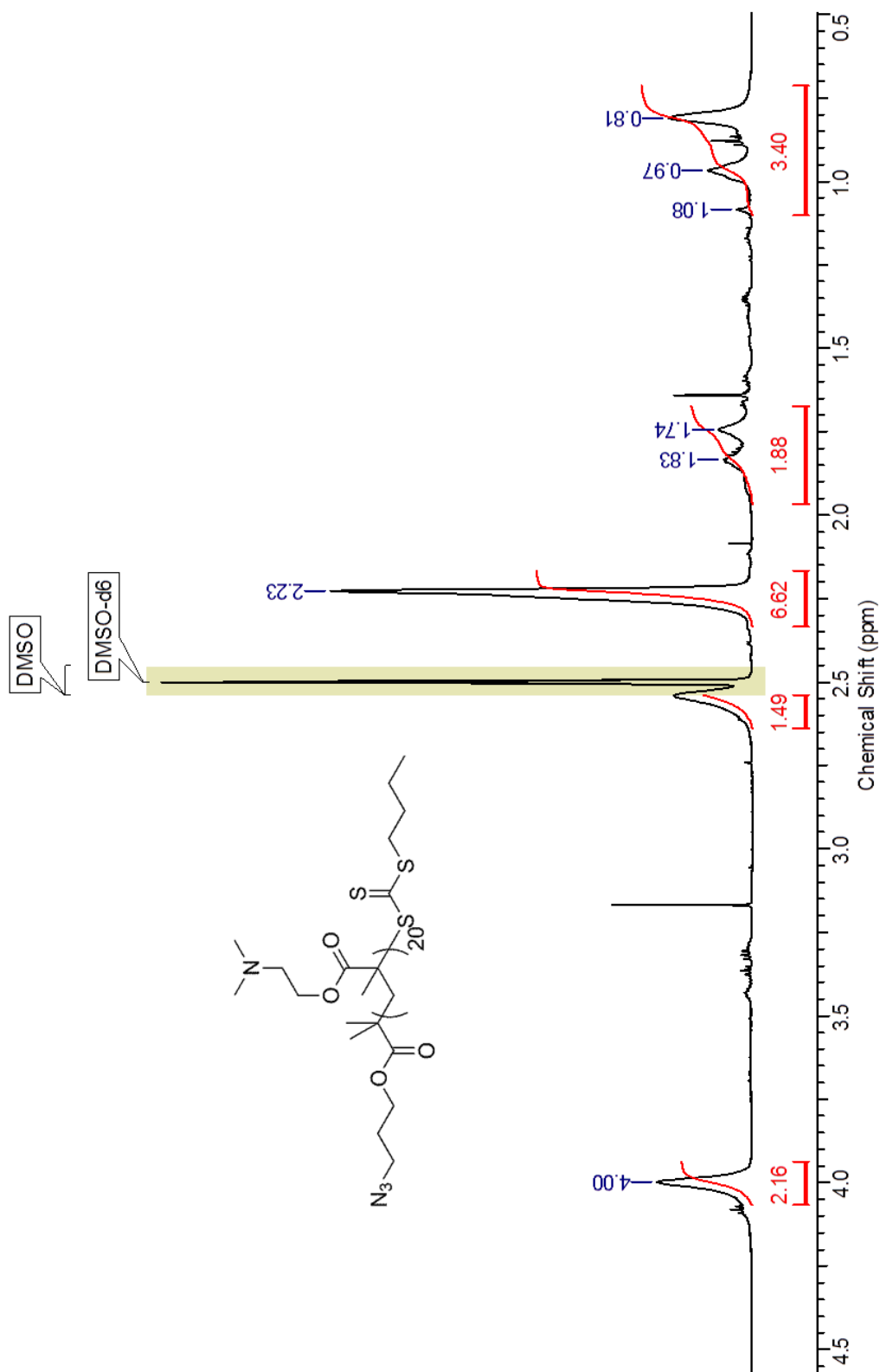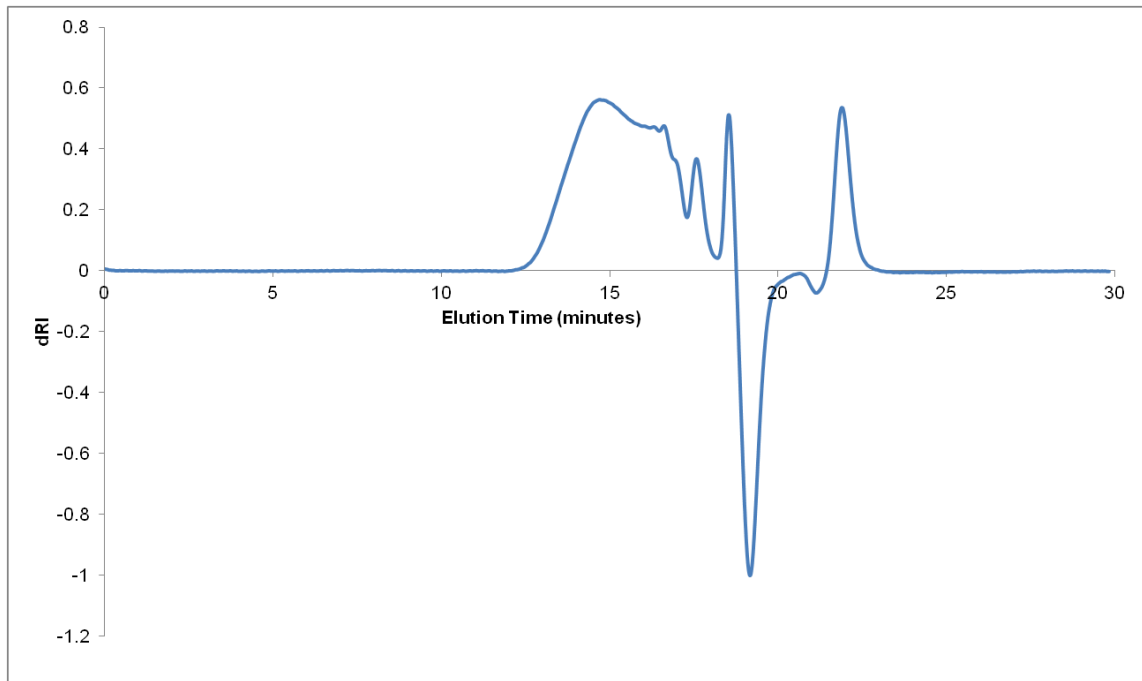
Figure A27: ¹H-NMR spectrum of compound **24**.

Appendix B: SEC Chromatograms
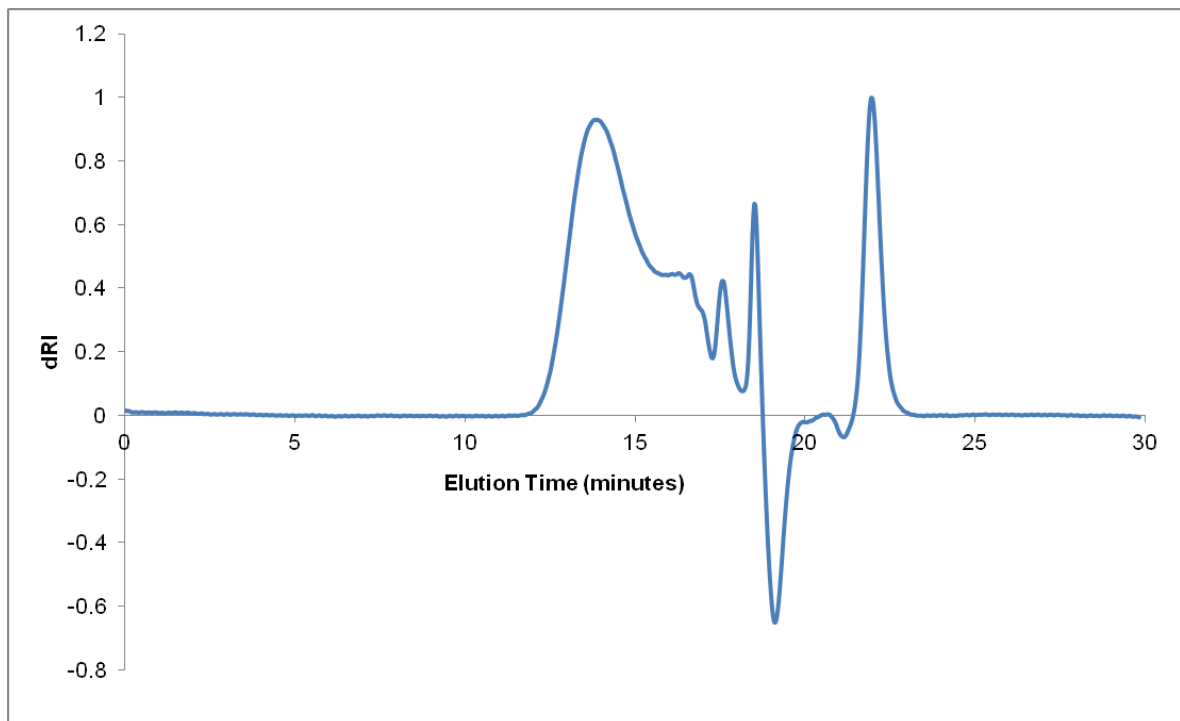

Figure B1: SEC chromatogram of polymer **S**.

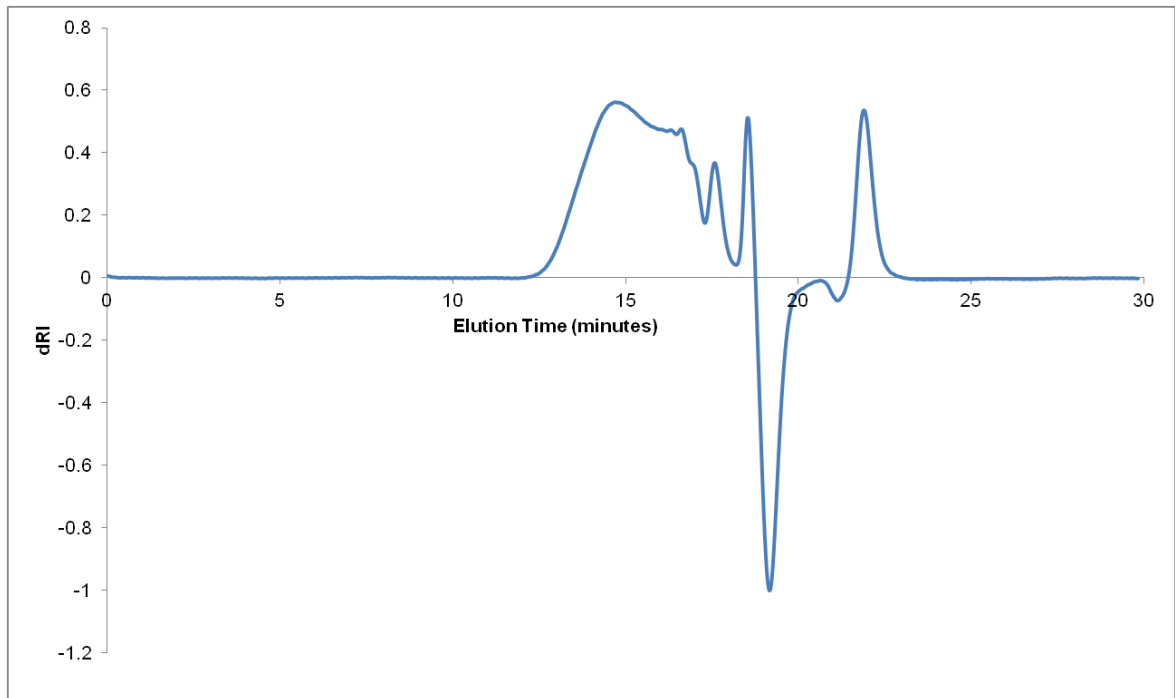Figure B2: SEC chromatogram of polymer **L**.

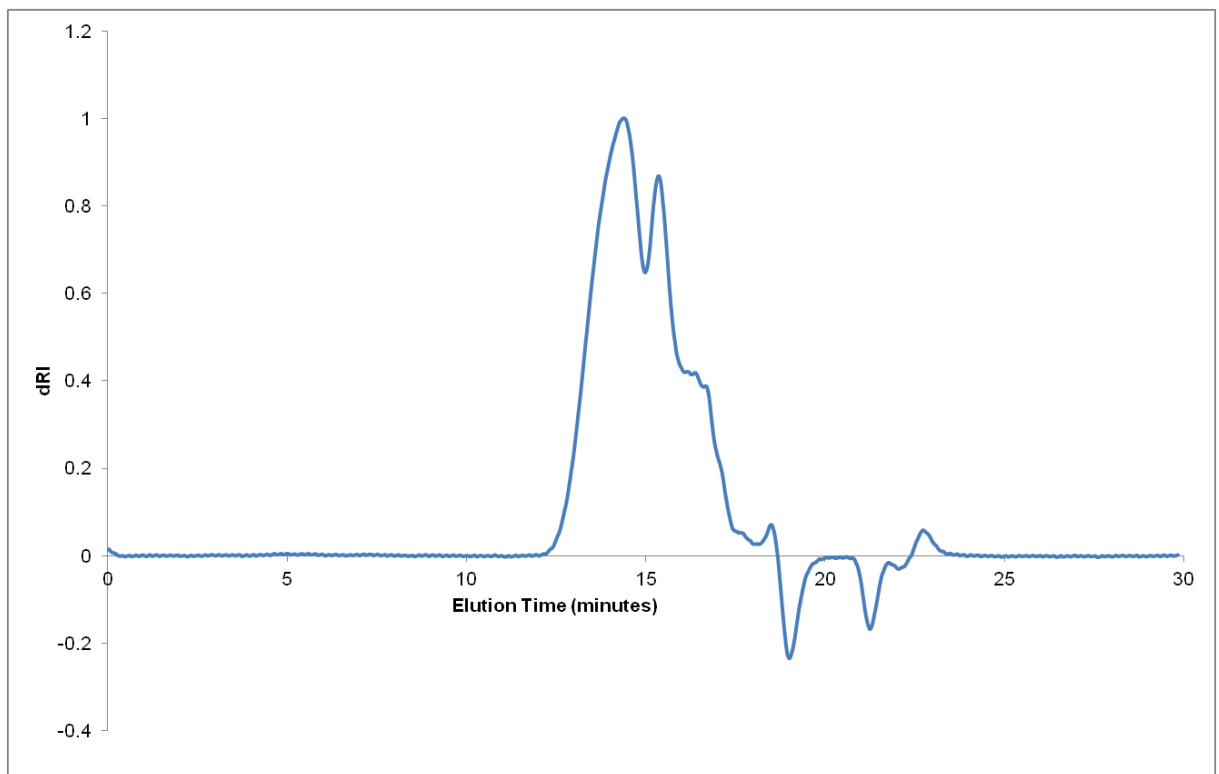Figure B3: SEC chromatogram of polymer **S-750**.
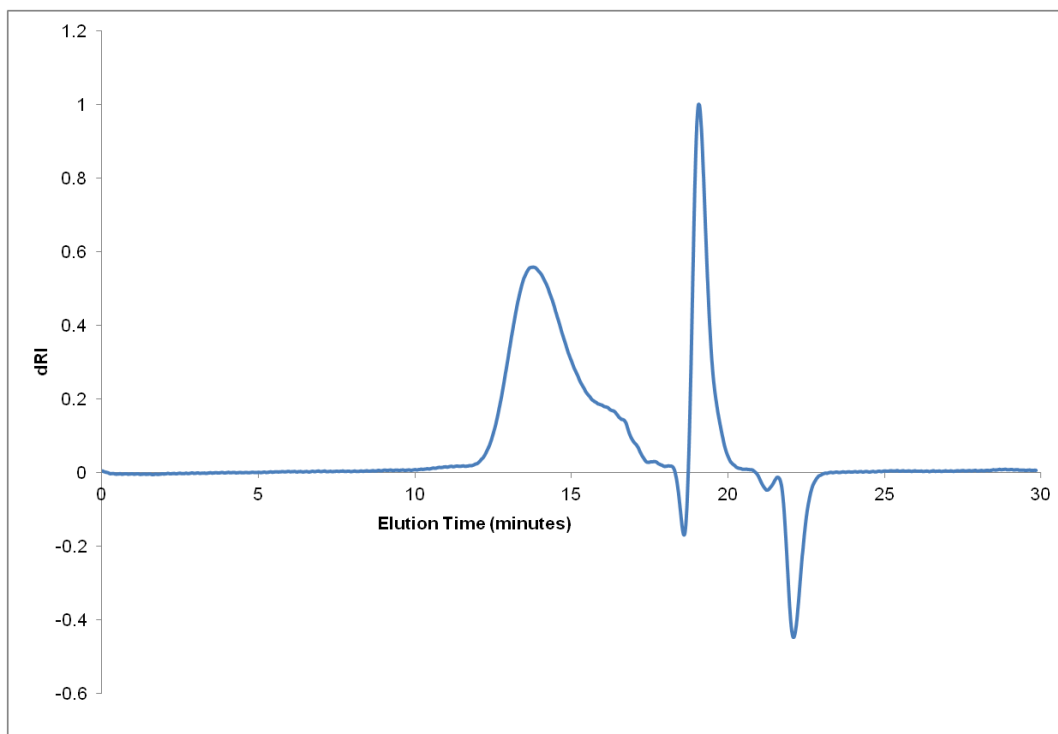

Figure B4: SEC chromatogram of polymer **S-2,000**.

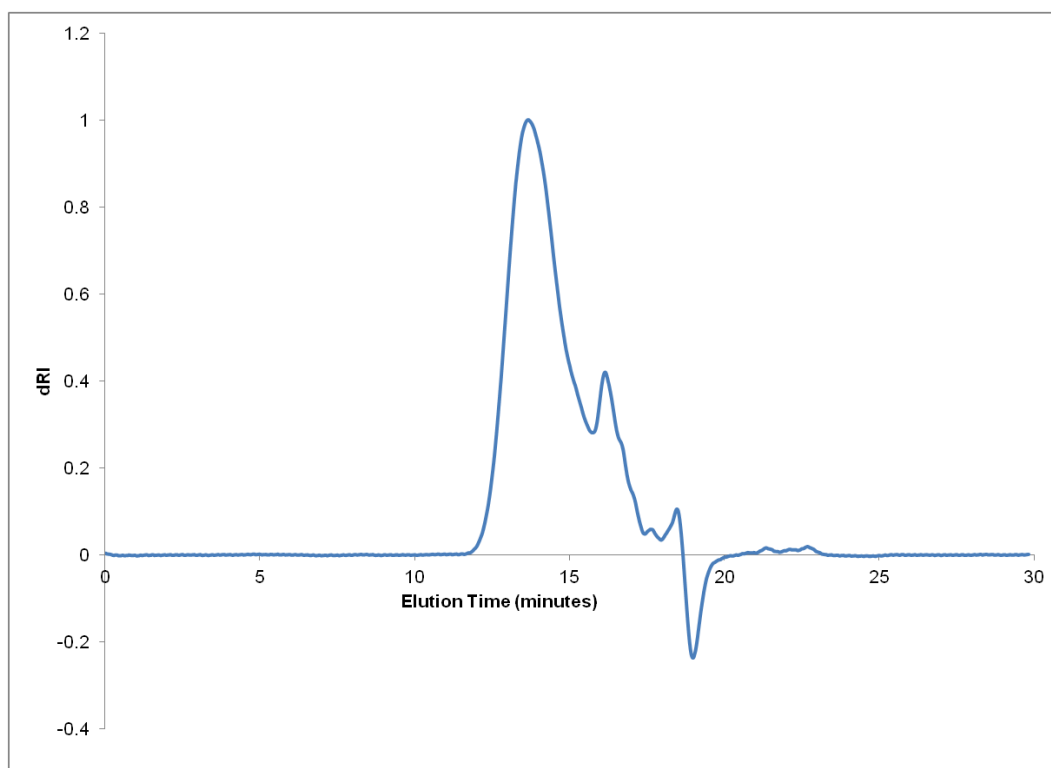Figure B5: SEC chromatogram of polymer **L-750**.

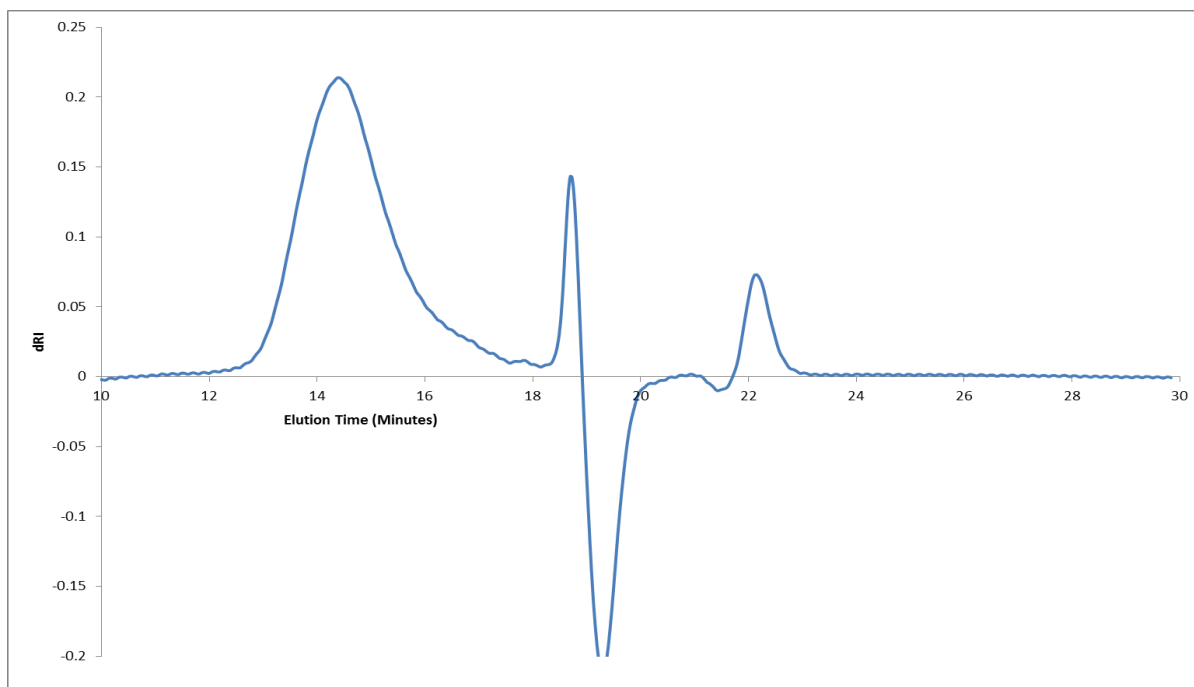Figure B6: SEC chromatogram of polymer **L-2,000**.
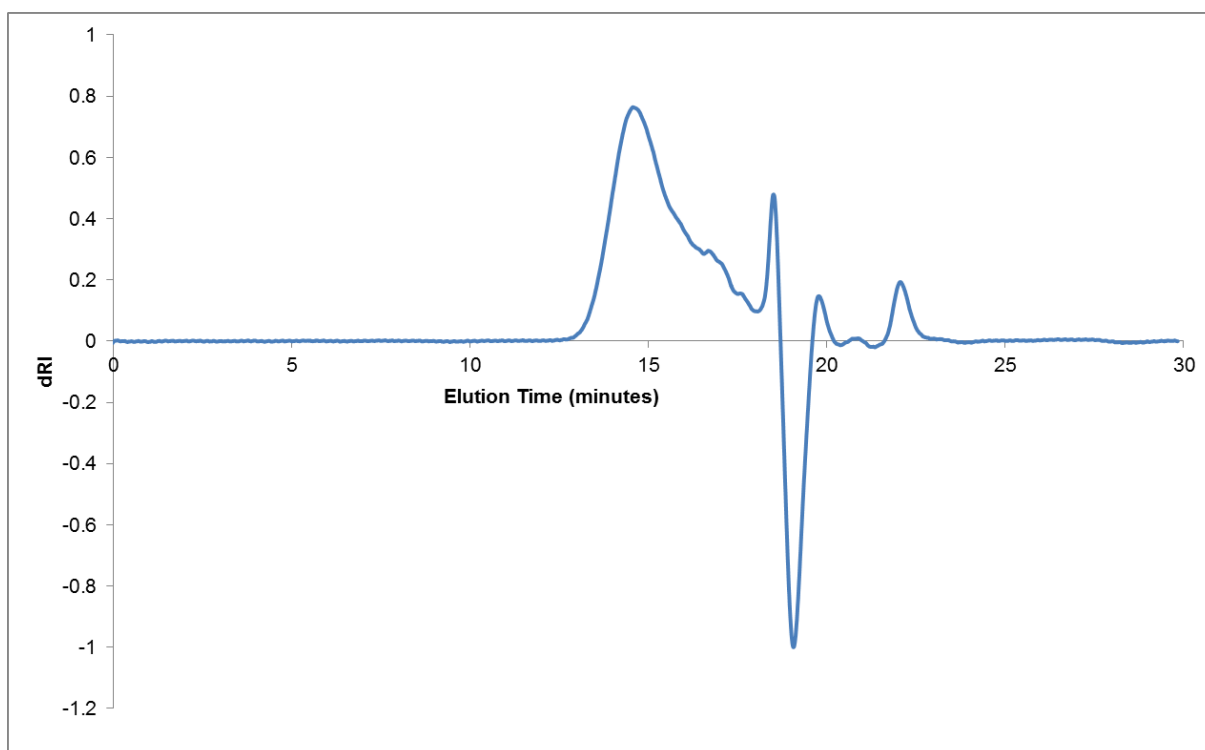
Figure B7: SEC chromatogram of polymer **C**.
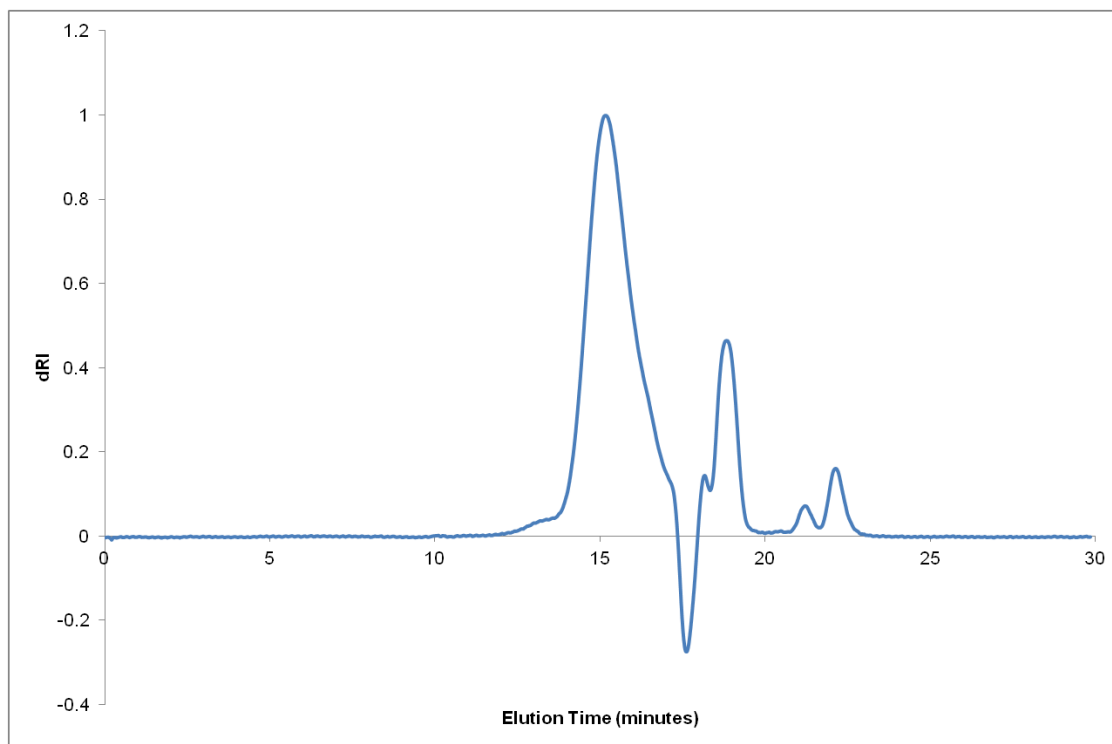

Figure B8: SEC chromatogram of copolymer **C-750**.

Figure B9: SEC chromatogram of polymer **24**.

Appendix C: Degradation Data

Data point	Hours	Raw count rate	Corrected count rate	% Release
X0	0	142904	122904	100
X1	24.13333	56918.63	36918.63	30.03859
X2	27.05	44530.6	24530.6	19.95916
X3	120.5167	35747.33	15747.33	12.81271
X4	151.0833	36498	16498	13.42348

Table C1: **L-2,000** Nile Red release data. The data points are labelled X0-X6. The "corrected" count rate is the fluoresence of the sample minus the fluoresence of the same concentration of Nile red in water.

Data point	Hours	Raw count rate	Corrected count rate	% Release
X0	0	249749	229749	100
X1	24.13333	131237.3	111237.3	52.54769
X2	27.05	109374.7	89374.67	43.79384
X3	120.5167	81424.83	61424.83	32.60267
X4	151.0833	79576.9	59576.9	31.86275

Table C2: **L-750** Nile Red release data.

Data point	Hours	Raw count rate	Corrected count rate	% Release
X0	0	103466	83466	100
X1	24.13333	78649.8	58649.8	76.01512
X2	27.05	77983.4	57983.4	75.37104
X3	120.5167	77087	57087	74.50467
X4	151.0833	76975	56975	74.39642

.

Table C3: Control copolymer Nile red release data.

Code	Time (minutes)	Count Rate (kcps)	Z-Ave. (nm)	PDI.
208Deg0	0	200.5	293	0.14
208Deg1	68	283	275	0.331
208Deg2	123	417	136	0.312
208Deg3	251	686	135	0.457
208Deg4	377	665	150	0.5
208Deg5	465	755	200	0.34
208Deg6	1514	631	133	0.376
208Deg7	1815	875	127	0.332
208Deg8	3190	950	101	0.33

Table C4: **L-2,000** DLS degradation data.

Code	Time (minutes)	Count Rate (kcps)	Z-Ave. (nm)	PDI.
216Deg0	0	327.8	171	0.14
216Deg1	57	271	205	0.13
216Deg2	122	218	211	0.196
216Deg3	251	205	212	0.144
216Deg4	377	177	221	0.164
216Deg5	464	160	216	0.136
216Deg6	1513	79	236	0.217
216Deg7	1814	77	242	0.182
216Deg8	3188	71	247	0.147

Table C5: **L-750** DLS degradation data.

Appendix D: DLS Data.

Results

		Size (d.nm):	% Volume	Width (d.nm):
Z-Average (d.nm): 145.1	**Peak 1:**	145.9	100.0	54.82
PdI: 0.143	**Peak 2:**	0.000	0.0	0.000
Intercept: 0.939	**Peak 3:**	0.000	0.0	0.000
Result quality : Good				
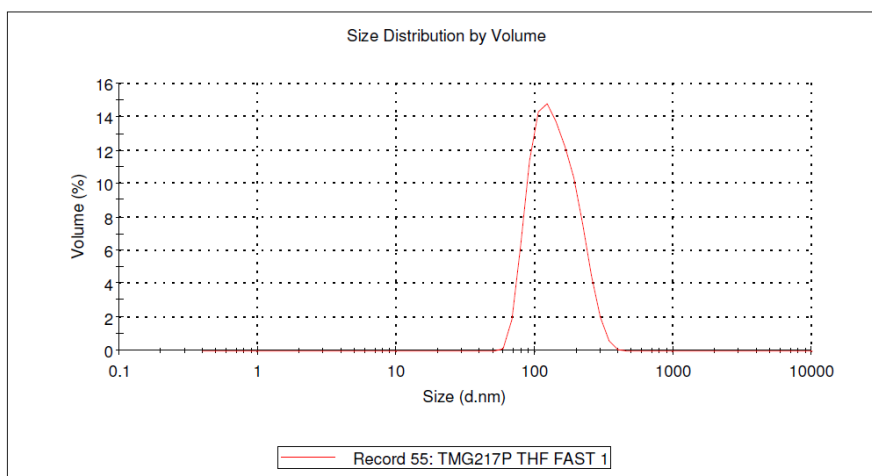
Results

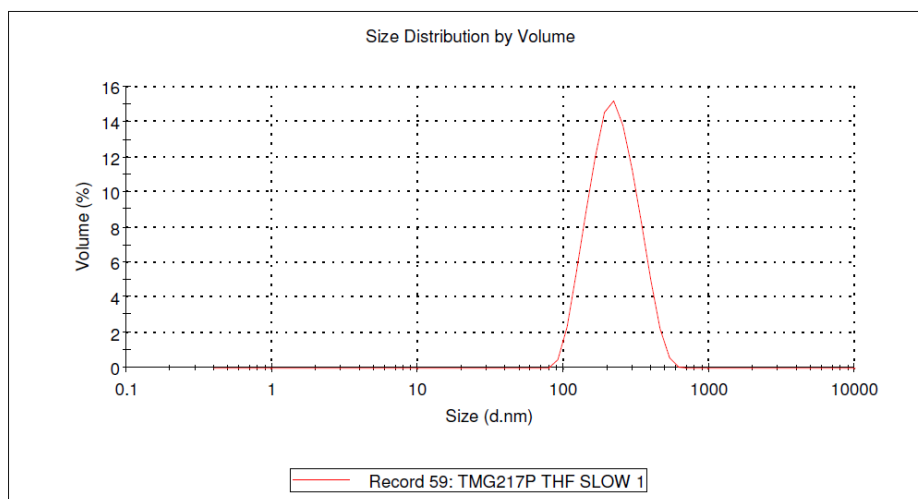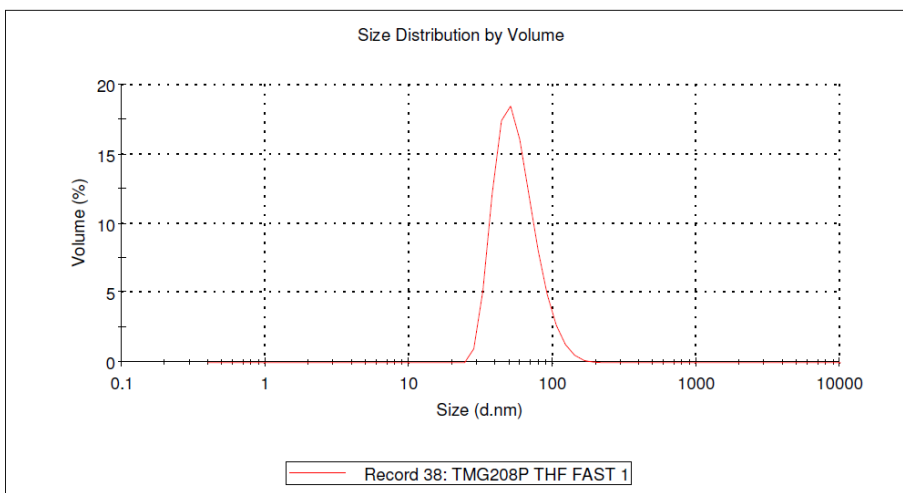|		Size (d.nm):	% Volume	Width (d.nm):
Z-Average (d.nm): 208.8	**Peak 1:**	233.2	100.0	85.51
PdI: 0.117	**Peak 2:**	0.000	0.0	0.000
Intercept: 0.954	**Peak 3:**	0.000	0.0	0.000
Result quality : Good				

Figure D1: The DLS traces of **S-750** following a) (top) fast aqueous self-assembly and b) (bottom) slow self-assembly.

Results

		Size (d.nm):	% Volume	Width (d.nm):
Z-Average (d.nm): 67.99	Peak 1:	57.60	100.0	20.36
PdI: 0.105	Peak 2:	0.000	0.0	0.000
Intercept: 0.959	Peak 3:	0.000	0.0	0.000
Result quality : Good				

Results

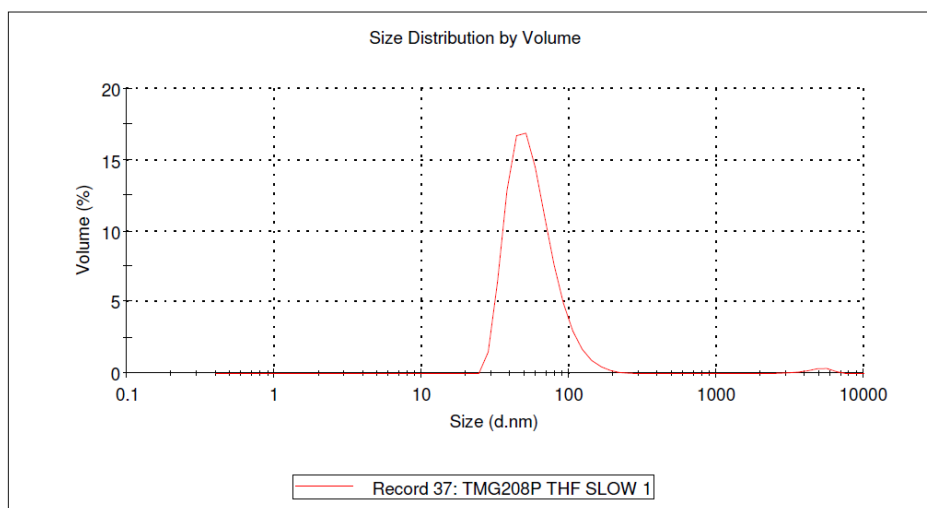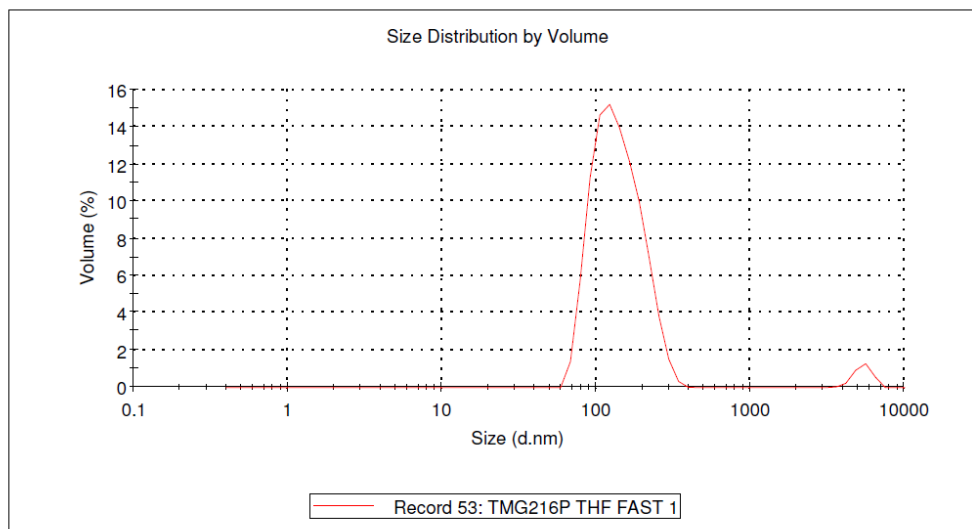|		Size (d.nm):	% Volume	Width (d.nm):
Z-Average (d.nm): 74.89	Peak 1:	58.41	98.8	23.95
PdI: 0.190	Peak 2:	4839	1.2	971.4
Intercept: 0.961	Peak 3:	0.000	0.0	0.000
Result quality : Good				

Figure D2: The DLS traces of **S-2,000** following a) (top) fast aqueous self-assembly and b) (bottom) slow self-assembly.

Results

			Size (d.nm):	% Volume	Width (d.nm):
Z-Average (d.nm):	147.4	Peak 1:	143.6	97.0	51.30
PdI:	0.153	Peak 2:	5369	3.0	681.2
Intercept:	0.940	Peak 3:	0.000	0.0	0.000
Result quality :	Good				

Size Distribution by Volume

Record 53: TMG216P THF FAST 1

Results

			Size (d.nm):	% Volume	Width (d.nm):
Z-Average (d.nm):	214.2	Peak 1:	233.6	100.0	80.73
PdI:	0.144	Peak 2:	0.000	0.0	0.000
Intercept:	0.944	Peak 3:	0.000	0.0	0.000
Result quality :	Good				

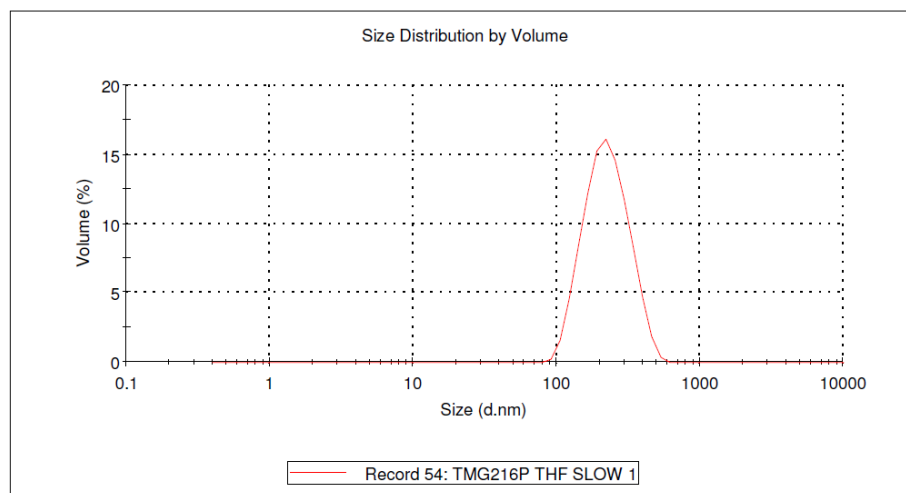Size Distribution by Volume
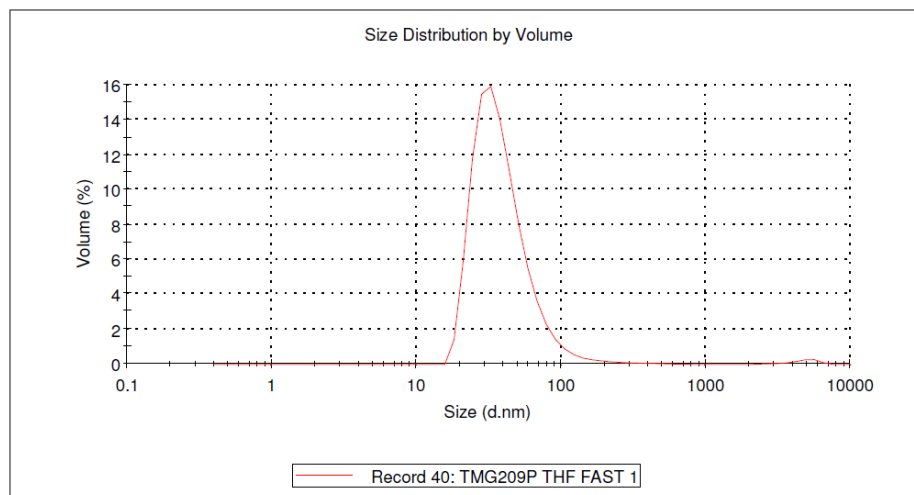
Record 54: TMG216P THF SLOW 1

Figure D3: The DLS traces of **L-750** following a) (top) fast aqueous self-assembly and b) (bottom) slow self-assembly.

Results

			Size (d.nm):	% Volume	Width (d.nm):
Z-Average (d.nm):	66.30	**Peak 1:**	42.07	99.1	31.55
PdI:	0.330	**Peak 2:**	4808	0.9	997.6
Intercept:	0.958	**Peak 3:**	0.000	0.0	0.000
Result quality :	Good				

Size Distribution by Volume

Record 40: TMG209P THF FAST 1

Results

			Size (d.nm):	% Volume	Width (d.nm):
Z-Average (d.nm):	480.0	**Peak 1:**	98.75	4.4	17.07
PdI:	0.530	**Peak 2:**	20.54	95.6	3.077
Intercept:	0.976	**Peak 3:**	0.000	0.0	0.000
Result quality :	Refer to quality report				

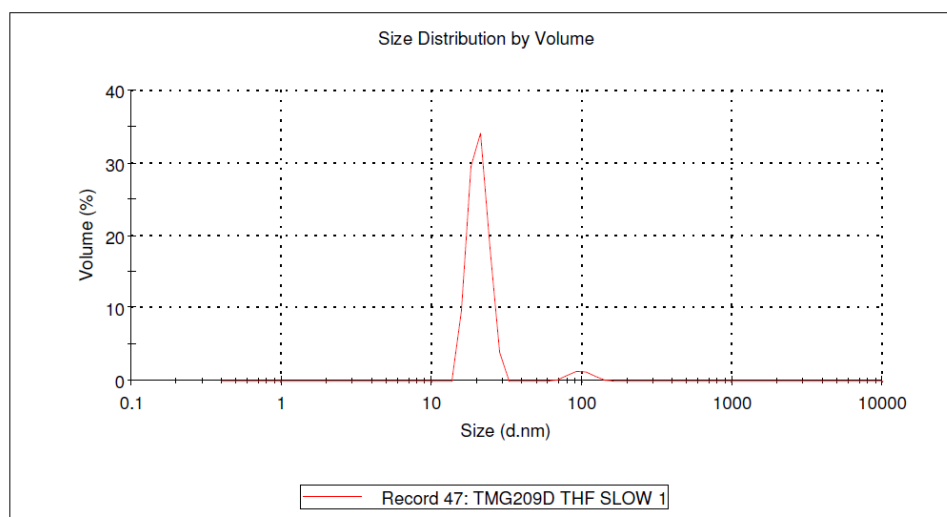Size Distribution by Volume

Record 47: TMG209D THF SLOW 1

Figure D4: The DLS traces of **L-2,000** following a) (top) fast aqueous self-assembly and b) (bottom) slow self-assembly.
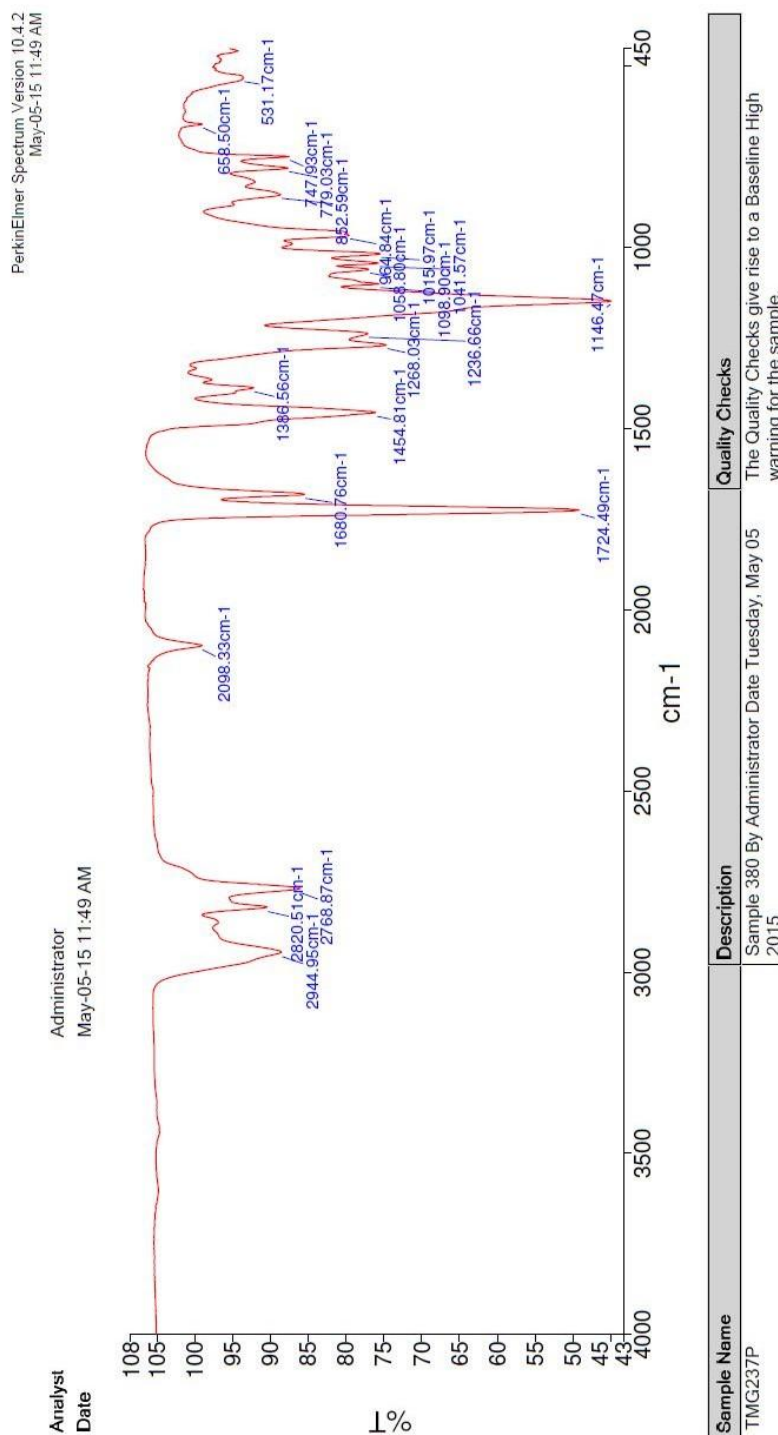
Appendix E: IR Spectrum

Figure E1: IR Spectrum of PDMAEMA polymer **24**

Curriculum Vitae

Name: Thomas Mackenzie Gungor

Post-secondary   University of Western Ontario
Education and   London, Ontario, Canada
Degrees: 2009-2013 HB.Sc.

                      The University of Western Ontario
                      London, Ontario, Canada
                      2013-2015 M.Sc. candidate

Publications:

Wong, A., Gungor, T.M., *ACS Macro Lett.*, **2014**, *3* (11), pp 1191–1195.